Integration of solar energy into a superheated steam process stream for the pre-treatment of lignocellulosic biomass

by

Dave Barchyn

A Thesis submitted to the Faculty of Graduate Studies of

The University of Manitoba

in partial fulfilment of the requirements of the degree of

MASTER OF SCIENCE

Department of Biosystems Engineering

University of Manitoba

Winnipeg

Abstract

The conversion of lignocellulosic wheat straw to bioethanol was found to benefit from pre-treatment using superheated steam (SS). A 2-step pre-treatment method using pressurized hot water at 119˚C followed by SS at 220˚C yielded the best results, with the most pronounced effect on enzymatic sugar liberation occurring after 2 minutes of SS treatment. The net sugar conversion efficiencies were 46.4 and 53.5% for glucose and xylose, respectively. The glucose was recovered from the treated biomass, while the majority of the xylose was recovered from the supernatant of the hot water phase. With an energy demand of approximately 1998 kJ/kg of biomass, pre-treatment with SS consumes approximately 78% as much energy as steam explosion, and can produce ethanol at a comparable price, based on a preliminary economic assessment.

Two technologies were examined for integration of solar energy into the SS process stream: evacuated tube solar collectors (ETSC) and parabolic trough solar collectors (PTSC). Utilization of ETSC was found not to be feasible for these applications due to low conversion efficiency (<12%) and progressive component failure at temperatures in excess of 175˚C. More promise was found with PTSC, which had higher conversion efficiencies of 36.4 and 55.8% at operating temperatures of 220 and 150˚C, respectively.

Experimental results were based on numerical simulation, and indicate that on a large scale, a PTSC facility is capable of generating energy at a rate competitive with conventional energy sources (<$0.021/kWh), though the capital expenditures are substantial, if not prohibitive.

Table of Contents

List of Figures

List of Tables

1. Introduction

1.1 Background

In 2010, global energy supply was reported as 12,717 MTOE (million tonnes oil equivalent, approximately 532 exajoules), 86.8% of which was derived from non-renewable sources such as fossil fuels and nuclear power (International Energy Agency, 2012). Non-renewable resources are defined as those that cannot be replenished at a rate suitable for sustainable economic extraction and utilization in meaningful human timeframes (National Research Council, 2010). Fossil fuels including coal, oil and natural gas represent the largest fraction of non-renewable energy sources, and make up 81.1% of the world's total energy supply (International Energy Agency, 2012).

Growing concern surrounding the sustainability of using fossil fuels was put into perspective with the concept of 'peak oil', when oil extraction would reach a maximum rate, independent of global demand. Increased fuel prices have rendered more costly extraction techniques economically feasible, thus postponing the date of 'peak oil'. Using the original work of M. King Hubbert, the projected date has been optimistically predicted as occurring later than 2020 (Cambidge Energy Research Associates (CERA), 2006), though other sources report that it will take place shortly (Koppelaar, 2005), or that it has already occurred (Zittel & Schindler, 2007).

Compounded with the diminishing supply of fossil fuels are environmental concerns associated with their combustion products. Carbon dioxide has been identified as a greenhouse gas, namely a substance whose anthropogenesis alters the atmospheric composition, contributing to climate change (Karl & Trenberth, 2003). Additionally,

health concerns have been identified related to exposure to particulate matter, another product of fossil fuel combustion (Grigg, 2002). Furthermore, as domestic reserves of conventional fossil fuels dwindle and imports are sought from regions where the political climate is volatile, energy security is taking the forefront in North American politics, with the focus shifting to energy sources which can be produced locally (Bradshaw, 2014). The development of alternative, sustainable fuel sources is therefore imperative for ongoing energy consumption at current rates and beyond.

Worldwide, one of the most prevalent uses of fossil fuels is in the transportation sector, accounting for 27.3% of total energy consumed, which represents 26,742 TWh (Swedish Energy Agency, 2010). Moreover, road transport is the major contributor to greenhouse gas emissions within the transport sector, representing 69.6% of total emissions generated (International Transport Forum, 2009). Reducing consumption of fossil fuel in the transportation sector would therefore have a significant impact on global utilization.

Many alternatives are currently being explored to supplant the sector's dependence on fossil fuels, including solar energy, hydrogen, wind energy, biofuels, and electricity from renewable sources (Metz, et al., 2007). Biofuels such as bioethanol and biodiesel are at the forefront for implementation for a variety of reasons. Bioethanol can be easily blended with gasoline for use in spark ignition engines (Rehnlund, 2004) and biodiesel can be blended with conventional diesel for use in compression ignition engines (Agarwal & Das, 2001). While blending with conventional fuels does not replace fossil fuels entirely, it displaces a significant portion leading to decreased emissions and can be implemented within the existing fuel distribution infrastructure (International Transport Forum, 2009). Moreover, the technology to produce and employ these fuels is well

established (Galbe & Zacchi, 2002), (Vasudevan & Briggs, 2008). The biofuel of interest in this study is ethanol.

Ethanol can be blended into unleaded gasoline in concentrations up to 25% with no reported impacts to engine operation. Furthermore, experimental results suggest that improvements in engine performance, exhaust emissions, brake power, brake thermal efficiency, volumetric efficiency and fuel consumption can be achieved though amendment of unleaded gasoline with ethanol, the most pronounced improvements reported at a 20% ethanol blend (Al-Hasan, 2003). However, ethanol has a significantly lower energy density than gasoline: 23.56 MJ/L versus 34.66 MJ/L, respectively (Argonne National Laboratory, 2010).

Currently, the production of virtually all fuel ethanol in North America is done by way of corn glucose fermentation (Lin & Tanaka, 2006). Ethanol produced from food crop feedstocks (such as corn) is referred to as a first-generation biofuel. Though these biofuels represent mature commercial markets and use well-understood technologies, they have inherent drawbacks. Competition with food crops, giving rise to the fuel-versus-food debate and driving food prices higher, limited greenhouse gas reduction benefits, and competition for water resources have increased the uncertainty surrounding the support of first-generation biofuels (Sims, et al., 2008). Additionally, use of these feedstocks has received widespread criticism, citing net energy loss, degradation of agricultural environment, displacement of food crops and economic sustainability among the primary concerns (Pimentel, 2003), (Taylor, 2009).

In order to be considered a viable substitute for conventional fuels, an alternative biofuel must possess several specific characteristics; net energy gains, environmental benefits, competitive economics, and large-scale yield without limiting food production being the most noteworthy (Hill, et al., 2006). This has encouraged research in the field of alternative feedstocks for ethanol production, paving the way for second-generation biofuels. Second-generation biofuels are those derived from agricultural and forest resides and non-food crop feedstocks (Sims, et al., 2008). Ethanol produced from second-generation sources is referred to as 'cellulosic ethanol' due to the utilization of cellulose as a substrate for fermentation in place of glucose or starch.

While development of second-generation biofuels shows promise in reducing impacts to crop production and agricultural environments and by extension increased reduction of greenhouse gas and combustion products (Sims, et al., 2008), there are still fundamental drawbacks to using cellulosic substrates, primarily relating to inherent recalcitrance to enzymatic digestibility (Mosier N. , et al., 2005). Raw cellulosic feedstocks are comprised of a combination of materials such as cellulose, hemicellulose and lignin and are collectively referred to as lignocellulose.

1.2 Research objectives

The design of a realistic pre-treatment technology must take into account the associated energy demands in order to properly assess its efficacy. Using superheated steam (SS) as the process medium stands to decrease the overall energy consumed during the process, and improve the overall energy yield of the conversion. Furthermore, since the generation of SS is a purely thermal process, improvements can be made to the energy source, and the integration of solar energy into the pre-treatment will be explored.

The three objectives addressed in this paper are as follows:

1) Determine the effectiveness of pre-treatment for lignocellulosic wheat straw using SS in terms of sugar conversion efficiency and energy demand

2) Investigate suitability of existing technologies for the integration of solar energy into the SS process stream

3) Develop a numerical model to predict the output and economy of integrating a solar energy collection field into SS generation

2. Literature review

2.1 Lignocellulose

Globally, biomass in the form of lignocellulose is a very abundant resource. It is generated at a rate of 731 million tons annually, which represents enough feedstock to produce 442 billion liters of bioethanol (Balat, 2011). Despite its abundance and low cost, lignocellulose as a feedstock is still a developing technology and has several barriers to overcome before it can be considered viable for implementation in industrial-scale ethanol production.

There is a large degree of variability between the compositions of lignocellulosic biomass feedstocks; the fractions of cellulose, hemicellulose and lignin differ substantially between sources (Kumar, et al., 2013). Cellulose is a tough, fibrous, water insoluble substance composed of organic polysaccharides. Linear chains of β(1→4) linked D-glucose $(C_6H_{10}O_5)n$ units form the main structures, and provide the source of fermentable

6-carbon sugars. Hemicellulose is an amorphous structure of several heteropolymers, with less strength than the ordered, crystalline cellulose. It is also a polysaccharide, but derived from several sugars in addition to glucose, including primarily xylose but also mannose, galactose, rhamnose and arabinose. Lignin is a biopolymer composed of phenylpropanoids that contributes to the structural integrity and mechanical strength of the cell wall. It is a complex chemical compound that covalently links to hemicellulose and cross-links the different polysaccharides (Tabil, Adapa, & Kashaninejad, 2011).

Cellulose and hemicellulose, once hydrolyzed into their constitutional 5- and 6-carbon sugars, can be fermented into ethanol by various microorganisms, including bacteria, fungi, and yeasts (Sun & Jiayang, 2002), (Currie, et al., 2013). While yeasts are used in many commercial operations due to high ethanol tolerance and rapid conversion rates, the utilization of anaerobic, thermophillic bacteria is also being explored for their ability to digest a wide variety of substrates (Lin & Tanaka, 2005). However, lignin binds these carbohydrates, rendering them recalcitrant to microbiological processes (Sanchez, Sierra, & Almeciga-Diaz, 2011). In order to render the lignocellulose susceptible to microbial conversion and enable its use as a fermentation substrate, treatment prior to processing is necessary.

The lignocellulosic biomass considered in this study is wheat straw; it is one of the most abundantly produced biomass sources in Manitoba, generally in the range of 4 to 6 million tons annually, representing and excess of approximately 2.6 to 3.8 million tons when conservation requirements are considered (Prairie Practitioners Group, 2008).

2.2 Pretreatment

Several factors inhibit hydrolysis of lignocellulose in addition to lignin content, such as degree of polymerization, moisture content and available surface area (Hendricks & Geeman, 2009). An ideal pretreatment process would address these problems and render 100% of the cellulose and hemicellulose contained within the structure fermentable while minimizing energy and chemical consumption (Mosier N. , et al., 2005). While the fundamental objectives of pretreatment are hydrolysis and delignification, other issues that must be addressed are the deterioration of post-hydrolysis sugars and the formation of toxic degradation products (Jönsson, Alriksson, & Nilvebrant, 2013). Many different pretreatment methods for lignocellulose exist, including thermal pretreatment, mechanical pretreatment, acid pretreatment, alkaline pretreatment and oxidative pretreatment (Hendricks & Geeman, 2009).

2.2.1 Thermal Pre-treatment

Thermal pretreatments operate on the basis of subjecting lignocellulose to high temperatures and pressures with the purpose of eliciting structural and chemical changes within the lignin (Mosier N. , et al., 2005). Such is the case for liquid-hot-water pretreatments; the lignin and hemicelluloses are solubilized and removed from the structure (Hendricks & Geeman, 2009). Conversely, steam explosion pretreatment hinges on an explosive decompression of biomass treated with high-pressure steam, resulting in a mechanical disruption of the fibres (Horn, Nguyen, Westereng, Nilsen, & Eijsink, 2011). Steam explosion is viewed as one of the most efficient means of pre-treating lignocellulosic biomass, and has been used successfully on a wide variety of substrates (Kim & Dale, 2004). Thermal processes are often catalyzed using dilute acids or alkalis.

Main concerns associated with thermal pre-treatment techniques are the formation of toxic degradation product, loss of fermentable hemicellulose, increased energy consumption, and repolymerization of lignin (Mosier N. , et al., 2005). In order to quantitatively compare thermal pre-treatments, a variable referred to as the 'severity factor' (S_0) is introduced, taking into account treatment time and temperature. The expression for S_0 is as follows (Overend & Chornet, 1987):

$$S_o = log(t \times e^{(T-100)/14.75}) \quad [2.1]$$

where

t = time (minutes)

T = temperature (°C)

An increased severity factor implies a more intense pre-treatment process. While the efficacy of pre-treatment increases with severity, lignin repolymerization also becomes more dominant (Li, Henriksson, & Gellerstedt, 2007). Furthermore, increased severity of pre-treatment processes can contribute to increased production of inhibitory compounds such as toxic degradation products, a result of the progression of chemical reactions beyond hydrolyzation (Jönsson, Alriksson, & Nilvebrant, 2013).

2.2.2 Mechanical Pre-treatment

The primary goal of mechanical pre-treatment is to reduce the particle size of the biomass. This increases the specific surface area susceptible to hydrolysis and fermentation reactions and decreases the degree of polymerization of the substrate, which contributes to an increased yield from the biomass. Milling and grinding are two

examples of mechanical pre-treatment currently in use (Sun & Jiayang, 2002) (Hendricks & Geeman, 2009). While shown to be an effective means of pre-treatment that produces few toxic by-products, due to high energy demands compared with the increase in fermentability, mechanical pre-treatments are viewed as not economically feasible (Fan, Gharpuray, & Lee, 1987).

2.2.3 Acid Pre-treatment

Acid pre-treatments have been employed using acids of varying concentrations, generally H_2SO_4 and HCl, at ambient to high temperatures (Sun & Jiayang, 2002). The main mode of action of acid pre-treatment is the hydrolysis of hemicelluloses, rendering the cellulose more accessible and susceptible to fermentation (Hendricks & Geeman, 2009). Increased temperatures result in more complete hydrolysis of hemicelluloses and increased cellulose hydrolysis, however yields are affected by sugar degradation with increasing process severity (Sun & Jiayang, 2002).

2.2.4 Alkaline Pre-treatment

Common pre-treatments involving alkaline compounds include ammonia fibre explosion (AFEX), ammonia recycle percolation (ARP), and soaking aqueous ammonia (SAA). Alkaline pre-treatments generally rely on solvation and saphonication reactions, which cause the biomass to swell and become accessible to enzymes and bacteria. While effective, alkaline treatment can result in the solubilization, redistribution, and condensation of lignin, and modifications to the crystallinity of the cellulose components (Gregg & Saddler, 1996). These side effects can decrease or even counteract the positive effect of the overall treatment (Hendricks & Geeman, 2009).

Treatments such as concentrated acids have been determined to be unfeasible due to economic constraints, however thermal and alkaline pre-treatments show more promise (Hendricks & Geeman, 2009). The main focus of this study was on thermal pre-treatment of lignocellulosic biomass. As lignin depolymerization occurs at approximately 180˚C, effective temperatures for thermal pre-treatment generally lie in the range of 170˚C to 270˚C (Agbor, et al., 2011). The temperature selected for the pre-treatment evaluated in this study is 220˚C.

2.3 Superheated steam processing

Generation of SS is achieved by heating wet steam beyond its saturation temperature (100˚C at atmospheric pressure) to increasing degrees of superheat. The advantages processing with SS is its ability to deliver high rates of energy prior to re-condensation, and achieve high penetration.

Traditionally, SS has been used to power steam turbines (Babcock and Wilcox Company, 2007), but recently it has been found to have applications in drying, decontamination, and pre-treatment of biological materials. It is effective in these areas due to high rate of energy delivery and high material penetration, resulting in reduced energy expenditure (Pronyk, Cenkowski, & Muir, 2004), (Cenkowski, et al., 2007).

2.4 Solar thermal technologies

Solar energy is the most abundant renewable resource on earth (Thirugnanasambandam, S., & Ranko, 2010); with increasing economic viability and technological advancements, it is projected to supply approximately 45% of global energy demand by the year 2050 (Mekhilef, Saidur, & Safari, 2011). Direct conversion of solar energy into electricity

through the use of photovoltaics is an attractive option; experimental efficiencies achieved in a laboratory setting have been reported as high as 38.8% (Green, Emery, Hishikawa, Warta, & Dunlop, 2014), however more realistic efficiencies deployable at industrial scales are closer to 15% (McGehee, 2013). Solar thermal technologies, which involve the conversion of solar radiation to heat instead of electricity, have an inherently higher efficiency. Operational efficiencies in excess of 80% have been reported over a range of temperature differentials (Kalogirou S. A., 2004).

Harnessing solar energy for the purposes of heat and power generation encompasses a wide variety of technology and applications. It has been proposed as a supplemental energy source for a variety of industrial processes, including drying, distillation, and product separation (Kalogirou S. , 2003), improving the overall efficiency of the system, most notably with solar thermal technologies, while simultaneously reducing the carbon footprint of the operation (Schnitzer, Christoph, & Gwehenberger, 2007).

Critical to the improvements in efficiency possible to achieve from integration of solar thermal technologies is the proper selection of collector (Mekhilef, Saidur, & Safari, 2011). While a wide variety of technology exists, not all are amenable to all industrial processes, depending primarily on operation temperature and tracking system. A summary of existing solar thermal technologies is shown in Table 2.1 (Kalogirou S. , 2003) with their respective tracking systems and operating temperatures. For a target pre-treatment temperature of 220˚C, the most appropriate technologies, which were selected as the focus of this study, are evacuated tube solar collectors (ETSC), and parabolic trough solar collector (PTSC).

Table 2.1. Thermal solar collectors and indicative operating temperatures

Motion	Collector type	Absorber type	Concentration ratio	Indicative temperature range (˚C)
Stationary				
	Flat plate collector	Flat	1	30-80
	Evacuated tube collector	Flat	1	50-200
	Compound parabolic reflector	Tubular	1-5	60-240
Single-axis tracking				
	Fresnel lens collector	Tubular	10-40	60-250
	Parabolic trough collector	Tubular	15-45	60-300
	Cylindrical trough collector	Tubular	10-50	60-300
Two-axis tracking				
	Parabolic dish collector	Point	100-1000	100-500
	Heliostat field collector	Point	100-1500	150-2000

2.4.1 Evacuated tube solar collectors

Evacuated tube solar collectors are a well-developed technology primarily used for heating, cooling and hot water applications (Hinotani, Kanatani, & Osumi, 1979). They have been demonstrated to operate with higher efficiency at high temperature differentials than their passive-tracking counterparts such as flat-plate collectors (Zambolin & Del Col, 2010). They are generally composed of a copper inner heating tube, sealed and evacuated, containing a small amount of distilled water. Attached at the apex of the tube is a copper terminus, to which the solar energy is transferred. Surrounding the evacuated tube is a shroud of borosilicate glass and aluminum heat transfer fins, all encased in protective glass. The outer glass layer serves the purpose of preventing convective losses from the tube, and the coppered glass and aluminum serve as a highly conductive manifold to transfer the collected solar energy into the evacuated

tube. The collector works on the basis of a thermosyphon, allowing the distilled water to evaporate at low temperatures and transferring the heat of vaporization into the copper terminus as the vapor condenses, returning to the base of the tube and restarting the cycle. The round shape of the tubes allows for passive solar tracking. An advantage of the evacuated tube collector system over other passive solar collection systems is its ability to generate high-quality heat in excess of 100˚C .

2.4.2 Parabolic trough solar collectors

Parabolic trough collectors have been in commercial use since the mid 1970s (Fernandez-Garcia, et al., 2010), though the technology has been used for applications such as steam generation since the early 1900s (Pytlinski, 1978).

Operation of a PTSC array relies on the concentration of direct solar radiation onto a focal line on the collector axis. A central absorber tube transfers the collected energy to the working fluid, generally a purpose-designed heat transfer fluid, or in some cases water. As the only component of the incident radiation that can be utilized by the PTSC is the direct normal radiation, single-axis tracking is required for efficient operation (Fernandez-Garcia, et al., 2010).

3. Methodology

3.1 Superheated steam apparatus

A schematic of the SS generator used for experimentation at the University of Manitoba is shown in Figure 3.1. Water at ambient temperature is fed from the process water tank (1) a Sussman ES18 boiler (8), which at its maximum capacity can generate 24.6 kg/h of

wet steam at 160˚C and corresponding pressure of 586 kPa . The unit operates at 208V, 50A on a 3-phase power supply. The high pressure saturated steam is depressurized at the pressure reducing valve (12). By lowering the pressure, the high pressure wet steam becomes low pressure (atmospheric pressure) superheated steam at 160C. As low pressure SS passes through 2 m stainless steel pipe it looses its sensible heat, therefore, the superheater (14) provides the additional heat required to elevate the SS needed for processing at a desired temperature. Once the desired temperature is achieved, the SS is fed into the processing chamber (20) where a sample is placed . Steam temperature in the superheater (14) is controlled using the main control panel and the steam rate is controlled with the globe valve (9).

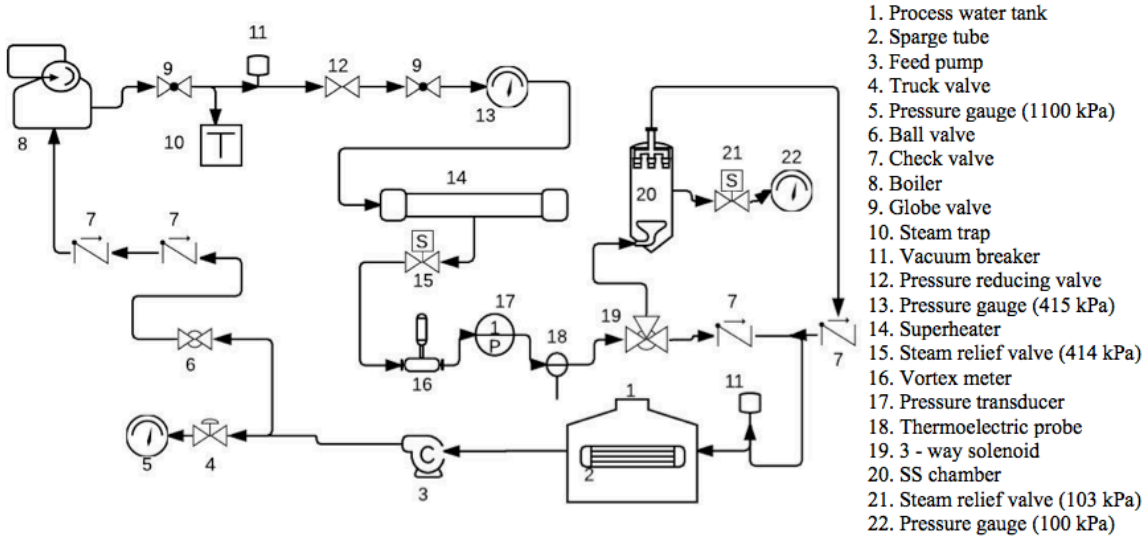

Fig. 3.1. Process flow diagram of superheated steam generator

3.2 Treatment with superheated steam

For the initial assessment of the effectiveness of a SS pre-treatment, samples of wheat straw were subjected to high temperature SS for varying amounts of time. In order to

measure the degree to which the cellulose and hemicellulose were rendered accessible for fermentation, the samples were subjected to enzymatic hydrolysis in accordance with the National Renewable Energy Laboratories (NREL) guidelines for saccharification of lignocellulosic biomass (Selig, Weiss, & Ji, 2008). Following enzymatic hydrolysis, the samples were analyzed using high performance liquid chromatography (HPLC) for the presence of glucose and xylose.

The model of HPLC used was the Breeze 2 system from Waters (Mississauga, ON). The system consisted of an HPX-87H column from Biorad (Hercules, CA) with Micro-guard Cation H+ guard column, and a 2414 refractive index detector. The HPLC system used 5 mM sulfuric acid as the mobile phase at a flow rate of 0.6 mL/min and a column temperature of 45°C.

Raw samples were obtained from Biovalco Inc. and assessed for constitutional components by the University of Saskatchewan College of Agriculture and Bioresources in accordance with Association of Official Agricultural Chemists (AOAC, 2011) and Association of American Feed Control Officials (AFFCO, 2009) standards.

Samples were ground and sieved to <355 µm particle size, and subjected to treatment in the SS chamber at 220˚C for 10, 20, and 20 minutes. Subsequently, enzymatic hydrolysis was conducted at a temperature of 50˚C +/- 1˚C for 144 hours, using aqueous cellulase and β-glucosidase from Novozymes (C-tec™ and H-tec™, respectively).

The intention was to establish a maximum severity treatment that would liberate the maximum possible cellulose and hemicellulose from the raw biomass using SS processing. As yield generally correlates with severity (Li, Henriksson, & Gellerstedt,

2007), an optimal length of time for thermal pre-treatment where energy expenditure, inhibitor formation, and sugar degradation begin to overcome product yield exists, and varies greatly between substrates and treatment methods. Similar high temperature pre-treatment methods have shown an initial increase in fermentable sugars, followed by a gradual decline in yield at various degrees of severity, with optimal times ranging from approximately 5 to 40 minutes (Lloyd & Wyman, 2005). To determine where the optimal treatment time would be, the treatment times selected were 10, 20, and 30 minutes.

3.3 Treatment with hot water and superheated steam

A second pre-treatment method was devised using a combination of hot water and SS. Liquid hot water under high pressure has been used successfully for the pre-treatment of lignocellulose, often in conjunction with acid catalysts (Hendricks & Geeman, 2009). As the goal of this pre-treatment was to avoid the use of excess chemicals, no outside catalysts were used.

The same size reduction methodology was followed as in 3.2. Following sieving, the samples were placed in a Lagostina 3L pressure cooker, where they were subjected to the hot water phase of the treatment. This involved processing in boiling water at 119˚C and 193 kPa for 15 minutes.

To better delineate the relationship between time of SS treatment and fibre liberation, treatment in the SS chamber was reduced to 2, 5, and 10 minutes. Enzymatic hydrolysis was carried out under the same protocol as in 2.2 (Selig, Weiss, & Ji, 2008), using lyophilized powder cellulase (from *Aspergillus niger*) and β-glucosidase (from *Prunus amygdalus*) supplied by Sigma-Aldrich.

Glucose and xylose concentrations in the hydrolyzed samples were determined by HPLC.

3.3.1 Xylose recovery

Since xylose solubilization is a common effect in thermal pre-treatments, determination of the solute concentration following the hot water phase of the treatment was undertaken. Water was collected from the treatment vessel following treatment and analyzed using HPLC for the presence of glucose, xylose, and cellobiose that could potentially have been solubilized during this phase of the process. Similarly, the condensate from the superheated steam generator was collected and tested for the presence of the same compounds.

3.4 Evacuated tube solar collector

(from *Performance of evacuated solar tube collectors at high temperature differentials*, Barchyn & Cenkowski, submitted to the Canadian Biosystems Engineering Journal, January 2015)

Solar energy was gathered using a bench-scale ETSC array composed of solar vacuum tubes (Jiaxing Sunergy Electric Co., HaiYan, China). The evacuated tube collectors were mounted inside of a parabolic reflector made of aluminum to maximize their exposure to incoming solar radiation. Aluminum was selected due to its propensity for reflecting thermal energy. Moreover, the frames into which they were mounted were tilted at an angle of 45° to the horizon, further increasing the radiation to which the tubes were exposed.

Heat exchangers were constructed out of oxygen-free, highly conductive soft copper tubing (Alloy 101), formed into tight coils to increase the residence time within the

manifold, shown in Figure 3.2. The nominal size of the copper was 1/8” O/D which, while it caused an increase in head loss through the system, was necessary to create coils small enough to be mounted on the evacuated tube collector terminals with maximum surface contact. The copper alloy selected was specifically designed for high thermal conductivity.

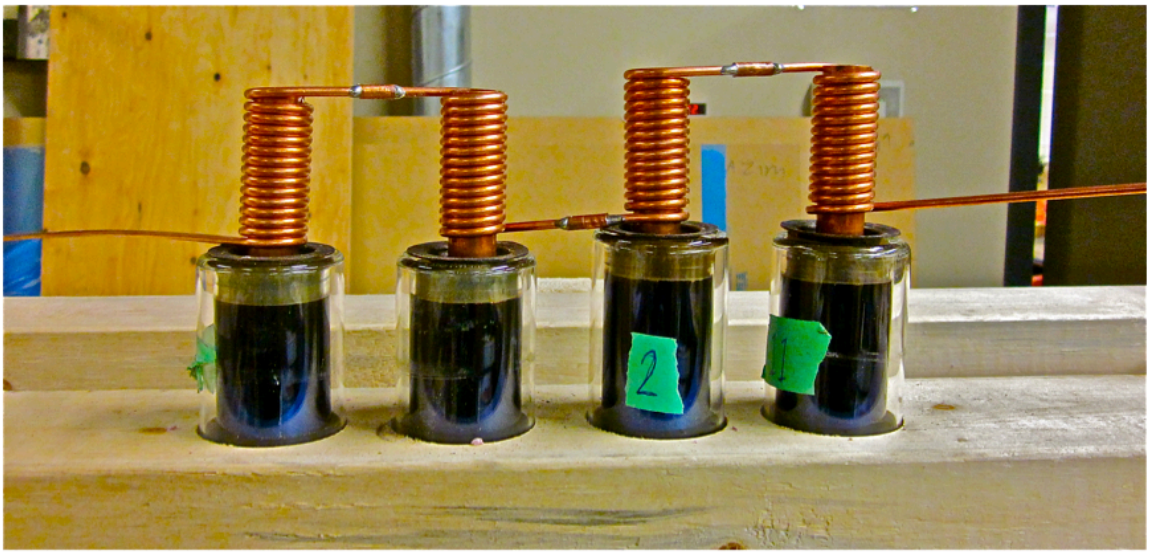

Fig. 3.2. Heat exchanger configuration using coiled soft copper tubing.

Water was fed through the system using a pressurized vessel to overcome the inherent head losses associated with the high fluid velocities resulting from the density decrease occurring during phase change from liquid to vapor. The reservoir was constructed using PVC and ABS plastics and pressurized using a hand pump up to pressures of 70 kPa. The entire setup is show in Figure 3.3.

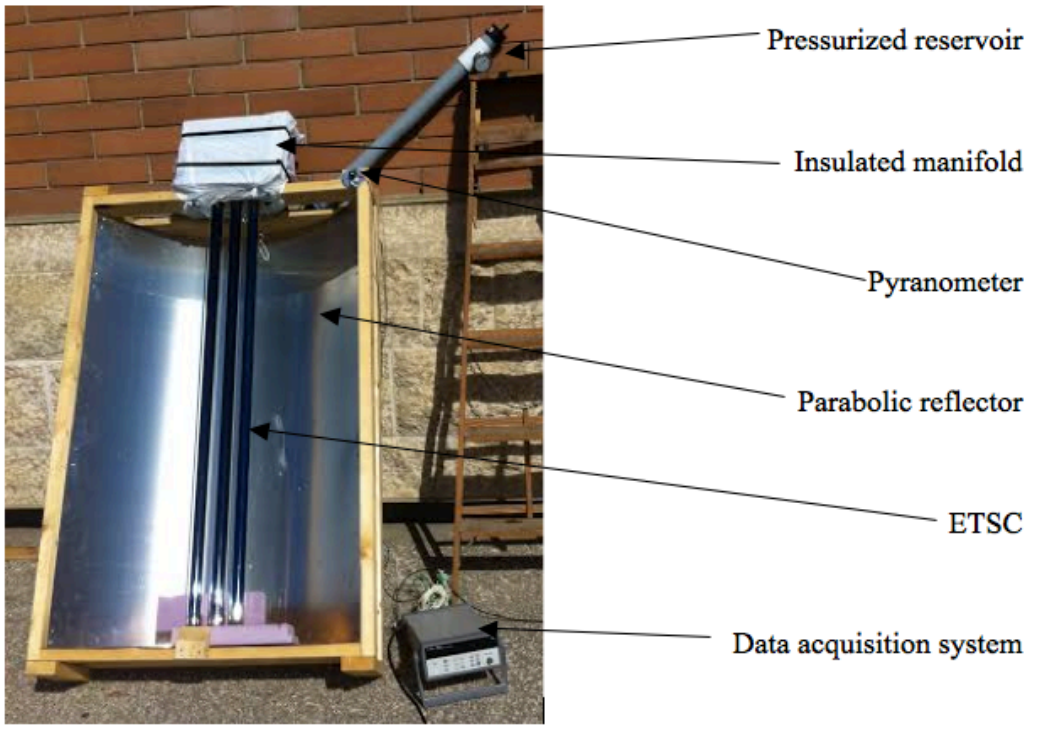

Fig. 3.3. Experimental setup of ETSC apparatus

Information pertinent to determining the performance parameters of the apparatus included temperature, incident solar radiation, rate of condensation and reservoir pressure.

Energy output of the system was calculated based on the maximum temperature reached by the superheated steam and the rate at which it was being produced. The energy input was calculated based on the specific radiation and the area of aperture of the collector tubes.

Temperature was measured by means of 4 type-K thermocouples, mounted on each of the manifold coils to measure the temperature of the steam and on the side of the frame to measure ambient temperature.

Radiation was measured by means of a LiCor LI-200 pyranometer, mounted on the frame, orthogonal to the incoming radiation.

Thermocouple and pyranometer readings were recorded at 10-second intervals. Condensation data was collected at intervals of 2 minutes.

In order to properly evaluate the rate at which energy was being delivered to the water vapor, a steady state needed to be achieved between the evacuated tube terminals and the water vapor. This was achieved using the pressurized reservoir to deliver the water at an equilibrium pressure to maintain a constant temperature in the downstream evacuated tube.

3.5 Parabolic trough solar collector

As PTSC are a mature and well-understood technology, techniques have been developed to simulate their operation using one- and two-dimensional heat transfer models (Forrestal, 2003)(Incropera & DeWitt, 2002). Using Matlab and Simulink, a simulation was constructed to model the behavior of a PTSC system operating in Winnipeg, Manitoba, Canada, and verified to accurately predict the output of the system (Mosallat & Bibeau, 2014). Modifications were made to accommodate the integration of statistically derived meteorological data for input, and produce results indicative of SS generation in the place of electrical power generation. The output generated by the model is indicative of the most basic scenario, ie: constant mass flow rate of heat transfer fluid and no onsite thermal storage.

3.5.1 Numerical model

The model described by Forrestal (2003) describes the performance of a PTSC linear collector element based on collector geometry, optical properties, heat transfer fluid thermodynamic properties and flow rate, and meteorological data, including direct normal irradiance, ambient temperature, and wind speed. The model takes into account the 1- and 2- dimensional energy balances in order to generate output, shown in Figure 3.4 and Figure 3.5, respectively (Forrestal, 2003). The model was constructed in accordance with the inclusion of a glass envelope surrounding the absorber pipe.

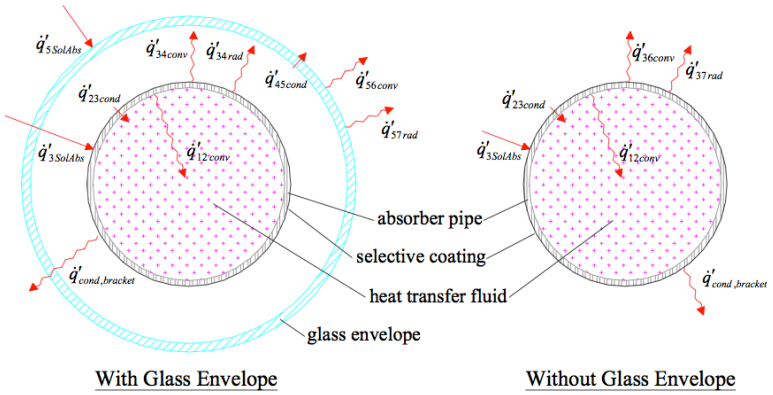

Fig. 3.4. One-dimensional steady-state energy flux balances

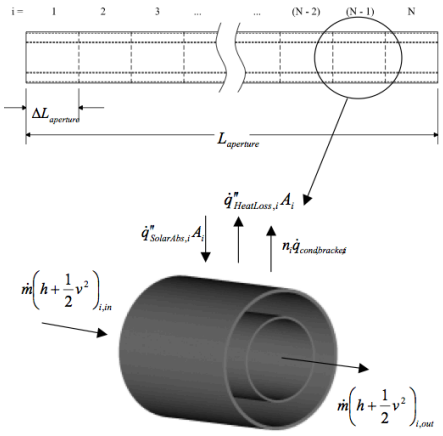

Fig. 3.5. Schematic of the two-dimensional heat transfer model

Assumptions made in the simulation of the PTSC performance associated with the materials used are listed in Table 3.1.

Table 3.1. Assumed values and parameters for the PTSC numerical simulation

Parameter	Assumption
Mirror reflectivity	0.9
Heat transfer fluid	Therminol 66 (Solutia, 1998)
Trough model	LS-3 (Mills, 2004)
Annulus gas	Air
Pipe volume	304 L
Absorber coating	Black chrome (Kennedy, 2002)
Tracking mode	East-west axis, continuous
Pipe length	50 m

Once programmed into the simulation, the numerical model was run for a period of one year using variable time-steps and the Dormand-Price ODE45 solver method.

3.5.2 Statistical model

Statistically derived data for direct normal irradiance (DNI), ambient temperature, and wind velocity were required as input variables to the simulation. Due to the unpredictable nature of these elements, a statistical model based on historical data from Environment Canada was constructed to generate an accurate representation of their expected behavior over the course of a year.

Statistical generalization for time series analysis is typically done by way of autoregressive integrated moving average (ARIMA) models, which can produce an

accurate forecast based on observed trends. A commonly used method in environmental monitoring is the Box-Jenkins method (Mihaela & Meghea, 2011), which was the method selected for this study.

The Box-Jenkins method requires four steps of analysis: model identification, estimation, diagnostics checking, and forecasting. The variable in question is first identified in the time series, and its stationarity and seasonality are established based on its autocorrelation function (ACF), partial autocorrelation function (PCF), and inverse autocorrelation function (IACF). Secondly, estimations are made based on the differencing periods to verify the invertibility of the model, and diagnostics checking is done in accordance with the Ljung-Box statistic. The forecasting is then done based on the differencing periods established, and to the accuracy desired by the analyst (Ngo, 2013). For this analysis, the most narrow confidence interval corresponding to the differencing periods was selected.

Historical meteorological data (Environment Canada, 2003) was used, representing the required variables for the model spanning from 1980 to 2001, collected from the Winnipeg International Airport in Manitoba, Canada. Input data was at intervals of 1 hour. The statistical forecast was generated using SAS 9.3 statistical analysis software and the ARIMA procedure.

4. Results and discussion

4.1 Compositional analysis

The results of the compositional analysis, shown in Table 4.1, indicate that the theoretical yield of cellulose and hemicellulose are 0.437 g/g and 0.240 g/g, respectively.

Table 4.1. Compositional analysis of raw biomass, Reported values are within 3% standard error.

Parameter	Composition (%)	Method
Moisture	4.82	AOAC 930.15
Dry matter	95.18	AOAC 930.15
Lignin	10.63	AOAC 973.18
ADF*	54.37	AOAC 973.18
NDF**	78.4	AOAC 2002.04
Cellulose	43.74	cellulose = ADF - lignin
Hemicellulose	24.03	hemicellulose = NDF - ADF

*ADF = acid detergent fibre

**NDF = neutral detergent fibre

4.2 Treatment with superheated steam

Figure 4.1 shows the pre-treated wheat straw and the samples following enzymatic hydrolysis. There was a visible change in colour between the raw and pre-treated biomass samples (Fig 4.1a). As a result of 10, 20 or 30 min pre-treatment with SS, the samples changed from beige to increasingly dark brown.(Fig. 4.1b)

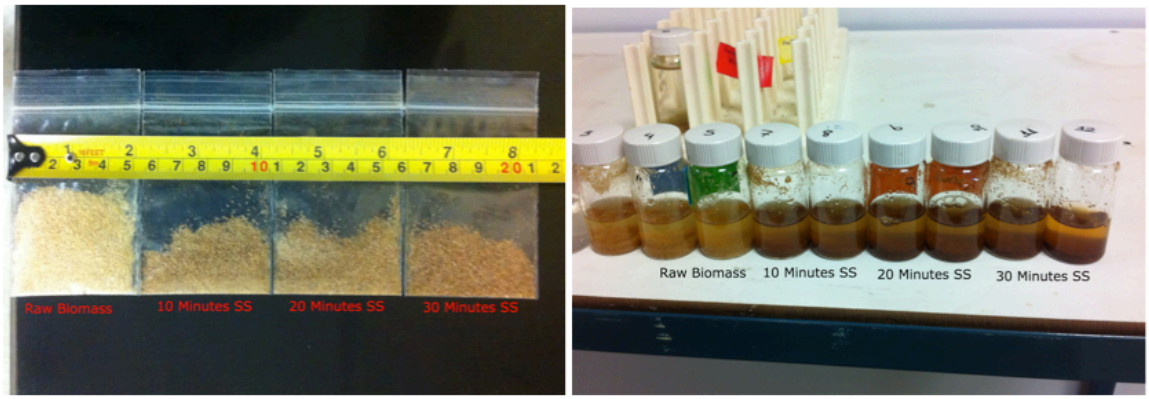

(a) **(b)**

Fig. 4.1. Wheat straw samples following SS pre-treatment (a) and enzymatic hydrolysis (b).

Figure 4.2 shows the yield of glucose and xylose as a result of SS pre-treatment followed by enzymatic hydrolysis. Complete data set and calibration curves can be found in appendix A.

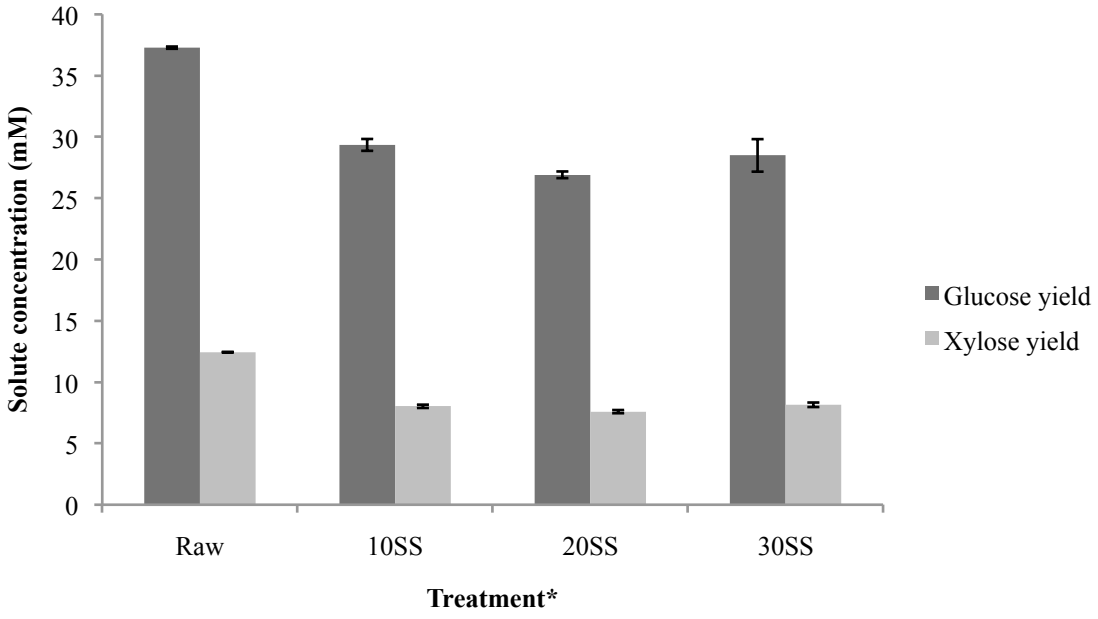

Fig. 4.2. Glucose and xylose production following SS pre-treatment
*xxSS denotes length of time (in minutes) of SS treatment applied to each sample

Contrary to the hypothesized outcome, both glucose and xylose production decreased as a result of pre-treatment at all severity levels. Furthermore, the effect of pre-treatment did not demonstrate a significant correlation with the level of severity.

It was concluded that the time of treatment should be reduced to accurately delineate the effect that SS has on the hydrolysable components, as the optimal treatment time was likely exceeded. Furthermore, in order to increase the capacity for lignin disruption, the moisture content would be increased in order to provide a medium into which it could solubilize.

Consequently, the pre-treatment methodology was modified to include a hot water phase prior to exposure to SS. This would at once reduce the required time of SS treatment, and provide a solvent into which the lignin could solubilize.

4.3 Treatment with hot water and superheated steam

Following the hot water phase of the treatment, there was a visible colour change to the biomass, though less dramatic than was observed for SS pre-treatment of raw biomass. Additionally, the water collected from the treatment vessel changed to brown with small particles precipitating when the solution cooled. The visible effects are shown in Figure 4.3.

Thermal pre-treatments often have the effect of solubilizing components of the hemicellulose, which may explain the presence of some solutes in the treatment water (Brodeur, et al., 2011).

(a) **(b)**

Fig. 4.3. Effect of hot water pre-treatment on wheat straw (a) and treatment water (b).

As SS processing is in effect a drying technology, there was a clear difference in the moisture content between treatments from saturated (only hot water) to dry (10 minutes SS). The visible effects of the combined hot water and SS treatment are shown in Figure 4.4.

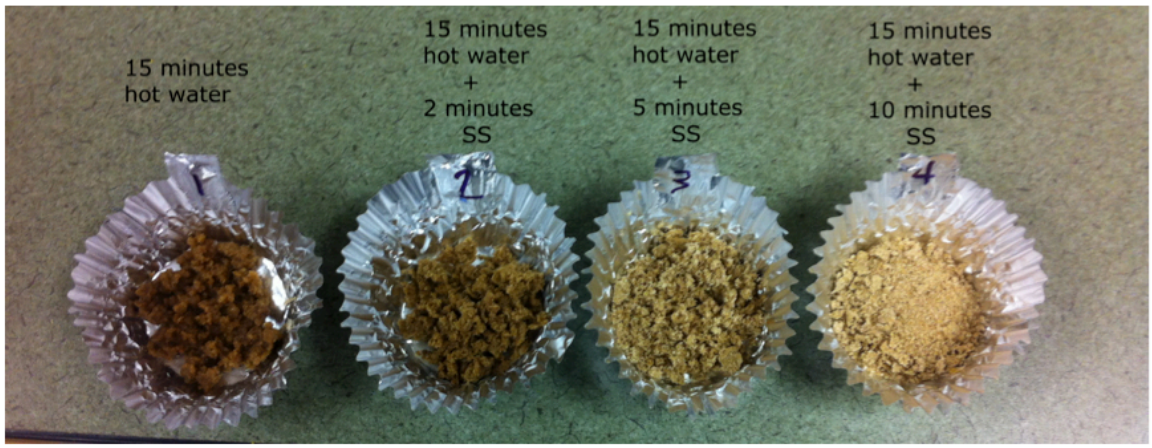

Fig. 4.4. Effects of combined hot water and SS pre-treatment.

The effects of enzymatic hydrolysis were evaluated based on the theoretical maximum yield of glucose and xylose. Xylose is considered the main constituent of wheat straw

hemicellulose, representing between 70% and 90% of the monomer units (Sun, Lawther, & Banks, 1996). For the purpose yield calculations, the hemicellulose was assumed to be composed of 78.7% xylose (Lawther, Sun, & Banks, 1995). Results of the HPLC following enzymatic hydrolysis are shown in Figure 4.5. Complete results of the HPLC can be found in Appendix B.

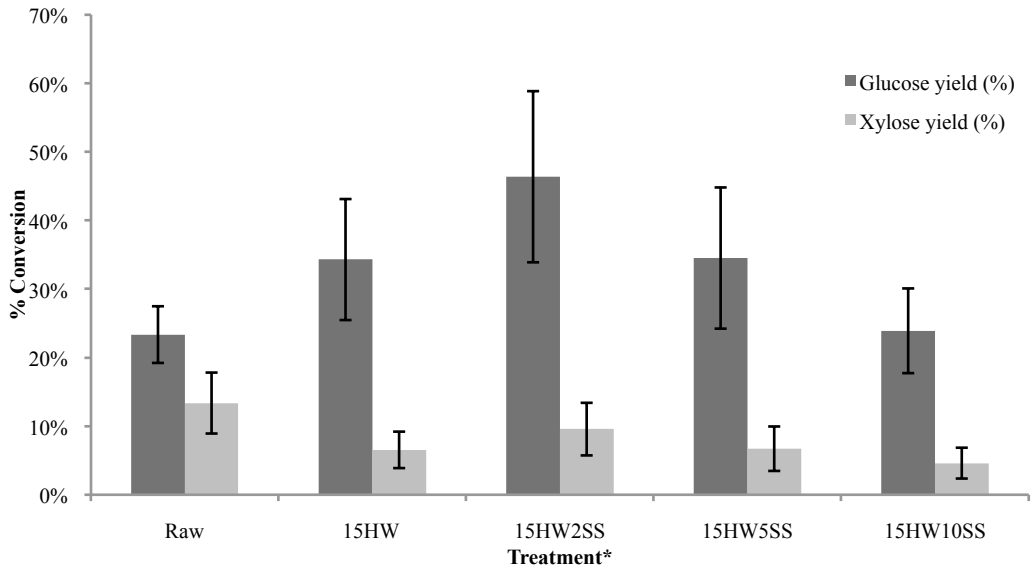

Fig. 4.5. Glucose and xylose conversion as a result of enzymatic hydrolysis
*15HW indicates 15 minutes treatment in hot water at 193 kPa, 119˚C, xSS indicates the number of minutes exposed to SS

There was a clear increase in the glucose production following combined hot water and SS pre-treatment. Xylose production followed a similar trend to the SS-only pre-treatment, showing a clear decline as a result of treatment with both hot water and SS. This reduction in xylose could have arisen as a result of solubilization during the hot water phase, as there were clearly solutes present in the water, and this is a common effect in hot water pre-treatments (Weil, et al., 1998). These results are similar to experiments carried out with steam explosion pre-treatment; an optimal treatment time was encountered beyond which yield began to decrease (Horn, et al., 2011). The optimal

conditions for glucose recovery appeared to occur at 15 minutes of hot water treatment and 2 minutes of SS. The decrease in glucose recovery is hypothesized to be the result of a redistribution of the lignin within the cellulose matrix.

While the treatment was successful in increasing the glucose yield from the substrate, there was a marked decrease in the xylose production from the biomass.

4.3.1 Xylose recovery

Results of the HPLC showed that in the treatment water, there was an average concentration of 16.6 mM of xylose present, representing a yield of 43.9%. No glucose was detected, and only trace amounts of cellobiose. Taking this into account, the yield of xylose as a result of the combined hot water and SS treatment is shown in Figure 4.6.

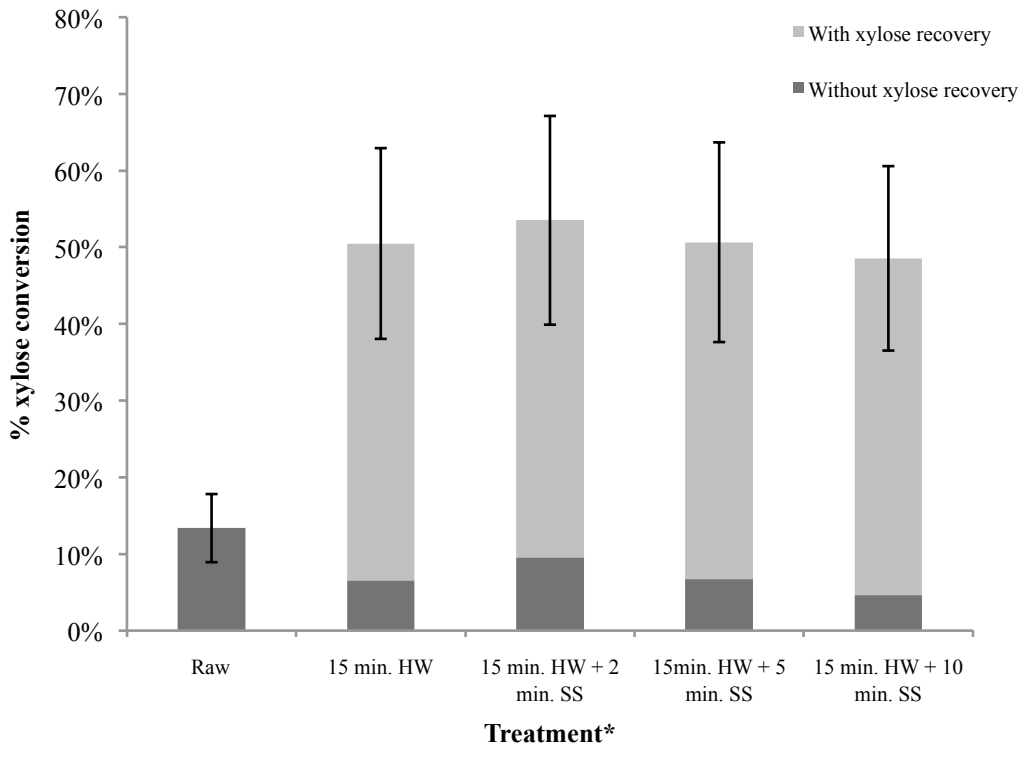

Fig. 4.6. Xylose conversion with and without recovery from hot water
*15HW indicates 15 minutes treatment in hot water at 193 kPa, 119˚C, xSS indicates the number of minutes exposed to SS

There is a substantial increase in xylose recovery if the fraction solubilized in the hot water phase of the treatment is accounted for. This significantly improves the total yield of sugars of the overall treatment.

The condensate from the superheated steam generator did not contain any glucose, xylose, or cellobiose.

4.4. Economic analysis

(From *Process analysis of superheated steam pre-treatment of wheat straw and its relative effect on ethanol selling price,* Barchyn & Cenkowski, published in Biofuel Research Journal, December 2014)

Proper assessment of a pre-treatment technology must include an economic analysis in order to evaluate its feasibility. Existing literature generally evaluates economic viability on the basis of a minimum ethanol selling price (MESP) resulting from production costs to compare different technologies (Eggeman & Elander, 2005). While this is a useful tool for evaluation, it is susceptible to uncertainties arising from the proprietary nature of ethanol corporate cost data, as well as the economies of scale (Gallagher, Brubaker, & Shapouri, 2005). Being a thermal process, SS pre-treatment of wheat straw will be compared to steam explosion, a well-developed technology for pre-treatment of lignocellulose.

4.4.1 Economic analysis methodology

An equation specific to the economics of cellulosic ethanol was proposed to calculate the cost of ethyl alcohol production (Soloman, Barnes, & Halvorsen, 2007) and is expressed as follows:

$$C_A = \frac{C_B}{95} + C_K + C_L + C_E + C_M + C_O - P_P \qquad [4.1]$$

where

C_A = cost of ethanol production ($/gal)

C_B = cost of biomass feedstock ($/dry short ton)

C_K = cost of capital investment

C_L = cost of labor

C_E = cost of energy

C_M = cost of raw materials

C_O = other costs

P_P = price of excess electric power byproduct to be sold

Naturally, many assumptions must be made in order to employ this equation, and are listed below.

Estimates pertaining to the cost of raw material are generally inconsistent, and in the range of $10/Mg to $25/Mg (Kaylen, et al., 2000), (Walsh, 1998). An extensive study of lignocellulosic biomass harvest systems concluded that, depending on crop yield, the cost of raw wheat straw can be estimated as being between $11.26 and $14.01 per Mg, which is the assumption made for this study (Thorsell, et al., 2004). An average sized (50 Mgal/year) ethanol plant typically requires approximately $65-$100 million in capital costs and $45-$60 million in annual operating costs (Urbanchuk, 2006). These costs are assumed to encompass the cost of labor and raw materials for this evaluation.

Energy costs associated with SS processing are generally evaluated based on the moisture removed from the biomass during the treatment (Berghel & Renstrom, 2002). Processing of wet, pressed agricultural pulps requires approximately 2900 kJ/kg of water removed (Mujumdar, 2006), and the assumption made for this study is that this is an appropriate number to use for the pre-treatment of wheat straw, for the moisture content prior to SS processing is 70-80%. Table 4.2 shows the energy consumed during the SS processing for each of the treatments. Steam explosion, by contrast, consumes approximately 1800 kJ/kg of biomass (Zhu, et al., 2010), (Zhu & Pan, 2010).

Similarly to the methodology used in SS processing, steam explosion occurs in 2 steps, the first being an acid impregnation to catalyze delignification. In order to achieve 80% of theoretical ethanol conversion from wheat straw, the raw material was soaked in 0.9% w/w H_2SO_4 at 45˚C for 18 hours prior to steam explosion (Ballesteros, et al., 2006). The

corresponding step in SS pre-treatment is soaking in hot water at 191 kPa (119˚C) for 15 minutes.

Table 4.2. Energy demand associated with SS treatment

Treatment	Change in moisture content* (kg/kg)	Corresponding energy demand (kJ/kg)
15 min. HW	0	0
15 min. HW + 2 min. SS	0.368	1068
15 min. HW + 5 min. SS	0.611	1772
15 min. HW + 10 min. SS	0.809	2348

HW = hot water treatment

*due to SS processing

In order to develop an estimate for comparison of the magnitude of energy consumption associated with these thermal processes, the severity factor for each shall be considered.

The ratio of severity factors between acid impregnation and hot water prior to SS to steam explosion are 0.42 and 0.52, respectively, so for the purposes of evaluation, it is assumed that the energy expenditure for the treatments are 760 kJ/kg and 930 kJ/kg, respectively.

Power generation from the combustion of excess biomass is assumed to generate energy based on a lower heating value of wheat straw of 16 MJ/kg (Jenkins, et al., 1998), and an electrical conversion efficiency of 25% (Energy and environmental analysis, 2008) and sold back to the grid at 0.04$/kWh (Eggeman & Elander, 2005).

4.4.2 Results and discussion

Referring back to Eq. 4.1, and operating under the assumptions from 4.4.1, an estimate can be put forth for the MESP of ethanol derived from wheat straw using SS and steam explosion for pre-treatment. The assumed price of H_2SO_4 is \$100/ton (\$0.11/kg) (Bout & Shewchuk, 2013). Table 4.3 shows the cost breakdown of the conversion of wheat straw to ethanol using steam explosion and SS pre-treatment based on the assumptions from 4.4.1. All costs are adjusted per unit volume of ethanol produced. The effect of xylose recovery is assumed to produce an additional 0.4 g of ethanol per gram of xylose recovered from the hot water. While the theoretical fermentation yield of xylose based on stoichiometry is 0.51 g ethanol/g xylose, in practice, the observed yields are closer to 0.4g/g (McMillan, 1993). Introduction of xylose recovery is assumed to increase the capital and operating costs by 3%.

Table 4.3. Cost breakdown of ethanol production

Pre-treatment method	**Steam explosion**	**Superheated steam**	**Superheated steam with xylose recovery**
Raw materials	\$0.06	\$0.10	\$0.07
Capital cost	\$0.44	\$0.44	\$0.45
Operating cost	\$0.28	\$0.28	\$0.29
Energy cost*	\$0.22	\$0.30	\$0.22
Other cost**	\$0.01	\$0.00	\$0.00
Energy revenue	\$0.20	\$0.34	\$0.26
MESP	**\$0.80**	**\$0.77**	**\$0.78**

*energy cost is assumed to be \$0.07 / kWh

**cost of H_2SO_4

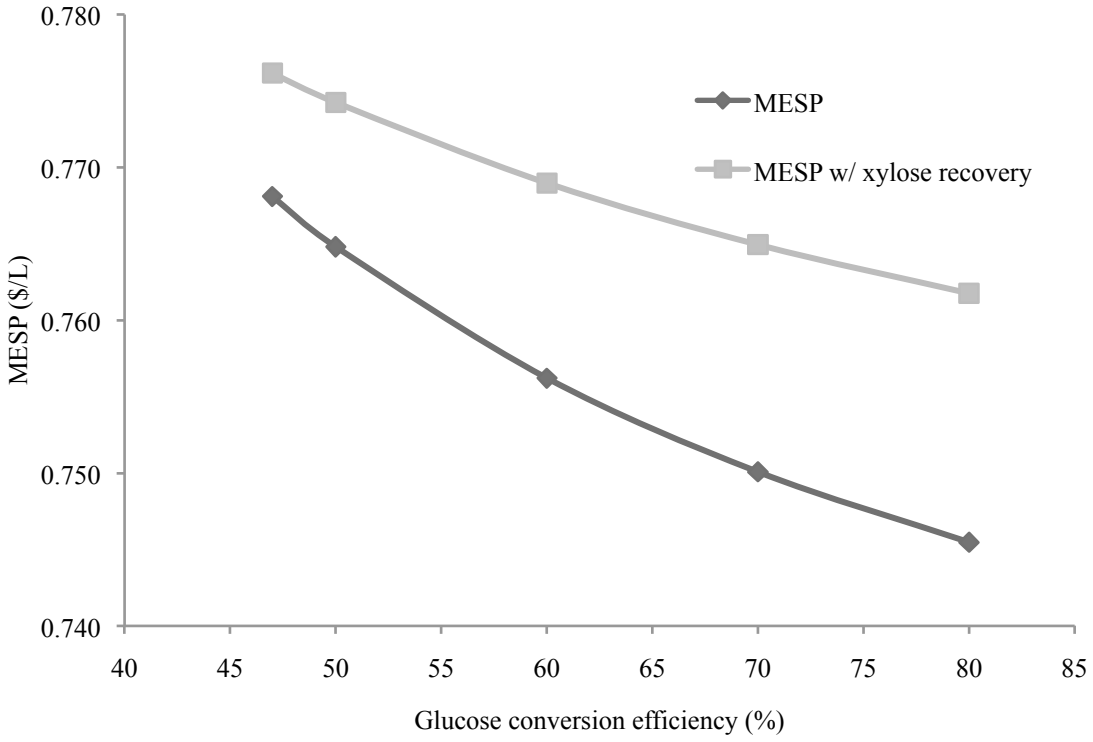

Fig. 4.7. Effect of glucose conversion efficiency on MESP of wheat straw pre-treated with SS with and without xylose recovery

While the MESP of ethanol produced with SS pre-treatment is lower than that using steam explosion, a significant portion is due to the increased revenue associated with the energy generated from excess biomass combustion, a result of the lower glucose conversion efficiency, and consequently, more excess biomass. However, if the efficiency of the pre-treatment increases, under the same assumptions, the MESP would decrease, shown in Figure 4.7. Xylose conversion efficiency is assumed to remain constant.

As the goal of this study was not to conduct a comprehensive economic evaluation of the production of cellulosic ethanol using SS pre-treated wheat straw, the preceding analysis yields a MESP significantly different than many in existing literature (Eggeman &

Elander, 2005) (Tao, et al., 2011). The MESP developed were meant to be used in relative terms, and not absolute (Barchyn & Cenkowski, 2014). The results are, however, conclusive in that they indicate that pre-treatment with SS is not only technically feasible, but produces a similar result in terms of economic viability to existing pre-treatment technologies. More importantly, SS pre-treatment stands to improve the energy efficiency of the pre-treatment process, as it was shown to consume only 78% of the energy of steam explosion pre-treatment per kg of biomass.

Pre-treatment of lignocellulosic wheat straw using SS has similar performance characteristics to developed technologies such as steam explosion in terms of economic viability. Furthermore, it is a promising technology in that it consumes less energy than steam explosion, reducing the energy requirements of the pre-treatment step, which is critical to developing viable cellulosic ethanol biorefineries at an industrial scale. Improvements can be made to the SS pre-treatment in order to improve the overall yield from the biomass, which is still comparatively low with regards to other pre-treatment technologies (Conde-Mejia, Jimenez-Gutierrez, & El-Halwagi, 2012).

4.5 Energy balance

The energy payback associated with biofuel production is generally evaluated in terms of the ratio of energy invested in the processing and conversion of the feedstock to the energy contained in the refined fuel. In the case of ethanol produced from wheat straw, this value has been calculated as 0.94 (Tampier, et al., 2004). This is a ‘negative payback’ in that less energy is obtained from the combustion of the fuel than is consumed producing it. This is at the heart of many arguments against the production of lignocellulosic ethanol at a commercial scale.

Energy expenditures associated with the pre-treatment phase of the processing and refining represent approximately 33% of the total energy invested in the feedstock conversion (Roy, 2014). Significant improvements can therefore be made in the overall process if the pre-treatment is made more energy efficient. If an equivalent, optimized SS pre-treatment method can be implemented with an energy demand of only 78% compared to existing technologies, the energy payback will shift to 1.014, making it a positive payback in terms of energy investment in the process. Further gains stand to be made if the energy utilized in the process is derived from renewable, efficient sources.

4.6 Evacuated tube solar collectors

In principle, at a constant mass flow rate through the system, each evacuated tube terminal would reach an equilibrium temperature and the rate of energy transfer could be calculated from the temperature differential and the condensation rate with the following formula:

$$Q = \overline{m} \times [c_{p,1}\Delta T_1 + \Delta H_{vap} + c_{p,2}\Delta T_2] \qquad [4.2]$$

Where: Q = rate of energy transfer (W)

m = mass flow rate (kg/s)

$c_{p,l}$ = specific heat capacity of liquid water (J/kgK)

ΔT_1 = temperature differential between ambient conditions and the boiling point of water (˚C)

ΔH_{vap} = heat of vaporization of water (J/kg)

$c_{p,v}$ = specific heat capacity of water vapor (J/kgK)

ΔT_2 = temperature differential between the boiling point of water and final steam temperature (˚C)

Once the rate of energy transfer was computed, the result could be compared with the theoretical maximum efficiency of evacuated tube collectors. It is represented by the empirically derived formula (Rai, 1987), (Budihardjo & Morrison, 2009):

$$\eta = 0.536 - 0.8240 \times \frac{(\bar{T} - T_a)}{G} - 0.0069 \times \frac{(\bar{T} - T_a)^2}{G} \qquad [4.3]$$

Where: η = theoretical maximum efficiency of the system (%)

$\bar{T}$ = average temperature in the evacuated tube system

T_a = ambient temperature

G = solar irradiance (W/m^2)

Using equation 4.3, it was predicted that producing SS at 175˚C with an ETSC array would have a theoretical efficiency of 25.1% (Vendan, et al., 2012). This was the level to which the performance of the experimental array was compared.

Once the system achieved steady state, the rate of energy transfer was computed and compared to the radiation to which the aperture of the collector was exposed, using equation 4.2. This analysis generated the data presented in Fig. 4.8, from August 20th, 2013. The observed efficiency was compared to the predicted efficiency (Budihardjo & Morrison, 2009).

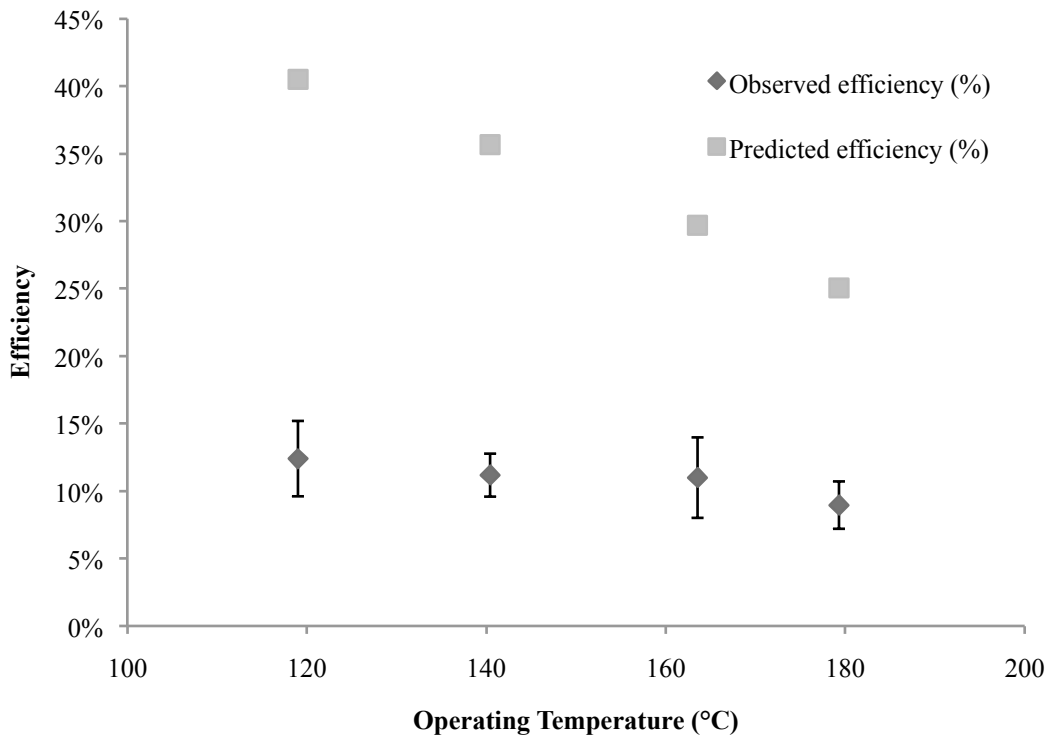

Fig. 4.8. Conversion efficiency at different maximum operating temperatures of working fluid

There is a clear negative correlation between the operating temperature and the energy conversion efficiency. This reflects the relationship predicted in literature, though the observed efficiency is markedly lower than the predicted values.

A decreased efficiency could have arisen as a result of component fatigue following repeated loading at high temperature differentials. At operating temperatures exceeding 200˚C during the first nine loading cycles, component failure occurred in two cases, at 257˚C and 234˚C respectively.

Subsequently, operating temperatures were maintained below 200˚C. However, during the 25th loading cycle, component failure occurred at 178˚C. The trend observed in the

trials during which component failure occurred appeared to follow declining temperatures, which may imply material fatigue as a result of repeated loading at high temperature differentials.

Mode of failure was the rupturing of the inner evacuated tube and consequent shattering of the outer glass shroud of the ETSC. Following failure, the damaged ETCS were no longer operational. Visual inspection of the failed ETSC suggested that failure arose from excessive pressure inside the tube, possibly as a result of elevated operating temperature. The loading cycle and component failure data are presented in Fig. 4.9.

Based on experimental results, it is possible to generate SS at temperatures approaching 180˚C with an ETSC array. As predicted, the efficiency decreases with operating temperature, with the experimental system shown to operate at an efficiency of 12.4% at 119˚C and 8.96% at 179˚C.

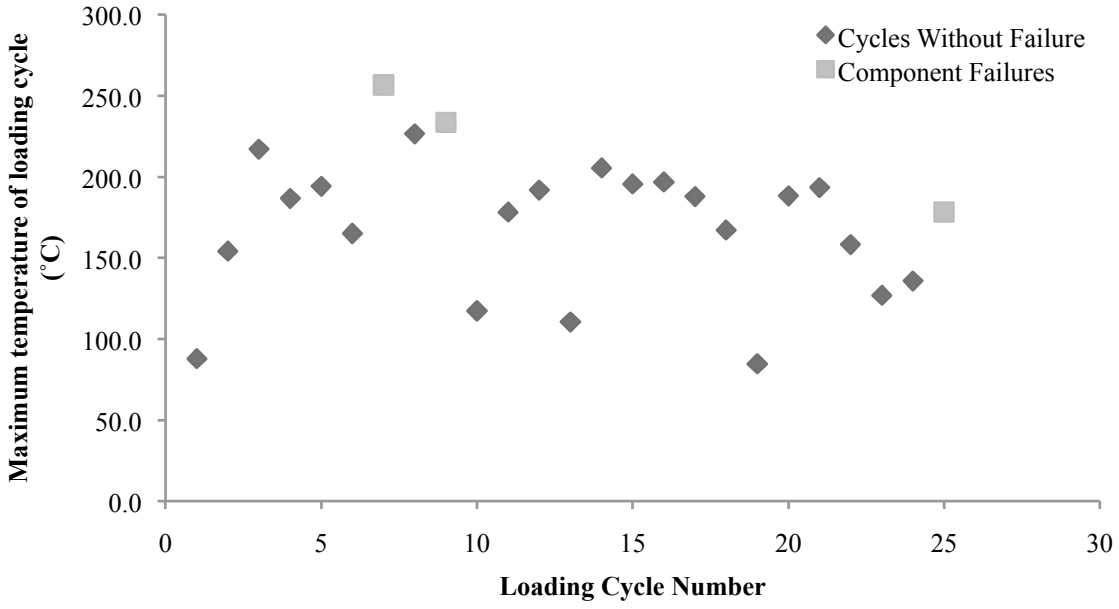

Fig. 4.9. Maximum temperature achieved by the system when component failure occurred

Implementation for industrial-scale use of ETSC for high-quality SS generation may not be feasible however, due to component failure after repeated loading cycles at high temperatures. Three component failures were observed, at 257˚C, 234˚C, and 178˚C, respectively. The diminishing temperature of failure is indicative of potential material fatigue and a result of loading at high temperature differentials, and implementation of an ETSC array into an industrial process stream would need to operate at temperatures below 180˚C.

For this reason, the examination of ETSC for their inclusion in a SS process stream was arrested, in favor of the more promising PTSC technology.

4.7 Parabolic trough solar collector

The variables selected for modeling all exhibited seasonality and stationarity at different differencing periods; the differencing periods (in hours) selected for DNI, temperature, and wind were 24 & 8760, 8760, and 8760, respectively. The complete results of the analysis and output from the SAS ARIMA procedure can be found in Appendix C. The results of the model forecast, along with the corresponding confidence intervals are shown in Figure 4.10.

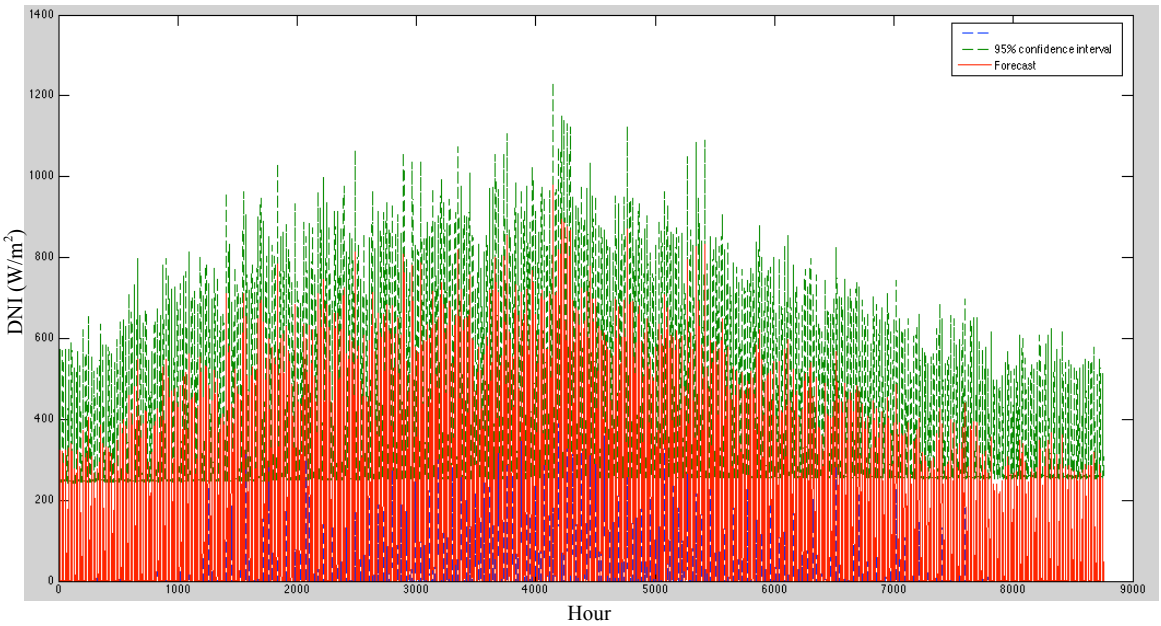

Fig. 4.10(a). Statistical forecast and 95% confidence interval for DNI

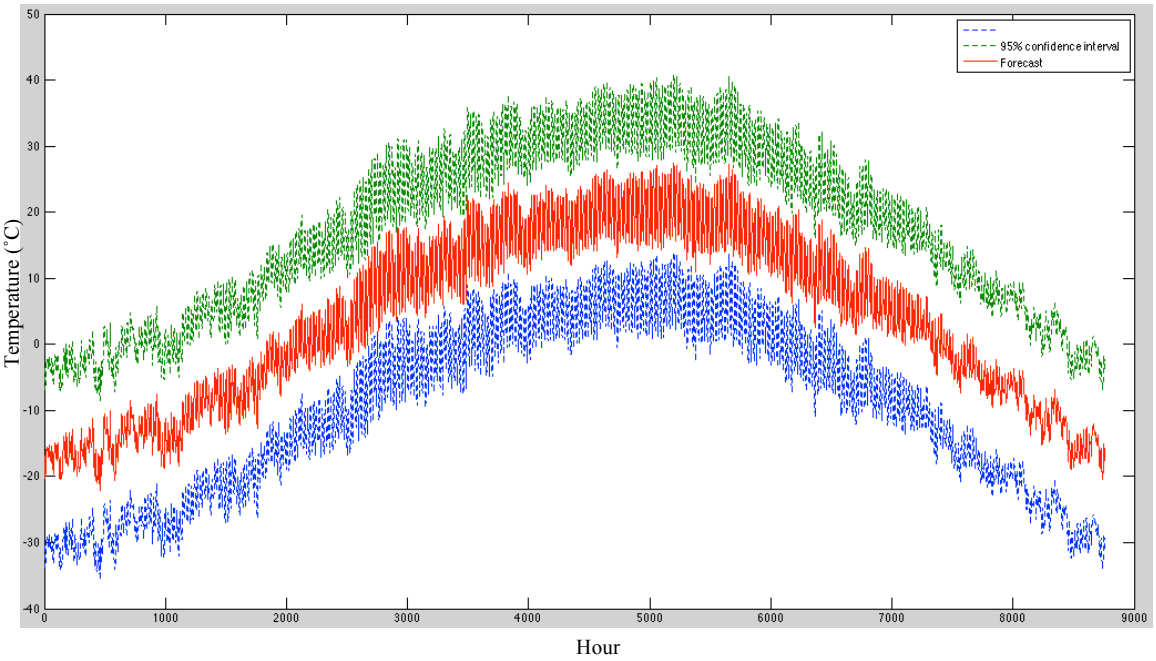

Fig. 4.10(b). Statistical forecast and 95% confidence interval for temperature

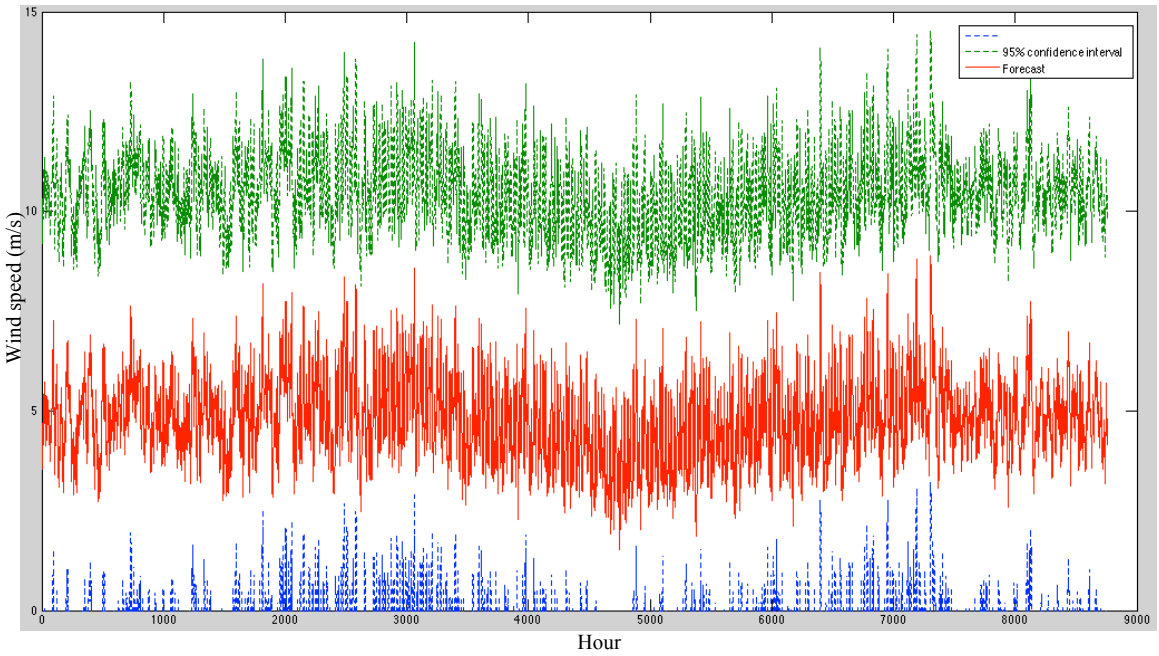

Fig. 4.10(c). Statistical forecast and 95% confidence interval for wind

The numerical simulation was run for steam production at 220˚C at constant mass flow rates of the heat transfer fluid of 2, 3, 4, and 6 kg/s. The purpose of running multiple simulations at different mass flow rates was to determine the optimal flow rate for energy collection, since the scope of this study was inclusive only of fixed-flowrate heat transfer fluid. The rate of energy delivery over the course of one year is shown in Figure 4.11, and the conversion efficiency shown is the ratio of thermal output at 3 kg/s to the total average incident DNI.

The low performance of the PTSC can be attributed to the low ambient temperature during the winter months, coupled with the reduced DNI during these periods. Still, the overall conversion efficiency is much higher than that observed using the ETSC. From Fig. 4.11, it is clear that the optimal mass flowrate of heat transfer fluid lies in the vicinity of 3 kg/s, and the peak conversion efficiency occurs in June. The reason for this is the DNI is highest in June, and the heat transfer fluid flow rate must be low enough to reach

the desired temperature, but sufficiently high to deliver enough energy to the steam generation system.

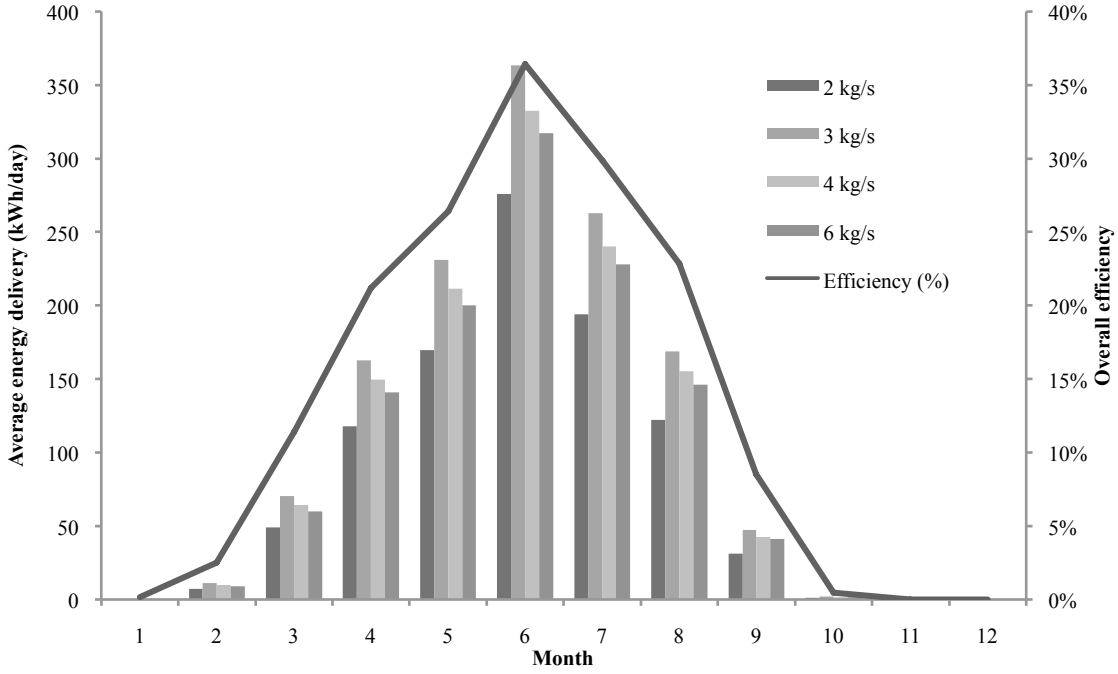

Fig. 4.11. Energy delivery of PTSC system at varying heat transfer fluid flow rates

In order to increase the efficiency of the system, the target temperature can be modified under the assumption that the residual energy required for the generation of SS at the target temperature will be acquired from a grid connection. If the target output temperature of the PTSC system is reduced to 150˚C, the overall efficiency increases, as show in Figure 4.12.

It is clear from Figs. 4.11 & 4.12 that operation of a PTSC system year-round is not necessarily realistic; the low efficiencies encountered due to high temperature differentials in the winter months affect the economy of the PTSC system.

A comprehensive study published by NREL (2003) of the economics of implementation for concentrating solar thermal energy technologies enumerates several components for which costs must be considered. Shown in Table 4.4, these values will be used to assess the operational configuration of the simulated PTSC (Sargent & Lundy, 2003). The costs shown are for a PTSC facility with a net power capacity of 150MWe, and 12 hours of available thermal storage.

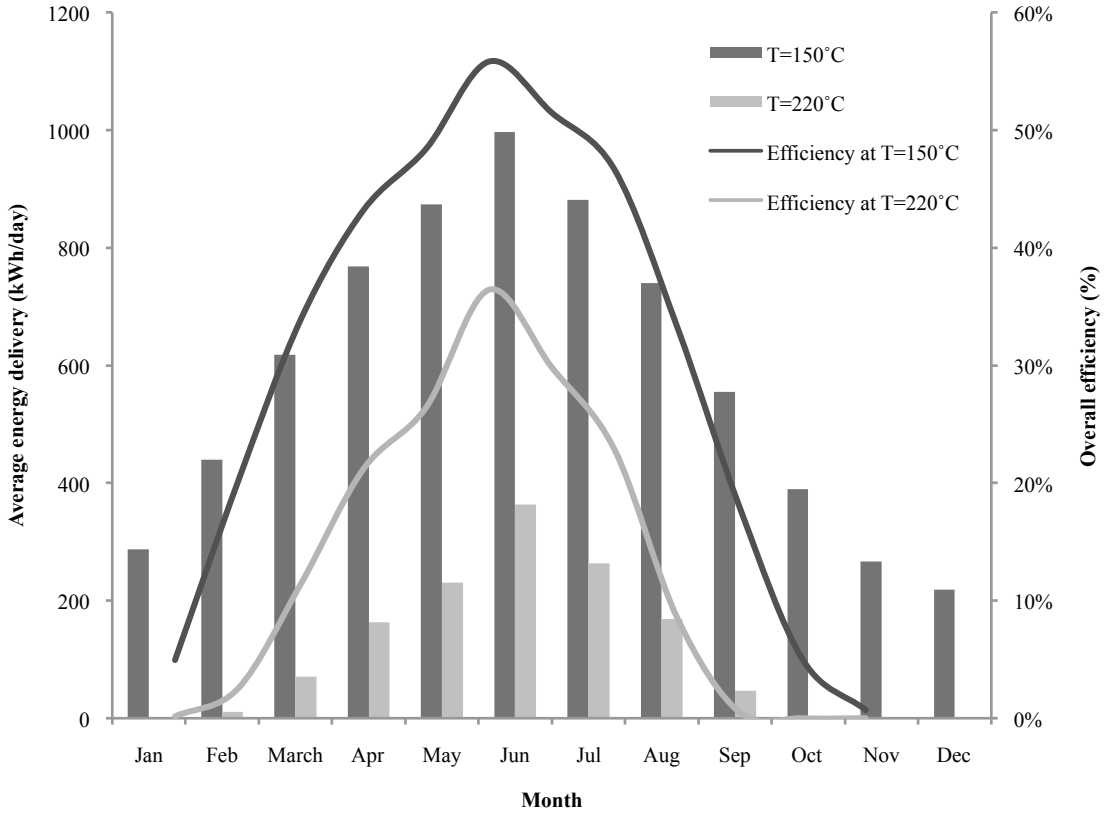

Fig. 4.12. Average energy delivery of a PTSC system operating at 150˚C and 220˚C

Table 4.4. Capital cost breakdown of PTSC components

Component	Fraction of total	Cost	Unit
Solar Collection System	**58%**	**$161.88**	**/m^2**
Receiver	12%	$28.00	/m^2
Mirror	11%	$28.00	/m^2
Support Structure	17%	$55.00	/m^2
Drive	3%	$9.54	/m^2
Piping	5%	$12.72	/m^2
Electronics & Control	4%	$11.13	/m^2
Pylon Foundations	2%	$6.36	/m^2
Heat Transfer Fluid	2%	$4.77	/m^2
Civil Works	2%	$6.36	/m^2
Thermal Storage System	**23%**	**$958.00**	**/kWe**
Power Block	**14%**	**$293.00**	**/kWe**
Steam Generation	**3%**	**$62.79**	**/kWe**
Structures and Improvements	**2%**	**$5.58**	**/m^2**

In order to appropriately scale the costs of a PTSC facility with respect to the capacity, a scaling equation [4.4] is introduced (Sargent & Lundy, 2003), expressed as follows:

$$\$B = \$A \times (B_{MW}/A_{MW})^{Sf} \qquad [4.4]$$

where B is larger than A,

$B = cost of plant B

$A = cost of plant A

B_{MW} = capacity of plant B, in MW

A_{MW} = capacity of plant A, in MW

Sf = scaling factor

The scaling factor is assumed to lie between 0.6 and 0.8, so for the purposes of this study, it is approximated as 0.7 (Sargent & Lundy, 2003). Using this approach, the cost of the simulated PTSC system can be estimated. Since the power generation capacity is not

necessarily representative of the size of the plant (the plants evaluated by Sargent & Lundy are used for electrical generation, and operate at higher temperatures), the costs associated with the simulated plant will be assumed to be comparable to a 30 kWe facility of approximately the same field size. Thermal output is assumed to scale proportionally with electrical power output, and the ratios still applicable to the scaling equation.

Operation and maintenance (O&M) costs are assumed to increase with the exclusion of thermal storage due to a decrease in the capacity factor of the plant, resulting in an increase in plant size. The electric conversion efficiency of the steam turbines studied by Sargent & Lundy (2003) was between 32 and 42.5%. This study will use a gross steam cycle efficiency of 37.5% to formulate an estimate for the relative power output for a PTSC plant designed for thermal output. Therefore, a 1 MW_e plant will be treated as equivalent to a 2.67 MW_{th} for the purposes of estimating O&M costs. The O&M costs were approximated as \$0.0278/kWh_e or \$0.0104/kWh_{th} (Sargent & Lundy, 2003).

4.7.1 Integration of solar thermal energy

For the integration of solar thermal energy to be feasible, it must supply energy at a price competitive with the utility. For the purposes of this study, the cost of electrical energy is assumed to be \$0.0718/kWh, and the cost of thermal energy as natural gas \$0.021/kWh (Manitoba Hydro, 2014). To properly assess the economy of scale, equation 4.3 was applied to the PTSC facility using the simulated thermal power generation at 150 and 220˚C. An assumed payback period of 30 years is used for the lifetime of the system (Sargent & Lundy, 2003), as well as a discount rate of 10% and an O&M cost escalation of 2%. The levelized energy costs associated with the plant scale-up are shown in Figure

4.13. It is assumed that the facility can operate year-round at 150˚C, and 8 months per year at 220˚C.

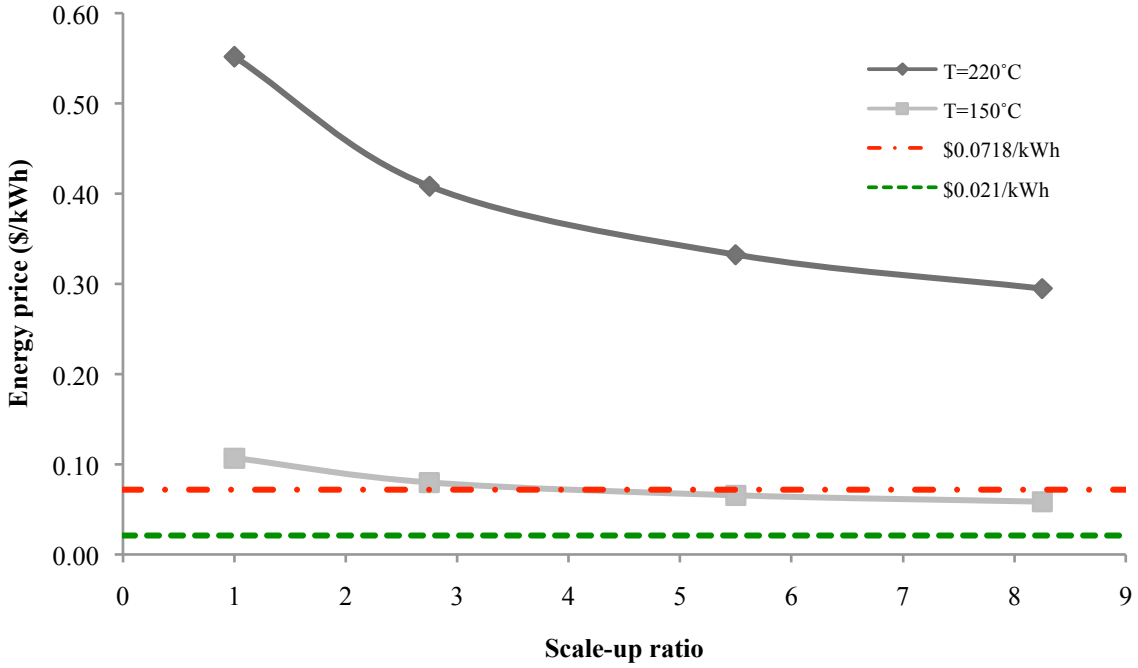

Fig. 4.13. Levelized cost of energy produced by a PTSC facility

Unsurprisingly, the PTSC facility operating at 150˚C generates energy at a much cheaper rate relative to the facility operating at 220˚C. If we return to the assumptions made in Section 4.4, a prospective ethanol production facility with a capacity of 50M gal/year would consume approximately 324 GWh_{th}/year for pre-treatment, corresponding to approximately 889 MWh/day. If the operator wished to displace 100% of this energy using the PTSC facility during peak operating time, a field aperture area of 37.3 ha or 13.6 ha would be required for operation at 220 or 150˚C, respectively. Even so, due to the annual variation in power production from the PTSC, this would only represent a total energy displacement of 30.4 or 58.9%, respectively. Depending on the available space on the site and the budget of the project, this may or may not be feasible. Table 4.5 shows

the budget and space requirements, as well as the resulting effective cost of energy associated with displacing different amounts of energy with a PTSC facility.

Table 4.5. Cost, energy displacement, and effective price of energy for integration of a PTSC facility

% of energy supplied at peak production	Temperature (˚C)	Capital cost ($ millions)	Total energy displaced (%)	Required field aperture area (ha)	Effective price of energy ($/kWh)
	220	$31.07	3.04%	3.73	$0.109
10%	150	$15.33	5.89%	1.36	$0.031
	220	$50.47	6.08%	7.47	$0.089
20%	150	$24.90	11.79%	2.72	$0.026
	220	$67.04	9.12%	11.20	$0.080
30%	150	$33.07	17.68%	4.08	$0.023
	220	$95.86	15.19%	18.67	$0.069
50%	150	$47.28	29.46%	6.80	$0.020
	220	$127.32	22.79%	28.00	$0.061
75%	150	$62.80	44.20%	10.20	$0.019
	220	$155.72	30.39%	37.34	$0.057
100%	150	$76.81	58.93%	13.60	$0.017

Denotes prices competitive with electricity

Denotes prices competitive with natural gas

From Table 4.5, it is clear that on this scale, the price of energy achieved through the integration of a PTSC facility can be competitive with electricity, but is only competitive with natural gas at the largest scales. Furthermore, operation at 220˚C is not only more costly, but does not reach energy prices competitive with natural gas, even at the largest scales. Additionally, the capital costs associated with the construction of the facility represent a large fraction of the capital cost of the ethanol plant itself, in some cases

exceeding it entirely. This would double the initial capital costs of the integrated facility, making this option even less attractive.

The superior technology for producing SS in the context of biomass processing is PTSC, which achieves significantly higher conversion efficiencies when compared to ETSC (55.8% vs 11.2%). The integration of a PTSC facility, while costly, has the potential to produce energy at a competitive cost to both electricity and natural gas, reaching unit energy prices as low as $0.017/kWh. This increase in cost however, is prohibitive for new developments, and the integration of a PTSC facility could likely only be undertaken when near unlimited capital was available, or the integration took place in an existing facility where the only capital associated with the project was for the PTSC array with the goal of improving the renewable energy ratio of the operation.

5. Conclusion

The results of this study indicate that the conversion of lignocellulosic wheat straw to bioethanol can benefit from pre-treatment using SS. A 2-step pre-treatment method using first pressurized hot water at 119˚C for 15 minutes followed by SS at 220˚C yielded the best results, with the most pronounced effect on sugar liberation occurring after 2 minutes of SS. The pre-treatment followed by enzymatic hydrolysis resulted in net sugar conversion efficiencies of 46.4 and 53.5% for glucose and xylose, respectively. The glucose was recovered from the treated biomass, while the majority of the xylose was recovered from the supernatant. With an energy demand of approximately 1998 kJ/kg of biomass, pre-treatment with SS consumes approximately 78% as much energy as steam

explosion, and can produce ethanol at a comparable price, based on a preliminary economic evaluation.

The integration of solar energy into a SS process stream depends on the technology used to collect the energy as well as the temperature of operation. Utilization of ETSC was found not to be feasible for high-temperature applications due to low conversion efficiency (<12%) and progressive component failure at temperatures in excess of 175˚C. More promise was found with PTSC, which had peak conversion efficiencies of 36.4 and 55.8% at operating temperatures of 220 and 150˚C, respectively.

Experimental results based on simulation, indicate that on a large scale, a PTSC facility is capable of generating energy at a rate competitive with conventional energy sources (<$0.021/kWh), though the capital expenditures are substantial, if not prohibitive.

Acknowledgments

The author would like to recognize the support of BioFuelNet Canada in the preparation of this work.

Further acknowledgement to:

Dale Bourns – Technician, Biosystems Engineering

Robert Lavallee – Technician, Biosystems Engineering

Matt McDonald – Technician, Biosystems Engineering

Peter Hildebrand – Technician, Biosystems Engineering

Faezeh Mosallat –Ph.D. Candidate, Mechanical Engineering

References

AAFCO. (2009). *Procedures manual.* Association of American Feed Control Officials, Inc. AAFCO.

Agarwal, A., & Das, L. (2001). Biodiesel Development and Characterization for use as a Fuel in Compression Ignition Engines. (A. S. Engineers, Ed.) *Journal of Engineering for Gas Turbines and Power , 123* (2), 440-447.

Agbor, V., Cicek, N., Sparling, R., Berlin, A., & Levin, D. (2011). Biomass pretreatment: Fundamentals toward application . *Biotechnology Advances* , 675-685.

Al-Hasan, M. (2003). Effect of Ethanol–unleaded Gasoline Blends on Engine Performance and Exhaust Emission. *Energy Conversion and Management* (44), 1547-1561.

Alvira, P., Tomas-Pejo, E., Ballesteros, M., & Negro, M. (2010). Pretreatment technologies for an efficient bioethanol production process based on enzymatic hydrolysis: a review. *Bioresource technology* , 4851-4861.

AOAC. (2011). Official Methods. *Journal of AOAC International* .

Argonne National Laboratory. (2010). *Greenhouse Gases, Regulated Emissions, and Energy Use in Transportation (GREET) Model, version 1.7.* Chicago, IL: Argonne National Laboratory.

Babcock and Wilcox Company. (2007). Superheated steam. In Babcock, & Wilcox, *Steam: its generation and use* (pp. 137-146). Gutenberg.

Balat, M. (2011). Production of Bioethanol from Lignocellulosic Materials via the Biochemical Pathway: A Review. *Energy Conversion and Management* (52), 858-875.

Ballesteros, I., Negro, M. J., Olivia, J., Cabanas, A., Manzanares, P., & Ballesteros, M. (2006). Ethanol production from steam-explosion pretreated wheat straw. *Applied biochemistry and biotechology , 129-132*, 496-508.

Barchyn, D., & Cenkowski, S. (2014). Process analysis of superheated steam pre-treatment of wheat straw and its relative effect on ethanol selling price. *Biofuel research journal , 4*, 123-128.

Beltrame, P., Carniti, P., Visciglio, A., Focher, B., & Marzetti, A. (1992). Fractionation and bioconversion of steam-exploded wheat straw. *Bioresource technology , 39*, 165-171.

Berghel, J., & Renstrom, R. (2002). Basic design criteria nad corresponding results performance of a pilot-scale fluidized superheated atmospheric condition steam dryer. *Biomass and bioenergy , 23*, 103-112.

Bjerre, A., Olesen, A., Fernqvist, T., Ploger, A., & Schmidt, A. (1996). Pretreatment of wheat straw using combined wet oxidation and alkaline hydrolysis resulting in convertible cellulose and hemicellulose. *Biotechnology and bioengineering , 49*, 568-577.

Bout, J., & Shewchuk, S. (2013). *2013 Agriculture, chemical and fertilizer outlook.* Toronto, Canada.

Bradshaw, M. (2014). *Global energy dilemmas.* Cambridge, UK: Polity Press.

Brodeur, G., Yau, E., Badal, K., Collier, J., Ramachandran, K., & Ramakrishnan, S. (2011). Chemical and physiochemical pretreatment of lignocellulosic biomass: a review. *Enzyme Research* , 1-18.

Budihardjo, I., & Morrison, G. (2009). Performance of water-in-glass evacuated tube water heaters. *Solar Energy* , 49-56.

Cambidge Energy Research Associates (CERA). (2006, 11 14). CERA Says Peak Oil is Faulty. *Energy Bulletin* . Cambridge, Massachusetts, United States: CERA.

Cenkowski, S., Pronyk, C., Zmidzinska, D., & Muir, W. (2007). Decontamination of food products with superheated steam. *Journal of food engineering* (83), 68-75.

Chang, V., Nagwani, M., & Holtzapple, M. (1998). Lime pretreatment of crop residues bagasse and wheat straw. *Applied biochemistry and biotechnology - Part A: Enzyme engineering and biotechnology , 74*, 135-159.

Conde-Mejia, C., Jimenez-Gutierrez, A., & El-Halwagi, M. (2012). A comparison of pretreatment methods for bioethanol production from lignocellulosic materials. *Process safety and environmental protection , 90*, 189-202.

Currie, D., Herring, C., Guss, A., Olson, D., Hogsett, D., & Lynd, L. (2013). Functional heterologous expression of an engineered full length CipA from Clostridium thermocellum in Thermoanaerobacterium saccharolyticum. *Biotechnology for Biofuels , 6* (32).

Eggeman, T., & Elander, R. (2005). Process and economic analysis of pretreatment technologies. *Bioresource technoogy , 96*, 2019-2025.

Energy and environmental analysis. (2008). *Technology characterization: steam turbines.* Environmental protection agency, Combined heat and power partnership. Washington, DC: USEPA.

Environment Canada. (2003). *Canadian weather energy and engineering data sets.* Meteorological service of Canada. National Research Council of Canada.

Fan, L., Gharpuray, M., & Lee, Y. (1987). *Cellulose Hydrolysis.* Berlin, Germany: Springer-Verlaug.

Fernandez-Garcia, A., Zarza, E., Valenzuela, L., & Perez, M. (2010). Parabolic trough solar collectors and their applications. *Renewable and sustainable energy reviews , 14*, 1695-1721.

Forrestal, R. (2003). *Heat Transfer Analysis and Modeling of a Parabolic Trough Solar Receiver Implemented in Engineering Equation Solver* . NREL. Golden, Colorado: U.S. Department of Energy.

Galbe, M., & Zacchi, G. (2002). A Review of the production of Ethanol from Softwood. *Applied Microbiology and Biotechnology* (59), 618-628.

Gallagher, P., Brubaker, H., & Shapouri, H. (2005). Plant size: capital cost relationships in the dry mill ethanol industry. *Biomass and bioenergy , 28* (6), 565-571.

Green, M. A., Emery, K., Hishikawa, Y., Warta, W., & Dunlop, E. D. (2014). Solar cell efficiency tables (version 43). *Progress in photovoltaics: research and applications* (22), 1-9.

Gregg, D., & Saddler, J. (1996). A techno-economic assessment of the pretreatment and fractionation steps in a biomass-to-ethanol process. *Applied biochemistry and biotechnology* , 711-727.

Grigg, J. (2002). The Health Effects of Fossil Fuel Derived Particles. *Archives of Disease in Childhood , 86* (2), 79-83.

Hendricks, A., & Geeman, Z. (2009). Pretreatments to Enhance the Digestibility of Lignocellulosic Biomass. *Bioresource Technology* (100), 10-18.

Hill, J., Nelson, E., Tilman, D., Polasky, S., & Tiffany, D. (2006). Environmental, economic, and energetic costs and benefits of biodiesel and ethanol biofuels. *Proceedings of the National Academy of Sciences of the United States of America , 103* (30), 11206–11210.

Hinotani, K., Kanatani, K., & Osumi, M. (1979). An evacuated glass tube collector and its application to a solar cooling, heating and hot water supply system for the hospital at Kinki University. *Solar Energy , 22* (6), 535-545.

Horn, S., Nguyen, Q., Westereng, B., Nilsen, P., & Eijsink, V. (2011). Screening of Steam Explosion Conditions for Glucose Production from Non-impregnated Wheat Straw. *Biomass and Bioenergy* (35), 4879-4886.

Incropera, F., & DeWitt, D. (2002). *Fundamentals of mass and heat transfer* (5th ed.). John Wiley & Sons.

International Energy Agency. (2012). *2012 Key World Energy Statistics.* Organization for Economic Co-operation and Development. Paris: I.E.A.

International Transport Forum. (2009). *Reducing Transport GHG Emissions.* OECD. OECD/ITF.

Jönsson, L., Alriksson, B., & Nilvebrant, N.-O. (2013). Bioconversion of Lignocellulose: Inhibitors and Detoxification. *Biotechnology for Biofuels , 6* (16).

Jenkins, B., Baxter, L., Miles, T. J., & Miles, T. (1998). Combustion properties of biomass. *Fuel processing technology , 54*, 17-46.

Kalogirou, S. A. (2004). Solar thermal collectors and applications. *Progress in energy and combustion science* (30), 231-295.

Kalogirou, S. (2003). The potential of solar industrial process heat applications. *Applied Energy , 76*, 337-361.

Kaparaju, P., & Felby, C. (2010). Characterization of lignin during oxidative and hydrothermal pre-treatment of wheat straw and corn stover. *Bioresource technology* , 3175-3181.

Karl, T., & Trenberth, K. (2003). Modern Global Climate Change. *Science , 302* (5651), 1719-1723.

Kaylen, M., VanDyne, D., Choi, Y., & Blase, M. (2000). Economic feasibility of producing ethanol from lignocellulosic feedstocks. *Bioresource technology , 72* (1), 19-32.

Kennedy, C. (2002). *Review of mid- to high- temperature solar selective absorber materials.* NREL, Golden, CO.

Kim, S., & Dale, B. (2004). Global Potential Bioethanol Production from Wasted Crops and Crop Residues. *Biomass and Bioenergy* (26), 361-375.

Kootstra, A., Beeftink, H., Scott, E., & Sanders, J. (2009). Comparison of dilute mineral and organic acid pretreatment for enzymatic hydrolysis of wheat straw. *Biochemical engineering journal , 46*, 126-131.

Koppelaar, R. (2005). *World Oil Production and Peaking Outlook.* Peak Oil Netherlands Foundation.

Kumar, R., Hu, F., Hubbell, C., Ragauskas, A., & Wyman, C. (2013). Comparison of Laboratory Delignification Methods, their Selectivity, and Impacts on Physiochemical Characteristics of Cellulosic Biomass. *Bioresource Technology* (130), 372-381.

Lawther, J. M., Sun, R., & Banks, W. (1995). Extraction, fractionation, and characterization of structural polysaccharides from wheat straw. *Journal of agriculture and food chemistry , 43*, 667-675.

Li, J., Henriksson, G., & Gellerstedt, G. (2007). Lignin Depolymerization/Repolymerization and its Critical Role for Delignification of Aspen Wood by Steam Explosion. *Bioresource Technology* (98), 3061–3068.

Lin, Y., & Tanaka, S. (2006). Ethanol Fermentation from Biomass Resources: Current State and Prospects. *Applied Mibrobiology and Biotechnology* (69), 627-642.

Lloyd, T., & Wyman, C. (2005). Combined sugar yields for dilute sulfuric acid pretreatment of corn stover followed by enzymatic hydrolysis of the remaining solids. *Bioresource technology , 96*, 1967-1977.

Lynd, L., VanZyl, W., McBride, J., & Laser, M. (2005). Consolidated bioprocessing of cellulosic biomass: an update. *Current opinion in biotechnology , 16* (5), 577-583.

Manitoba Hydro. (2014). NFAT Review. *Load Forecast & DSM* . Winnipeg, Manitoba, Canada.

McGehee, M. D. (2013). Materials Science: Fast-track solar cells. *Nature , 501*, 323-325.

McMillan, J. (1993). *Xylose fermentation to ethanol: a review.* Golden, CO: NREL.

Mekhilef, S., Saidur, R., & Safari, A. (2011). A review on solar energy use in industries. *Renewable and sustainable energy reviews* , 1777-1790.

Metz, B., Davidson, O., Bosch, P., & Dave, R. (2007). *Contribution of Working Group III to the Fourth Assessment Report of the Intergovernmental Panel on Climate Change, 2007.* Cambridge University. Cambridge: Cambridge University Press.

Mihaela, M., & Meghea, I. (2011). Box Jenkins methodology applied to the environmental monitoring data. *Applied sciences , 13*, 74-81.

Mills, D. (2004). Advances in solar thermal energy. *Solar Energy* , 19-31.

Mosallat, F., & Bibeau, E. (2014). Internal communication, University of Manitoba, Winnipeg.

Mosier, N., Wyman, C., Dale, B., Elander, R., Lee, Y. Y., Holtzapple, M., et al. (2005). Features of Promising Technologies for Pretreatment of Lignocellulosic Biomass. *Bioresource Technology* (93), 673-686.

Mosier, N., Wyman, C., Dale, B., Elander, R., Lee, Y., Holtzapple, M., et al. (2005). Features of promising technologies for pretreatment of lignocellulosic biomass. *Bioresource technology* , 673-686.

Mujumdar, A. (2006). Superheated steam drying. In A. Mujumdar, *Handbook of industrial drying* (pp. 421-432). Boca Raton, FL: Taylor & Francis.

National Research Council. (2010). *Advancing the science of climate change.* Board on Atmospheric Sciences and Climate, Division of Earth and Life Sciences. Washington, D.C., United States: National Academies Press.

Ngo, T. H. (2013). *The box-jenkins methodology for time series models.* SAS Global Forum, Statistics and Data Analysis. Burbank, California: Warner Bros. Entertainment.

Overend, R., & Chornet, E. (1987). Fractionation of Lignocellulosics by Steam- Aqueous Pretreatments. *Philosophical Transactions of the Royal Society* (321), 523–536.

Pedersen, M., & Meyer, A. (2009). Influence of substrate particle size and wet oxidation on physical surface structures and enzymatic hydrolysis of wheat straw. *Biotechnology progress , 25*, 399-408.

Perez, J., Ballesteros, I., M., B., Suez, F., Negro, M., & Manzanares, P. (2008). Optimizing liquid hot water pretreatment conditions to enhance sugar recovery from wheat straw for fuel ethanol production. *Fuel , 87*, 3640-3647.

Pimental, D. (2003). Ethanol fuels: energy balance, economics, and environmental impacts are negative. *Natural resources research , 12* (2), 127-134.

Pimentel, D. (2003). Ethanol Fuels: Energy Balance, Economics, and Environmental Impacts are Negative. *Natural Resources Research , 12* (2), 127-134.

Prairie Practitioners Group. (2008). *Final report: straw procurement business case.* Winnipeg, Manitoba, Canada: PPG.

Pronyk, C., Cenkowski, S., & Muir, W. (2004). Drying Foodstuffs with Superheated Steam. *Drying technology , 22* (5), 899-916.

Pytlinski, J. (1978). Solar installations for pumping irrigation water. *Solar energy , 21*, 255-258.

Rai, G. (1987). *Solar Energy Utilization* (3 ed.). Khanna Publishers.

Rehnlund, B. (2004). *Blending of Ethanol in Gasoline for Spark Ignition Engines.* Contribution of Working Group III to the Fourth Assessment Report of the Intergovernmental Panel on Climate Change, 2007.

Roy, P. (2014). *Life cycle assessment of ethanol produced from lignocellulosic biomass: techno-economic and environmental evaluation.* University of Guelph, Guelph, ON.

Saha, B., Iten, L., Cotta, M., & Wu, Y. (2005). Dilute acid pretreatment, enzymatic saccharification and fermentation of wheat straw to ethanol . *Processes in Biochemistry , 40*, 3693-3700.

Sanchez, O., Sierra, R., & Almeciga-Diaz, C. (2011). Delignification Process of Agro-Industrial Wastes an Alternative to Obtain Fermentable Carbohydrates for Producing Fuel. In D. M. Manzanera (Ed.), *Alternative Fuel* (pp. 111-154). In-Tech.

Sargent & Lundy. (2003). *Assessment of parabolic trough and power tower solar technology cost and performance forecasts.* United States Department of Energy, NREL. Golden, CO: NREL.

Schell, D., Torget, R., Power, A., Walter, P., Grohmann, K., & Hinman, N. (1991). A technical and economic analysis of acid-catalyzed steam explosion and dilute acid pretreatments using wheat straw and aspen wood chips. *Applied biochemistry and biotechnology , 28/29*, 87-97.

Schnitzer, H., Christoph, B., & Gwehenberger, G. (2007). Minimizing greenhouse gas emissions through the application of solar thermal energy in industrial processes. *Journal of cleaner production , 15*, 1271-1286.

Selig, M., Weiss, N., & Ji, Y. (2008). *Enzymatic saccharification of lignocellulosic biomass.* NREL. Golden, CO: NREL.

Shapouri, H., Duffield, J., & Wang, M. (2002). The energy balance of corn ethanol: an update. *Agricultural economic report* .

Sims, R., Taylor, M., Saddler, J., & Mabee, W. (2008). *From 1st to 2nd Generation Biofuels.* International Energy Agency, Global Bioenergy Partnership. OECD/IEA.

Soloman, B., Barnes, J., & Halvorsen, K. (2007). Grain and cellulosic ethanol: history, economics, and energy policy. *Biomass and bioenergy , 31*, 416-425.

Solutia. (1998). *Therminol 66 high performance highly stable heat transfer fluid.* St Louis, MO: Solutia.

Sun, R., Lawther, J. M., & Banks, W. (1996). Fractional and structural characterization of wheat straw hemicellulose. *Carbohydrate polymers* , 325-331.

Sun, Y., & Jiayang, C. (2002). Hydrolysis of Lignocellulosic Materials for Ethanol Production: A Review. *Bioresource Technology* (83), 1-11.

Swedish Energy Agency. (2010). *Energy in Sweden - Fact and Figures 2010.* Swedish Energy Agency.

Tabil, L., Adapa, P., & Kashaninejad, M. (2011). Biomass Feedstock Pre-processing - Part 1: Pretreatment. In D. M. Bernardes (Ed.), *Biofuel's Engineering Process Technology* (pp. 411-437). Rijeka, Croatia: In-Tech.

Talebnia, F., Karakashev, D., & Angelidaki, I. (2010). Production of bioethanol from wheat straw: an overview on pretreatment, hydrolysis and fermentation. *Bioresource Technology , 101*, 4744-4753.

Tampier, M., Smith, D., Bibeau, E., & Beauchemin, P. (2004). *Stage 2 report: life-cycle GHG emission reduction benefits of selected feedstock-to-product threads.* Envirochem Services, Inc. North Vancouver, BC: Natural Resources Canada.

Tao, L., Aden, A., Elander, R., Pallapolu, V., Lee, Y., Garlock, R., et al. (2011). Process and technoeconomic analysis of leading pretreatment technologies for lignocellulosic ethanol production using switchgrass. *Bioresource technology , 102*, 11105-11114.

Taylor, J. (2009). An Economic Critique of Corn Ethanol Subsidies. *Federal Reserve Bank of St Louis, Regional Economic Development , 5* (1), 78-97.

Thirugnanasambandam, M., S., I., & Ranko, G. (2010). A review of solar thermal technologies. *Renewable and sustainable energy reviews , 14*, 312-322.

Thorsell, S., Epplin, F., Huhnke, R., & Taliaferro, C. (2004). Economics of a coordinated biorefinery feedstock harvest system: lignocellulosic biomass harvest cost. *Biomass and bioenergy , 27*, 327-337.

Urbanchuk, J. (2006). *Contribution of the ethanol industry to the economy of the United States.* Renewable fuels association, Washington, DC.

Vasudevan, P., & Briggs, M. (2008). Biodiesel Production - Current State of the Art and Challenges. *Society for Industrial Microbiology* (35), 421-430.

Vendan, S., Shunmuganathan, L., Manojkumar, T., & Shiva Thanu, C. (2012). Study on Design of an Evacuated Tube Solar Collector for High Temperature Steam Generation. *International Journal of Emerging Technology and Advanced Engineering , 2* (12), 539-541.

von Blottnitz, H., & Curran, M. (2007). A review of assessments conducted on bio-ethanol as a transportation fuel from a net energy, greenhouse gas, and environmental life cycle perspective. *Journal of cleaner production , 15*, 607-619.

Walsh, M. (1998). U.S. bioenergy crop economic analyses: status and needs. *Biomass and bioenergy , 14* (4), 341-350.

Weil, J., Sarikaya, A., Rau, S., Goetz, J., Ladisch, C., Brewer, M., et al. (1998). Pretreatment of corn fibre by pressure cooking in water. *Applied biochemistry and biotechnology , 73*, 1-17.

Wyman, C. (2007). What is (and is not) vital to advancing cellulosic ethanol. *Trends in biotechnology , 25* (4), 153-157.

Zambolin, E., & Del Col, D. (2010). Experimental analysis of thermal performance of flat plate and evacuated tube solar collectors in stationary standard and daily conditions. *Solar Energy , 84* (8), 1382-1396.

Zhu, J., & Pan, X. (2010). Woody biomass pretreatment for cellulosic ethanol production: Technology and energy consumption evaluation. *Bioresource technology* , 4992-5002.

Zhu, W., Zhu, J., Gleisner, R., & Pan, X. (2010). On energy consumption for size-reduction and yields from subsequent enzymatic saccharification of pretreated lodgepole pine. *Bioresource technology* , 2782-2792.

Zittel, W., & Schindler, J. (2007). *Crude Oil, The Supply Outlook.* Ottobrunn: Energy Watch Group.

Appendix A. HPLC output for SS pre-treatment

Treatment	Glucose (HPLC output)	Xylose (HPLC output)	Glucose concentration (mM, 1/10 dilution)	Xylose concentration (mM, 1/10 dilution)	Glucose concentration (mM)	Xylose concentration (mM)
Raw Biomass	408802	124828	3.721218	1.24228	37.21218	12.4228
Raw Biomass	410227	125202	3.734043	1.24602	37.34043	12.4602
10SS	324048	81847	2.958432	0.81247	29.58432	8.1247
10SS	327383	82152	2.988447	0.81552	29.88447	8.1552
10SS	315321	79378	2.879889	0.78778	28.79889	7.8778
10SS	318820	80091	2.91138	0.79491	29.1138	7.9491
20SS	296387	75645	2.709483	0.75045	27.09483	7.5045
20SS	296581	75570	2.711229	0.7497	27.11229	7.497
20SS	290070	76566	2.65263	0.75966	26.5263	7.5966
20SS	294159	78371	2.689431	0.77771	26.89431	7.7771
30SS	298982	80596	2.732838	0.79996	27.32838	7.9996
30SS	300385	80761	2.745465	0.80161	27.45465	8.0161
30SS	329340	84514	3.00606	0.83914	30.0606	8.3914
30SS	318814	82596	2.911326	0.81996	29.11326	8.1996

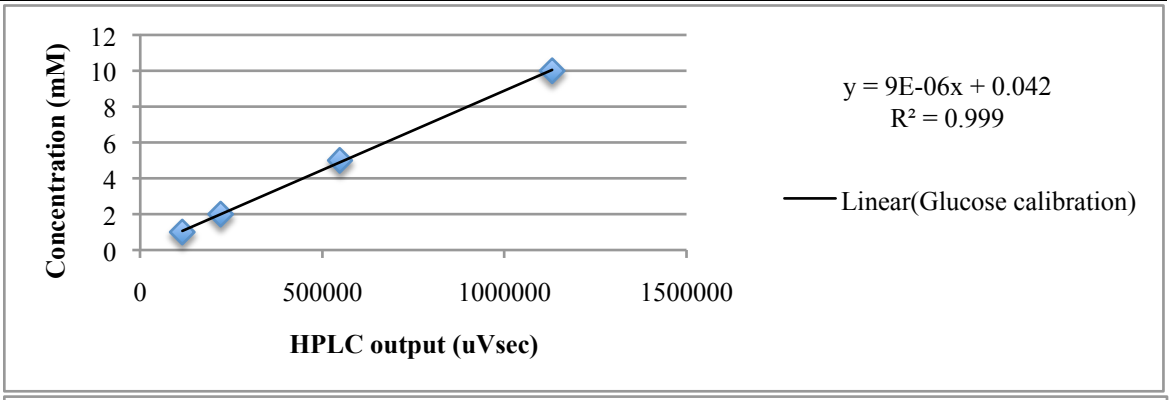

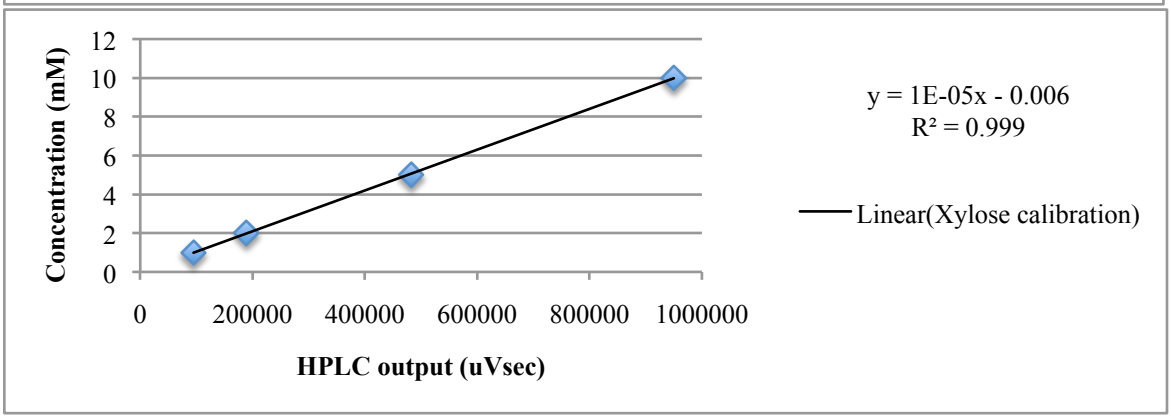

Appendix B. HPLC output for combined pre-treatment

Treatment	Dilution	HPLC Output (µVsec)		Concentration (mM)		Yield (%)	
		Glucose	Xylose	Glucose	Xylose	Glucose	Xylose
Raw	1:10	73022	23583	6.492	2.358	18.76%	10.34%
Raw	1:10	69295	22419	6.157	2.242	17.79%	9.83%
Raw	1:10	115893	24534	10.350	2.453	29.78%	10.71%
Raw	1:10	121586	25653	10.863	2.565	31.25%	11.19%
Raw	1:20	57226	18316	10.141	3.663	29.31%	20.40%
Raw	1:20	58859	18546	10.435	3.709	30.16%	20.65%
15HW	1:10	105409	8793	9.407	0.879	25.98%	3.68%
15HW	1:10	109793	9316	9.801	0.932	27.07%	3.90%
15HW	1:10	105130	11438	9.382	1.144	25.82%	4.78%
15HW	1:10	100084	10724	8.928	1.072	24.57%	4.48%
15HW	1:20	92007	7729	16.401	1.546	45.30%	8.23%
15HW	1:20	95464	7946	17.024	1.589	47.02%	8.46%
15HW	1:20	93560	10135	16.681	2.027	45.91%	10.75%
15HW	1:20	91246	10162	16.264	2.032	44.77%	10.78%
15HW+2SS	1:10	102644	10168	9.158	1.017	33.86%	5.70%
15HW+2SS	1:10	104202	10357	9.298	1.036	34.38%	5.81%
15HW+2SS	1:10	108484	11566	9.684	1.157	35.60%	6.45%
15HW+2SS	1:10	106467	11320	9.502	1.132	34.94%	6.31%
15HW+2SS	1:20	91790	9139	16.362	1.828	60.49%	13.02%
15HW+2SS	1:20	93513	9408	16.672	1.882	61.64%	13.40%
15HW+2SS	1:20	88548	9807	15.779	1.961	58.02%	13.89%
15HW+2SS	1:20	104378	11247	18.628	2.249	68.49%	15.93%
15HW+5SS	1:10	78726	5738	7.005	0.574	21.18%	2.63%
15HW+5SS	1:10	78447	5934	6.980	0.593	21.11%	2.72%
15HW+5SS	1:10	106807	12780	9.533	1.278	28.92%	5.88%
15HW+5SS	1:10	107341	13023	9.581	1.302	29.06%	5.99%
15HW+5SS	1:20	85745	6387	15.274	1.277	46.19%	7.44%
15HW+5SS	1:20	89149	6720	15.887	1.344	48.04%	7.83%
15HW+5SS	1:20	88497	10521	15.769	2.104	47.84%	12.30%
15HW+5SS	1:20	85430	9987	15.217	1.997	46.16%	11.67%
15HW+10SS	1:10	105859	7562	9.447	0.756	17.35%	2.11%
15HW+10SS	1:10	108694	7609	9.702	0.761	17.81%	2.12%
15HW+10SS	1:10	113690	14023	10.152	1.402	18.73%	3.92%
15HW+10SS	1:10	111137	13824	9.922	1.382	18.31%	3.87%
15HW+10SS	1:20	92431	6615	16.478	1.323	30.25%	4.68%
15HW+10SS	1:20	100412	7174	17.914	1.435	32.89%	5.08%
15HW+10SS	1:20	94978	11452	16.936	2.290	31.24%	8.14%
15HW+10SS	1:20	100678	12448	17.962	2.490	33.14%	8.85%
Rxn Blank	1:10	14057	14254	1.185	1.425	3.53%	6.44%
Rxn Blank	1:10	13607	13895	1.145	1.390	3.41%	6.28%
Rxn Blank	1:10	4209	501	0.299	0.050	1.35%	0.34%
Rxn Blank	1:10	4360	513	0.312	0.051	1.41%	0.35%
Rxn Blank	1:20	12295	12583	2.053	2.517	6.11%	14.44%
Rxn Blank	1:20	12912	13335	2.164	2.667	6.45%	15.30%
Rxn Blank	1:20	8383	0	1.349	0.000	6.07%	0.00%
Rxn Blank	1:20	0	676	0.000	0.000	0.00%	0.00%

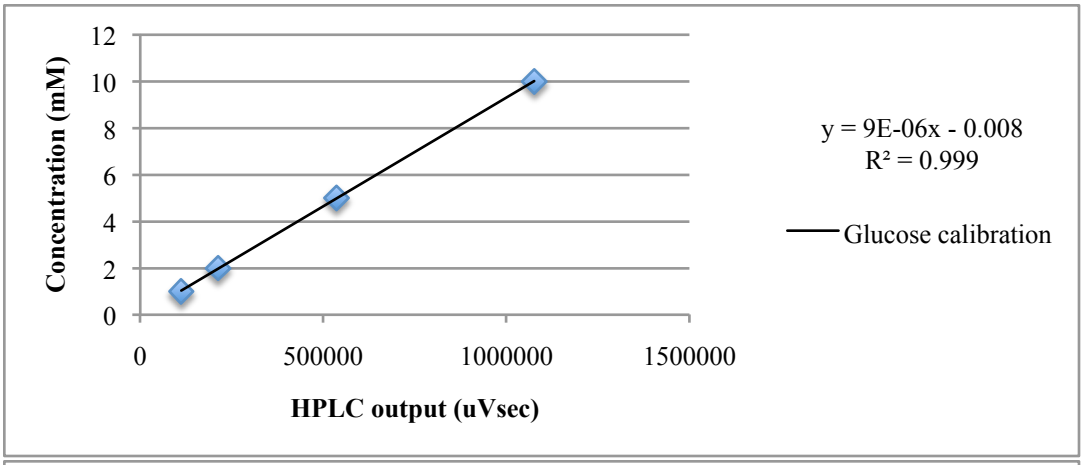
Concentration (mM)
12
10
8
6
4
2
0
0
500000
1000000
1500000
HPLC output (uVsec)
y = 9E-06x - 0.008
R² = 0.999
Glucose calibration

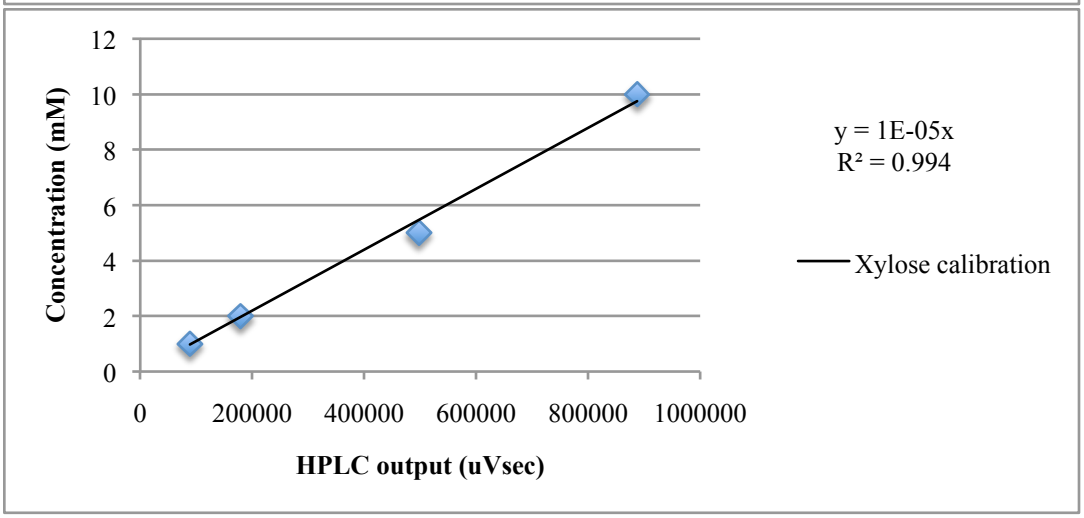
Concentration (mM)
12
10
8
6
4
2
0
0
200000
400000
600000
800000
1000000
HPLC output (uVsec)
y = 1E-05x
R² = 0.994
Xylose calibration

Appendix C. Output from the SAS 9.3 ARIMA Procedure

Direct normal irradiance (DNI)

The ARIMA Procedure

Name of Variable = DNI	
Mean of Working Series	162.4784
Standard Deviation	233.4067
Number of Observations	280320

Autocorrelation Check for White Noise

To Lag	Chi-Square	DF	Pr > ChiSq	Autocorrelations					
6	9999.99	6	<.0001	0.923	0.774	0.596	0.406	0.218	0.045
12	9999.99	12	<.0001	-0.105	-0.226	-0.317	-0.381	-0.418	-0.430
18	9999.99	18	<.0001	-0.418	-0.381	-0.319	-0.229	-0.113	0.029
24	9999.99	24	<.0001	0.189	0.357	0.517	0.651	0.742	0.773
30	9999.99	30	<.0001	0.739	0.647	0.512	0.351	0.184	0.025
36	9999.99	36	<.0001	-0.116	-0.231	-0.320	-0.382	-0.418	-0.430
42	9999.99	42	<.0001	-0.418	-0.382	-0.320	-0.232	-0.116	0.024
48	9999.99	48	<.0001	0.182	0.348	0.506	0.639	0.729	0.761

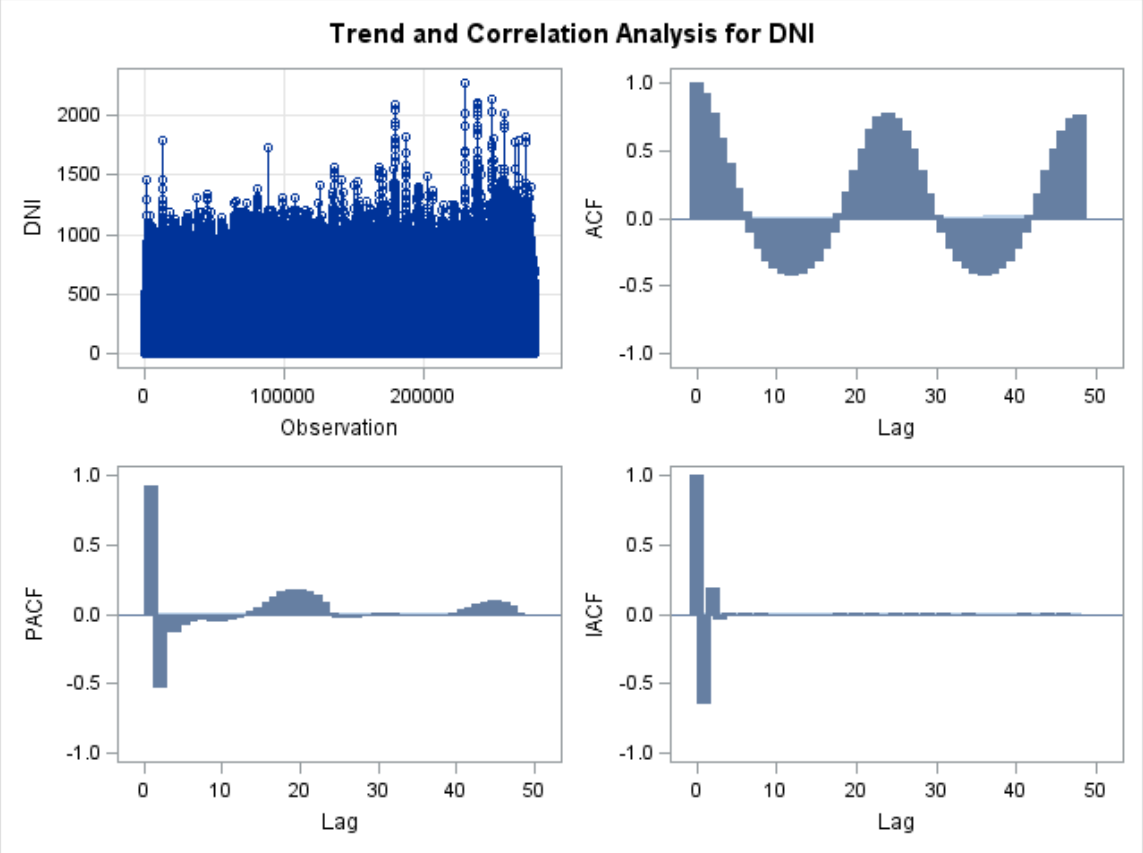

Name of Variable = DNI	
Period(s) of Differencing	1
Mean of Working Series	1.8E-18
Standard Deviation	91.48599
Number of Observations	280319
Observation(s) eliminated by differencing	1

Autocorrelation Check for White Noise

To Lag	Chi-Square	DF	Pr > ChiSq	Autocorrelations					
6	9999.99	6	<.0001	0.469	0.191	0.078	-0.015	-0.095	-0.156
12	9999.99	12	<.0001	-0.186	-0.192	-0.183	-0.171	-0.162	-0.157
18	9999.99	18	<.0001	-0.160	-0.168	-0.176	-0.177	-0.162	-0.122
24	9999.99	24	<.0001	-0.049	0.050	0.167	0.285	0.386	0.424
30	9999.99	30	<.0001	0.379	0.282	0.163	0.047	-0.055	-0.122
36	9999.99	36	<.0001	-0.162	-0.175	-0.172	-0.167	-0.159	-0.156
42	9999.99	42	<.0001	-0.159	-0.166	-0.173	-0.175	-0.162	-0.119
48	9999.99	48	<.0001	-0.048	0.050	0.166	0.280	0.376	0.418

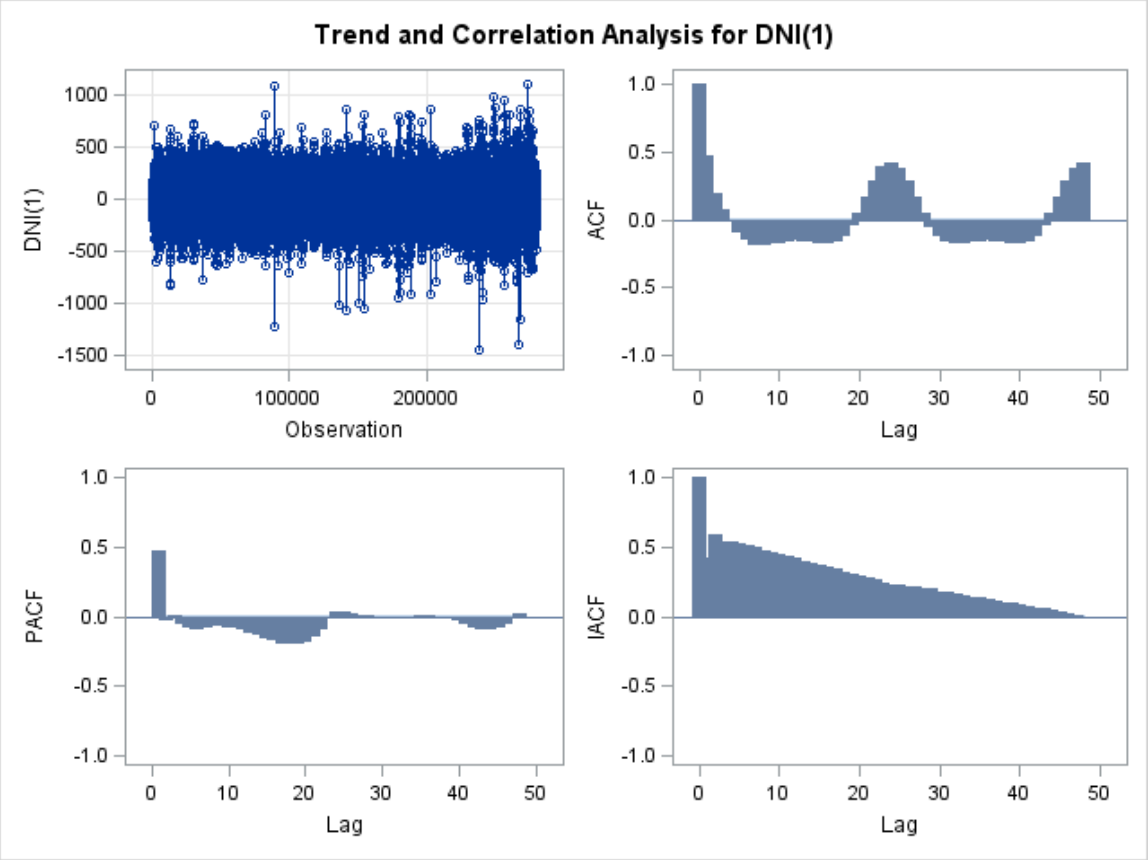

Name of Variable = DNI

Name of Variable = DNI	
Period(s) of Differencing	24
Mean of Working Series	0.000158
Standard Deviation	157.2612
Number of Observations	280296
Observation(s) eliminated by differencing	24

Autocorrelation Check for White Noise

To Lag	Chi-Square	DF	Pr > ChiSq	Autocorrelations					
6	9999.99	6	<.0001	0.805	0.552	0.361	0.229	0.139	0.079
12	9999.99	12	<.0001	0.041	0.020	0.009	0.004	0.002	0.001
18	9999.99	18	<.0001	0.000	-0.000	-0.001	-0.003	-0.010	-0.025
24	9999.99	24	<.0001	-0.050	-0.090	-0.153	-0.245	-0.372	-0.473
30	9999.99	30	<.0001	-0.382	-0.261	-0.172	-0.111	-0.070	-0.040
36	9999.99	36	<.0001	-0.022	-0.011	-0.005	-0.003	-0.001	-0.001
42	9999.99	42	<.0001	-0.000	-0.001	-0.002	-0.005	-0.008	-0.012
48	9999.99	48	<.0001	-0.016	-0.019	-0.021	-0.024	-0.027	-0.027

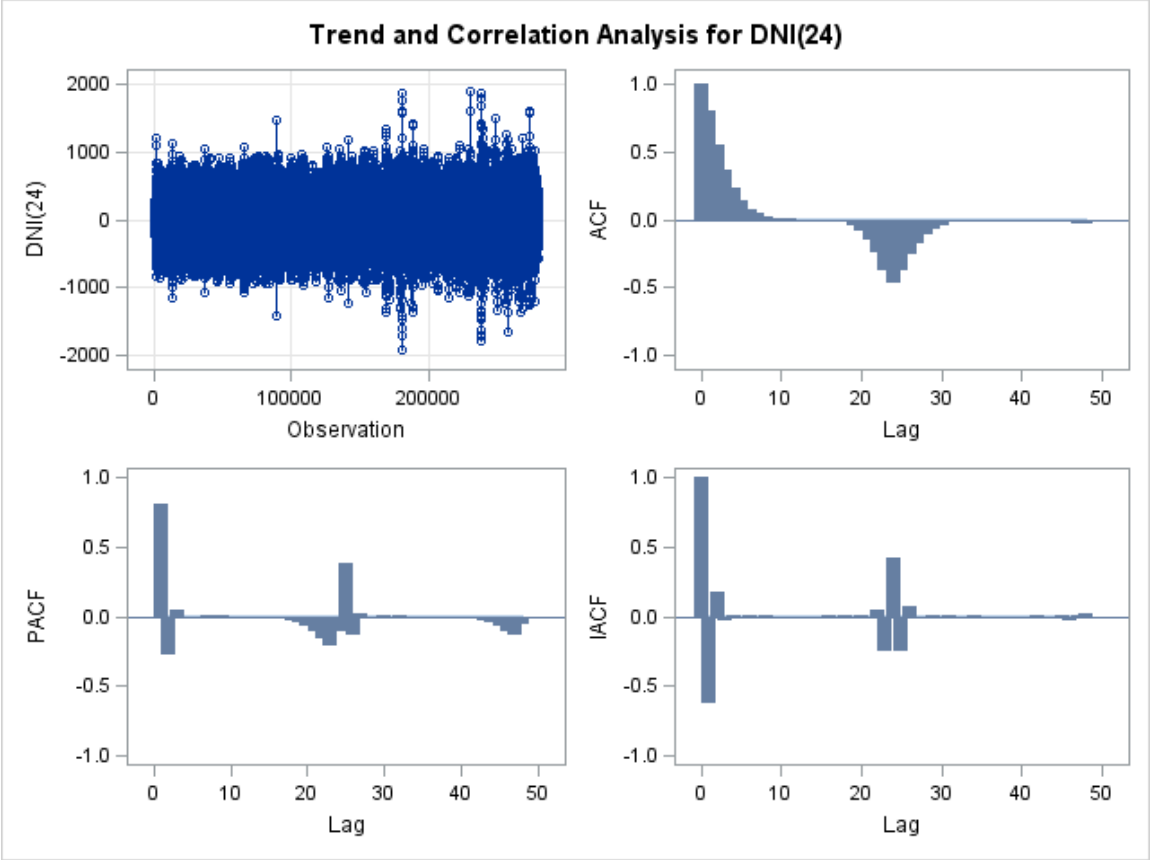

Name of Variable = DNI

Name of Variable = DNI	
Period(s) of Differencing	8760
Mean of Working Series	0.175291
Standard Deviation	165.0256
Number of Observations	271560
Observation(s) eliminated by differencing	8760

Autocorrelation Check for White Noise

To Lag	Chi-Square	DF	Pr > ChiSq	Autocorrelations					
6	9999.99	6	<.0001	0.820	0.578	0.388	0.251	0.154	0.089
12	9999.99	12	<.0001	0.049	0.025	0.012	0.005	0.002	0.002
18	9999.99	18	<.0001	0.002	0.003	0.005	0.009	0.015	0.024
24	9999.99	24	<.0001	0.036	0.052	0.068	0.084	0.095	0.095
30	9999.99	30	<.0001	0.085	0.069	0.050	0.033	0.020	0.012
36	9999.99	36	<.0001	0.007	0.003	0.002	0.001	0.000	0.000
42	9999.99	42	<.0001	0.000	-0.001	-0.001	-0.001	0.002	0.006
48	9999.99	48	<.0001	0.013	0.021	0.029	0.038	0.045	0.050

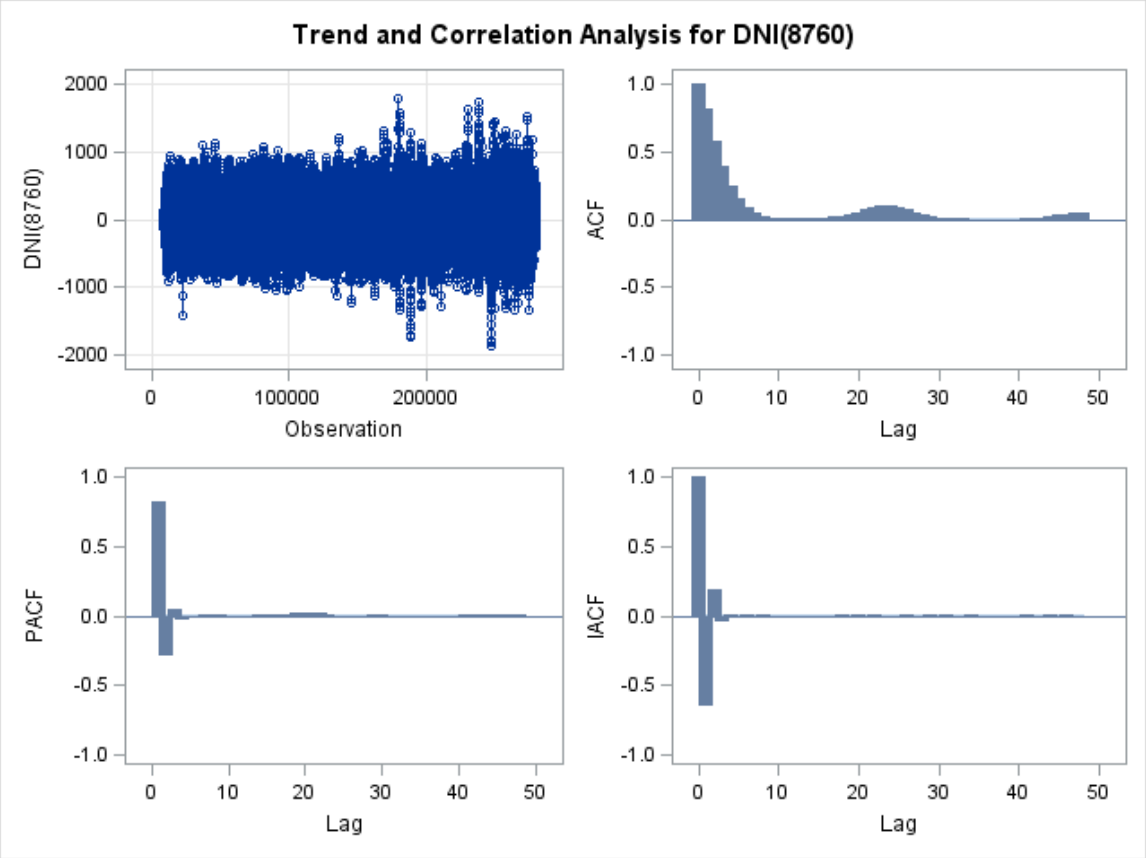

Name of Variable = DNI

Name of Variable = DNI	
Period(s) of Differencing	1,24
Mean of Working Series	-743E-20
Standard Deviation	98.17594
Number of Observations	280295
Observation(s) eliminated by differencing	25

Autocorrelation Check for White Noise

To Lag	Chi-Square	DF	Pr > ChiSq	Autocorrelations					
6	9999.99	6	<.0001	0.150	-0.161	-0.151	-0.109	-0.074	-0.059
12	9999.99	12	<.0001	-0.040	-0.028	-0.015	-0.007	-0.003	-0.002
18	9999.99	18	<.0001	-0.000	0.001	0.004	0.012	0.019	0.028
24	9999.99	24	<.0001	0.039	0.056	0.079	0.086	-0.064	-0.495
30	9999.99	30	<.0001	-0.075	0.079	0.073	0.053	0.029	0.029
36	9999.99	36	<.0001	0.018	0.013	0.009	0.003	0.002	0.002
42	9999.99	42	<.0001	0.001	0.002	0.004	0.002	0.001	-0.000
48	9999.99	48	<.0001	-0.001	-0.002	0.002	-0.001	-0.008	-0.007

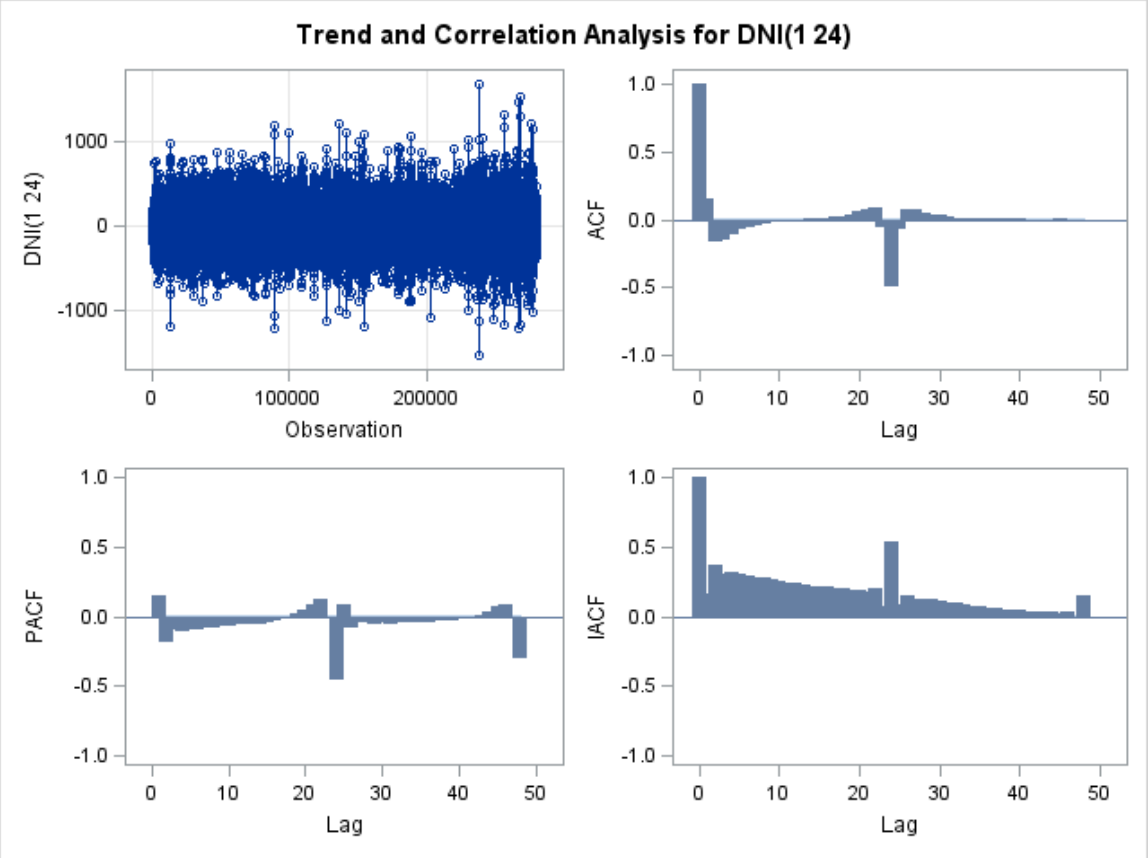

Name of Variable = DNI

Name of Variable = DNI	
Period(s) of Differencing	1,8760
Mean of Working Series	-184E-19
Standard Deviation	98.96138
Number of Observations	271559
Observation(s) eliminated by differencing	8761

Autocorrelation Check for White Noise

To Lag	Chi-Square	DF	Pr > ChiSq	Autocorrelations					
6	9999.99	6	<.0001	0.174	-0.147	-0.145	-0.113	-0.088	-0.069
12	9999.99	12	<.0001	-0.046	-0.030	-0.018	-0.010	-0.006	-0.003
18	9999.99	18	<.0001	-0.003	-0.004	-0.005	-0.006	-0.007	-0.010
24	9999.99	24	<.0001	-0.008	-0.004	0.003	0.015	0.027	0.029
30	9999.99	30	<.0001	0.020	0.005	-0.004	-0.012	-0.015	-0.006
36	9999.99	36	<.0001	-0.005	-0.005	-0.002	-0.002	-0.001	0.001
42	9999.99	42	<.0001	0.001	-0.000	-0.002	-0.005	-0.007	-0.005
48	9999.99	48	<.0001	-0.004	-0.003	0.002	0.001	0.009	0.016

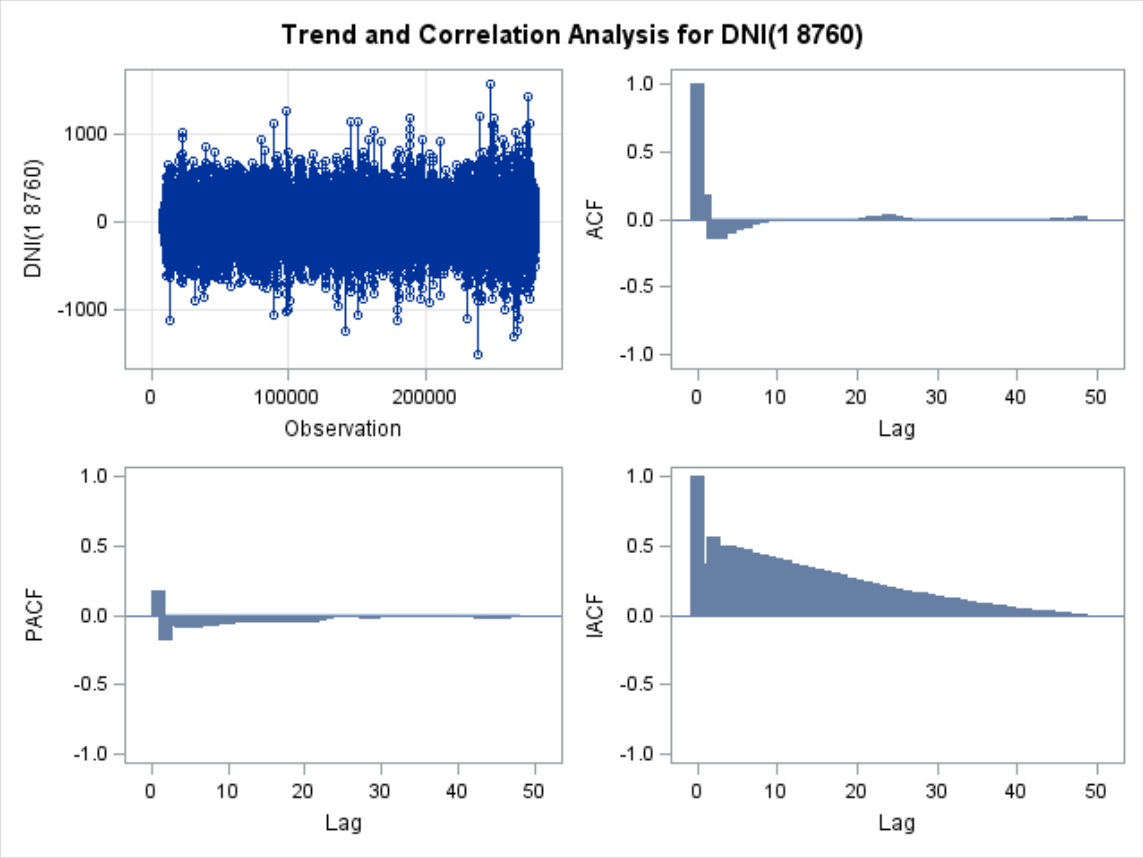

Name of Variable = DNI

Name of Variable = DNI	
Period(s) of Differencing	24,8760
Mean of Working Series	0.0035
Standard Deviation	222.0156
Number of Observations	271536
Observation(s) eliminated by differencing	8784

Autocorrelation Check for White Noise

To Lag	Chi-Square	DF	Pr > ChiSq	Autocorrelations					
6	9999.99	6	<.0001	0.807	0.554	0.364	0.231	0.140	0.079
12	9999.99	12	<.0001	0.042	0.021	0.010	0.004	0.002	0.001
18	9999.99	18	<.0001	0.000	0.000	-0.001	-0.004	-0.011	-0.026
24	9999.99	24	<.0001	-0.052	-0.093	-0.155	-0.247	-0.374	-0.475
30	9999.99	30	<.0001	-0.386	-0.268	-0.179	-0.116	-0.072	-0.041
36	9999.99	36	<.0001	-0.023	-0.012	-0.006	-0.003	-0.001	-0.001
42	9999.99	42	<.0001	-0.001	-0.002	-0.003	-0.005	-0.008	-0.011
48	9999.99	48	<.0001	-0.014	-0.018	-0.021	-0.023	-0.024	-0.021

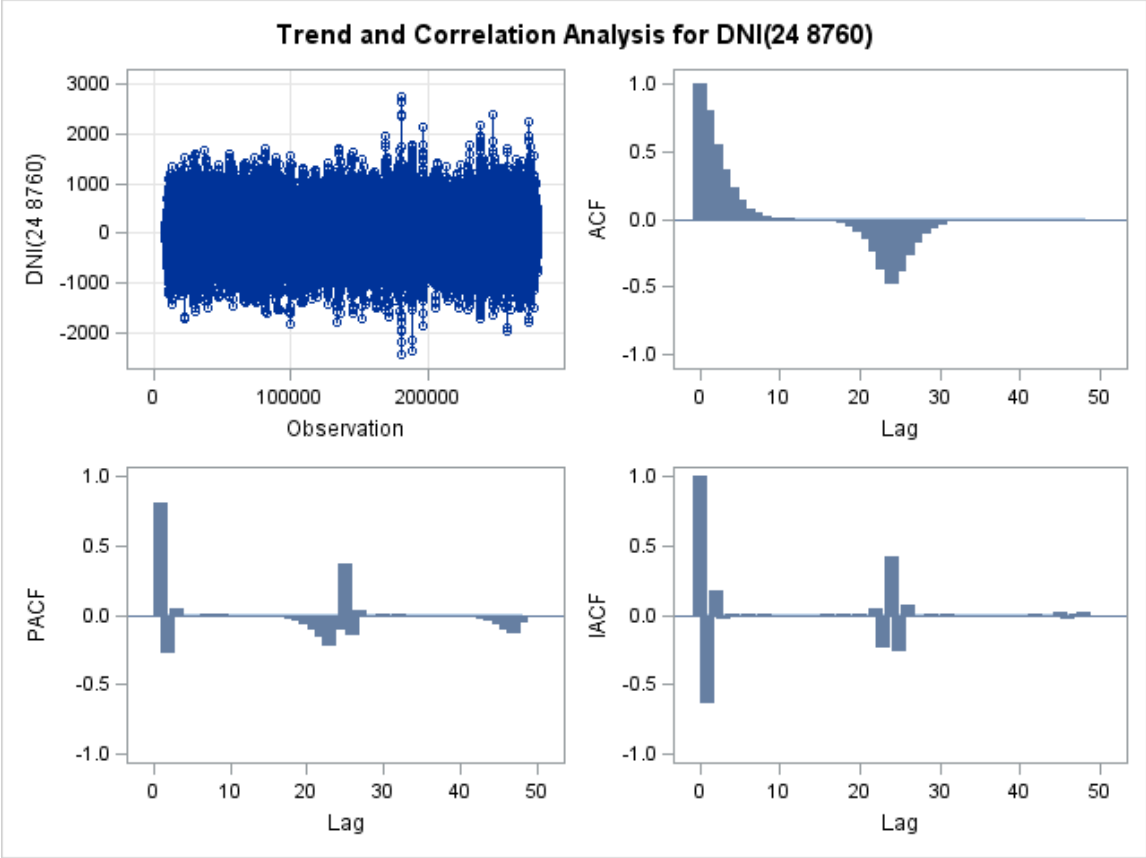

Name of Variable = DNI

Name of Variable = DNI	
Period(s) of Differencing	1,24,8760
Mean of Working Series	-761E-20
Standard Deviation	137.9339
Number of Observations	271535
Observation(s) eliminated by differencing	8785

Autocorrelation Check for White Noise

To Lag	Chi-Square	DF	Pr > ChiSq	Autocorrelations					
6	9999.99	6	<.0001	0.155	-0.162	-0.149	-0.108	-0.078	-0.062
12	9999.99	12	<.0001	-0.041	-0.026	-0.014	-0.007	-0.004	-0.002
18	9999.99	18	<.0001	-0.000	0.002	0.005	0.012	0.020	0.027
24	9999.99	24	<.0001	0.039	0.055	0.077	0.090	-0.066	-0.493
30	9999.99	30	<.0001	-0.075	0.075	0.068	0.049	0.033	0.033
36	9999.99	36	<.0001	0.020	0.012	0.008	0.003	0.002	0.002
42	9999.99	42	<.0001	0.002	0.001	0.002	0.001	0.001	0.001
48	9999.99	48	<.0001	0.001	-0.003	0.000	-0.006	-0.008	-0.008

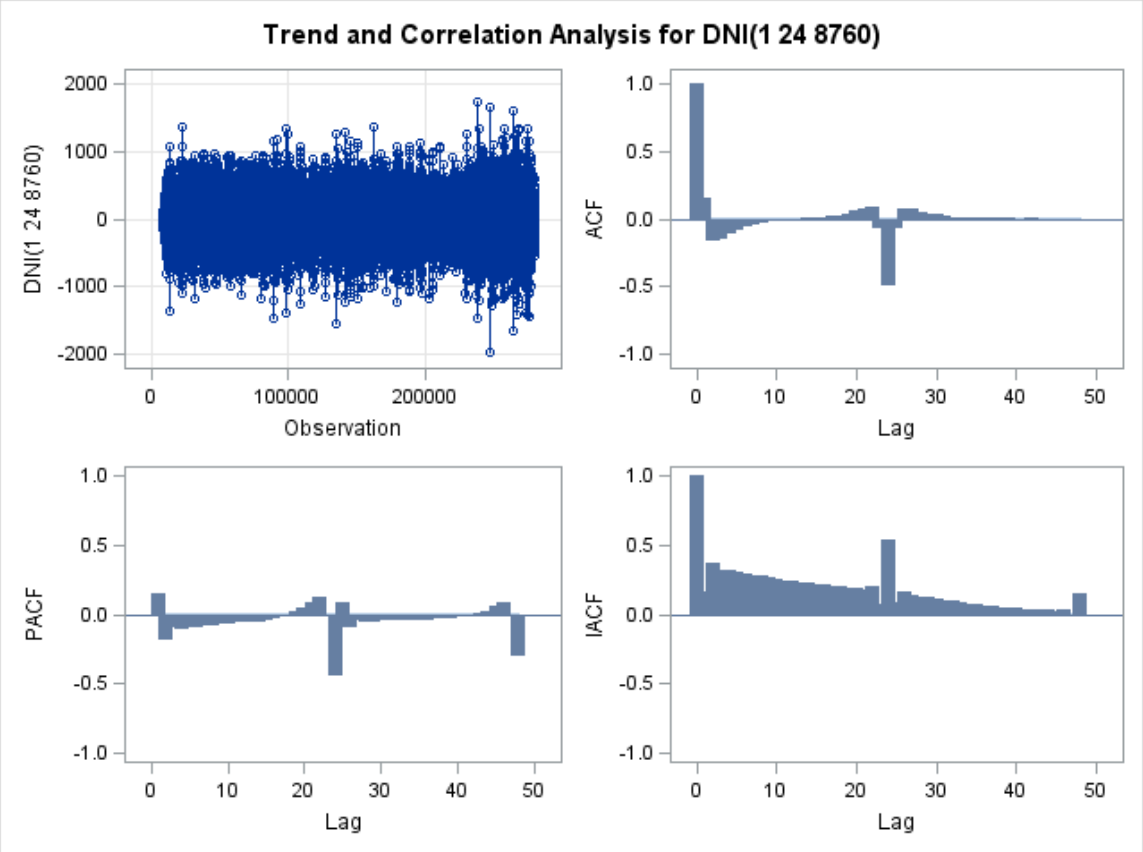

Temperature (T)

The ARIMA Procedure

Name of Variable = T	
Mean of Working Series	2.902963
Standard Deviation	14.85018
Number of Observations	280320
Embedded missing values in working series	4

Autocorrelation Check for White Noise

To Lag	Chi-Square	DF	Pr > ChiSq	Autocorrelations					
6	9999.99	6	<.0001	0.996	0.989	0.979	0.968	0.956	0.943
12	9999.99	12	<.0001	0.931	0.919	0.909	0.900	0.894	0.890
18	9999.99	18	<.0001	0.888	0.889	0.892	0.896	0.902	0.908
24	9999.99	24	<.0001	0.915	0.922	0.927	0.932	0.934	0.933
30	9999.99	30	<.0001	0.929	0.923	0.914	0.904	0.893	0.882
36	9999.99	36	<.0001	0.872	0.862	0.853	0.846	0.841	0.839
42	9999.99	42	<.0001	0.838	0.840	0.844	0.850	0.857	0.864
48	9999.99	48	<.0001	0.872	0.880	0.886	0.892	0.895	0.896

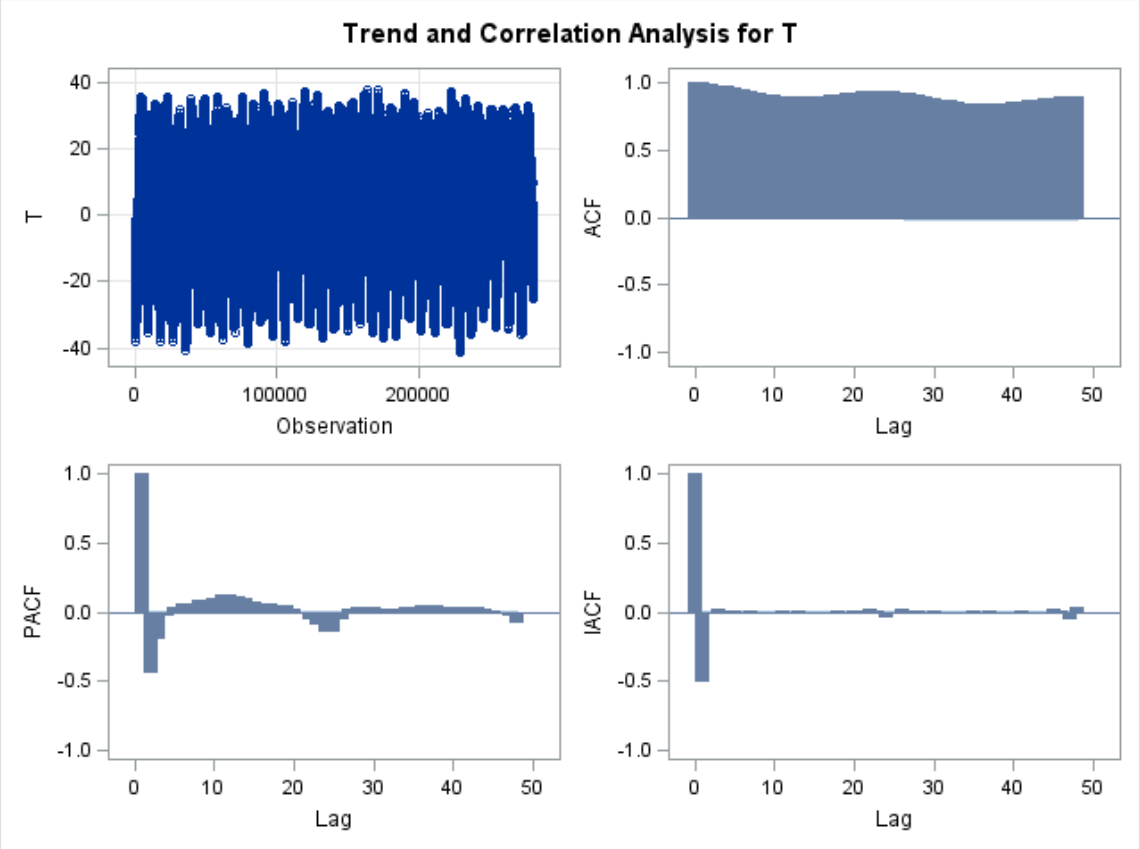

Name of Variable = T	
Period(s) of Differencing	1

Name of Variable = T	
Mean of Working Series	3.567E-7
Standard Deviation	1.287317
Number of Observations	280319
Observation(s) eliminated by differencing	1
Embedded missing values in working series	7

Autocorrelation Check for White Noise

To Lag	Chi-Square	DF	Pr > ChiSq	Autocorrelations					
6	9999.99	6	<.0001	0.438	0.352	0.229	0.127	0.035	-0.040
12	9999.99	12	<.0001	-0.109	-0.171	-0.228	-0.279	-0.313	-0.325
18	9999.99	18	<.0001	-0.312	-0.274	-0.221	-0.165	-0.104	-0.041
24	9999.99	24	<.0001	0.031	0.108	0.196	0.285	0.370	0.413
30	9999.99	30	<.0001	0.369	0.280	0.190	0.100	0.023	-0.048
36	9999.99	36	<.0001	-0.108	-0.166	-0.221	-0.269	-0.302	-0.311
42	9999.99	42	<.0001	-0.300	-0.263	-0.215	-0.160	-0.105	-0.039
48	9999.99	48	<.0001	0.030	0.108	0.189	0.278	0.360	0.400

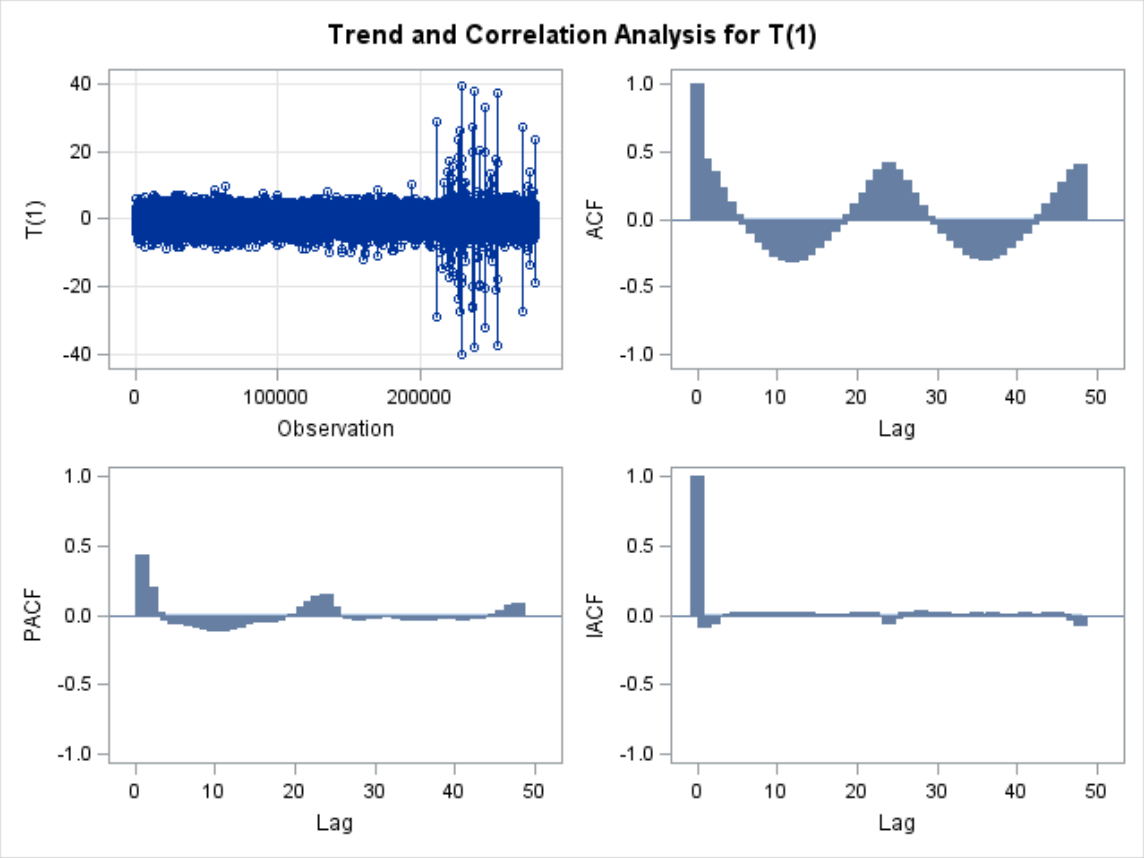

Name of Variable = T

Name of Variable = T	
Period(s) of Differencing	24
Mean of Working Series	-0.00064
Standard Deviation	5.431019
Number of Observations	280296
Observation(s) eliminated by differencing	24
Embedded missing values in working series	8

Autocorrelation Check for White Noise

To Lag	Chi-Square	DF	Pr > ChiSq	Autocorrelations					
6	9999.99	6	<.0001	0.967	0.926	0.878	0.825	0.770	0.714
12	9999.99	12	<.0001	0.657	0.601	0.545	0.491	0.437	0.383
18	9999.99	18	<.0001	0.331	0.279	0.227	0.175	0.124	0.071
24	9999.99	24	<.0001	0.019	-0.032	-0.083	-0.132	-0.178	-0.220
30	9999.99	30	<.0001	-0.230	-0.237	-0.240	-0.240	-0.239	-0.237
36	9999.99	36	<.0001	-0.233	-0.229	-0.225	-0.221	-0.216	-0.211
42	9999.99	42	<.0001	-0.207	-0.202	-0.198	-0.194	-0.189	-0.183
48	9999.99	48	<.0001	-0.177	-0.171	-0.165	-0.158	-0.151	-0.144

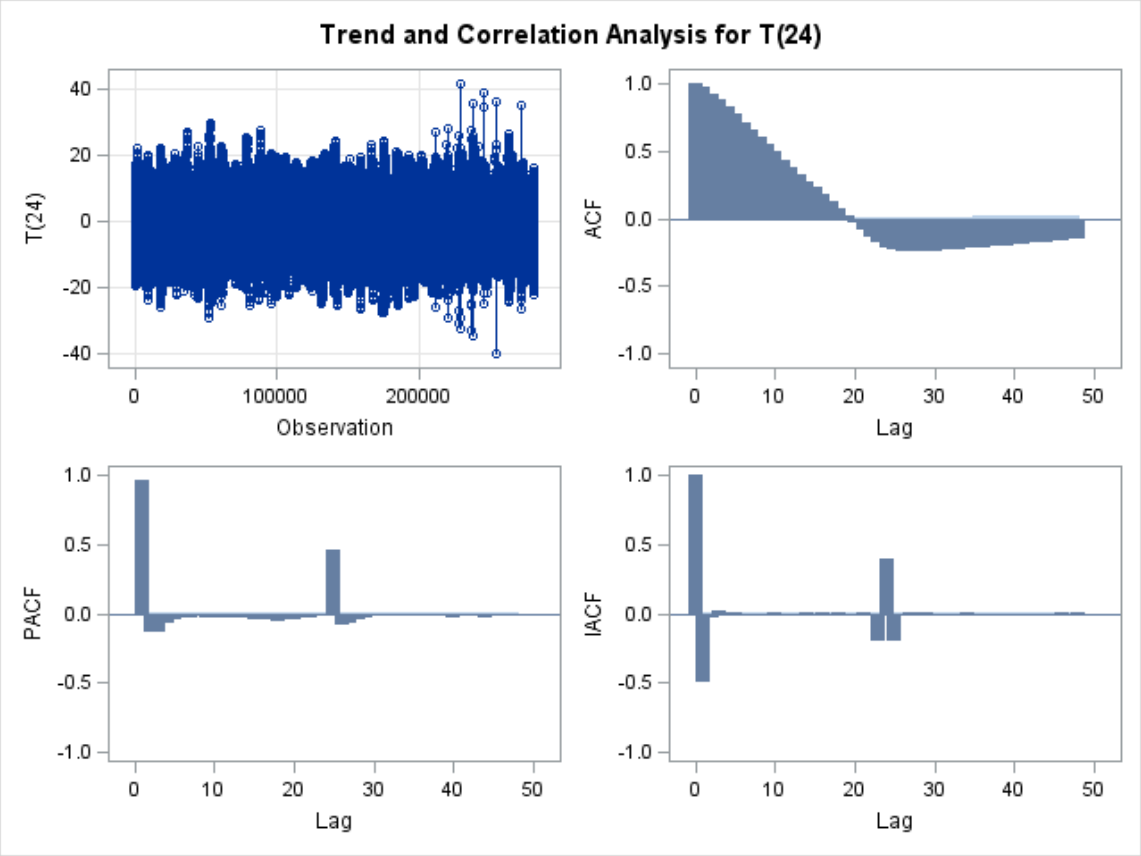

Name of Variable = T	
Period(s) of Differencing	8760
Mean of Working Series	0.084532
Standard Deviation	8.879835
Number of Observations	271560
Observation(s) eliminated by differencing	8760
Embedded missing values in working series	8

Autocorrelation Check for White Noise

To Lag	Chi-Square	DF	Pr > ChiSq	Autocorrelations					
6	9999.99	6	<.0001	0.987	0.970	0.950	0.928	0.906	0.883
12	9999.99	12	<.0001	0.861	0.839	0.819	0.800	0.782	0.765
18	9999.99	18	<.0001	0.751	0.737	0.725	0.714	0.703	0.693
24	9999.99	24	<.0001	0.683	0.673	0.664	0.654	0.644	0.632
30	9999.99	30	<.0001	0.620	0.606	0.592	0.578	0.564	0.551
36	9999.99	36	<.0001	0.539	0.527	0.516	0.505	0.496	0.488
42	9999.99	42	<.0001	0.481	0.474	0.468	0.463	0.459	0.455
48	9999.99	48	<.0001	0.452	0.448	0.445	0.442	0.438	0.433

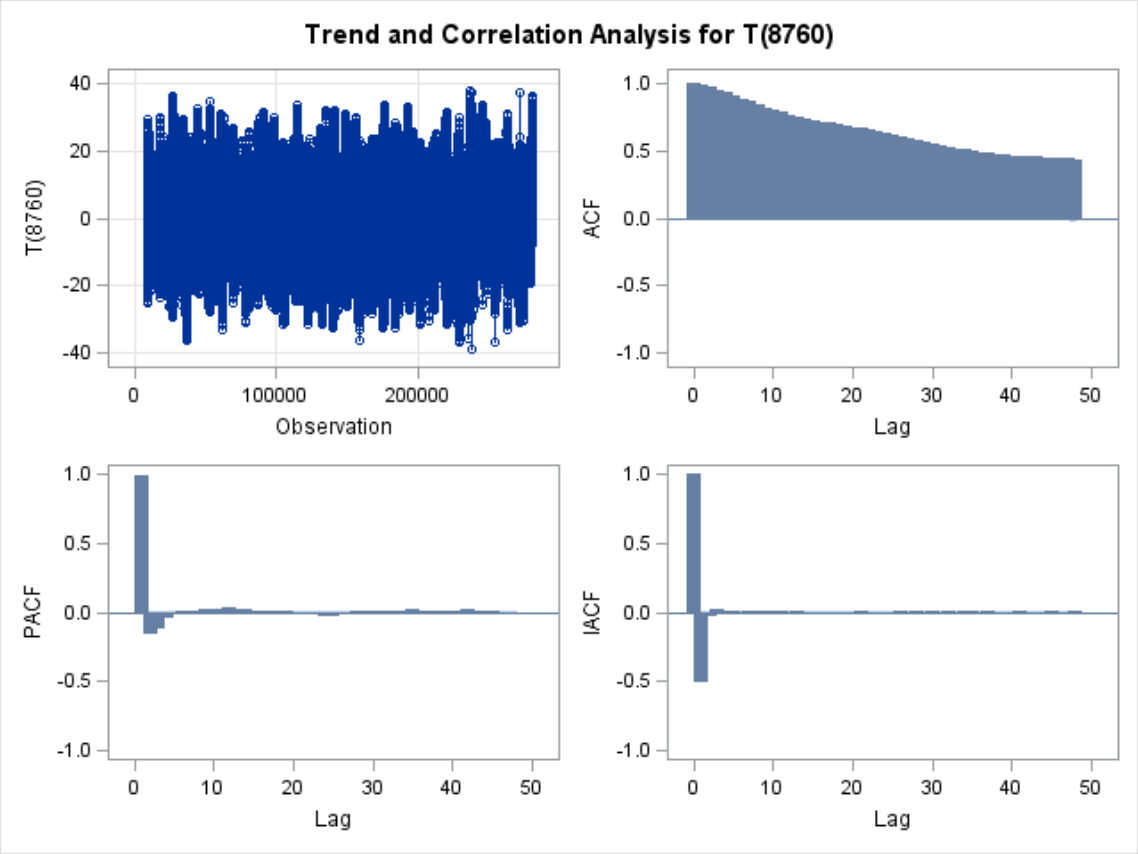

Name of Variable = T	
Period(s) of Differencing	1,24
Mean of Working Series	0.000039
Standard Deviation	1.394477
Number of Observations	280295
Observation(s) eliminated by differencing	25
Embedded missing values in working series	14

Autocorrelation Check for White Noise

To Lag	Chi-Square	DF	Pr > ChiSq	Autocorrelations					
6	9403.16	6	<.0001	0.117	0.120	0.060	0.038	0.014	0.008
12	9586.73	12	<.0001	-0.006	-0.010	-0.011	-0.012	-0.011	-0.011
18	9630.55	18	<.0001	-0.009	-0.006	0.000	0.002	0.005	-0.003
24	9999.99	24	<.0001	-0.003	-0.016	-0.022	-0.052	-0.050	-0.489
30	9999.99	30	<.0001	-0.053	-0.061	-0.034	-0.027	-0.017	-0.016
36	9999.99	36	<.0001	-0.007	-0.004	-0.004	-0.003	-0.001	0.003
42	9999.99	42	<.0001	0.002	0.001	-0.003	-0.005	-0.009	-0.004
48	9999.99	48	<.0001	-0.005	-0.001	-0.009	-0.004	-0.006	-0.007

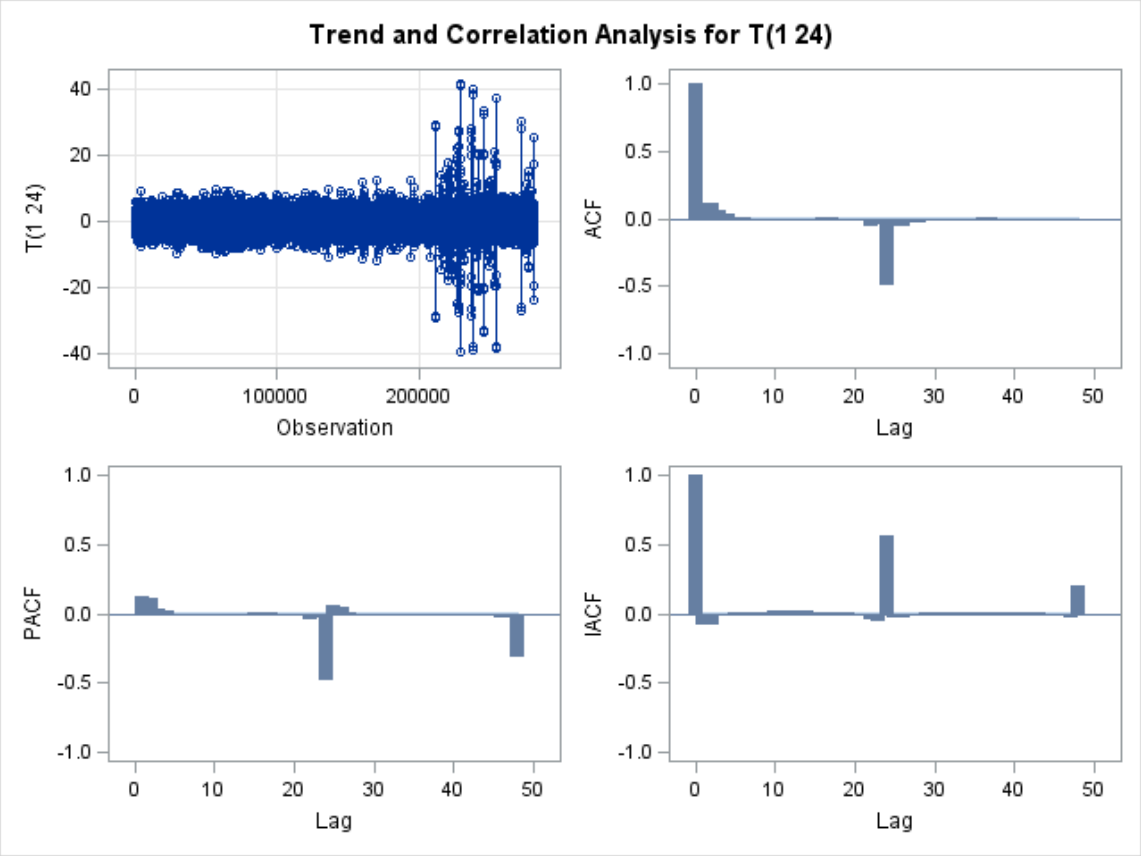

Name of Variable = T	
Period(s) of Differencing	1,8760
Mean of Working Series	0.000073
Standard Deviation	1.427128
Number of Observations	271559
Observation(s) eliminated by differencing	8761
Embedded missing values in working series	14

Autocorrelation Check for White Noise

To Lag	Chi-Square	DF	Pr > ChiSq	Autocorrelations					
6	9999.99	6	<.0001	0.149	0.132	0.065	0.029	-0.001	-0.013
12	9999.99	12	<.0001	-0.029	-0.039	-0.046	-0.055	-0.059	-0.056
18	9999.99	18	<.0001	-0.057	-0.045	-0.037	-0.027	-0.020	-0.014
24	9999.99	24	<.0001	-0.008	0.000	0.010	0.026	0.037	0.046
30	9999.99	30	<.0001	0.035	0.017	0.004	-0.012	-0.020	-0.025
36	9999.99	36	<.0001	-0.025	-0.032	-0.035	-0.039	-0.039	-0.033
42	9999.99	42	<.0001	-0.033	-0.028	-0.026	-0.024	-0.024	-0.012
48	9999.99	48	<.0001	-0.007	-0.001	0.005	0.015	0.022	0.026

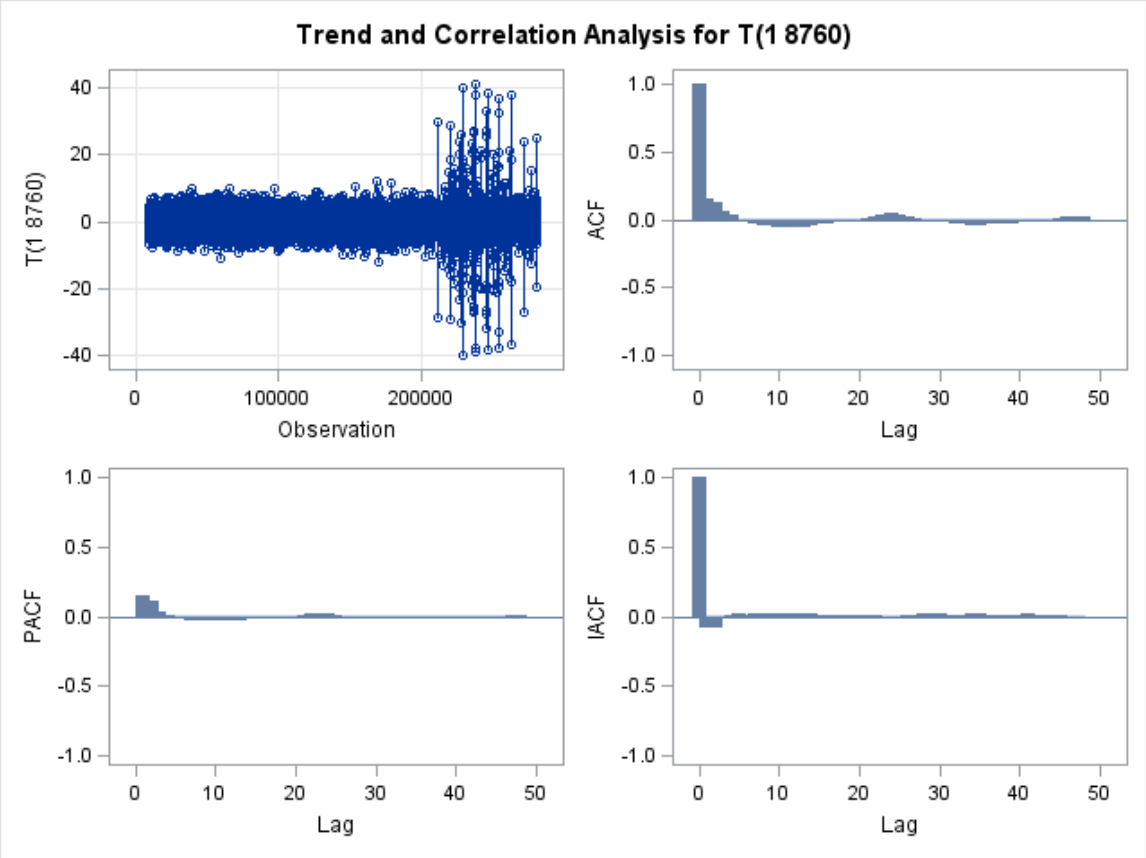

Name of Variable = T	
Period(s) of Differencing	24,8760
Mean of Working Series	0.001115
Standard Deviation	7.615524
Number of Observations	271536
Observation(s) eliminated by differencing	8784
Embedded missing values in working series	16

Autocorrelation Check for White Noise

To Lag	Chi-Square	DF	Pr > ChiSq	Autocorrelations					
6	9999.99	6	<.0001	0.966	0.925	0.876	0.822	0.767	0.710
12	9999.99	12	<.0001	0.653	0.596	0.540	0.485	0.431	0.377
18	9999.99	18	<.0001	0.324	0.272	0.221	0.169	0.117	0.064
24	9999.99	24	<.0001	0.012	-0.040	-0.091	-0.141	-0.187	-0.230
30	9999.99	30	<.0001	-0.239	-0.246	-0.248	-0.248	-0.247	-0.244
36	9999.99	36	<.0001	-0.240	-0.235	-0.231	-0.226	-0.220	-0.215
42	9999.99	42	<.0001	-0.210	-0.205	-0.200	-0.195	-0.190	-0.183
48	9999.99	48	<.0001	-0.177	-0.170	-0.163	-0.156	-0.148	-0.141

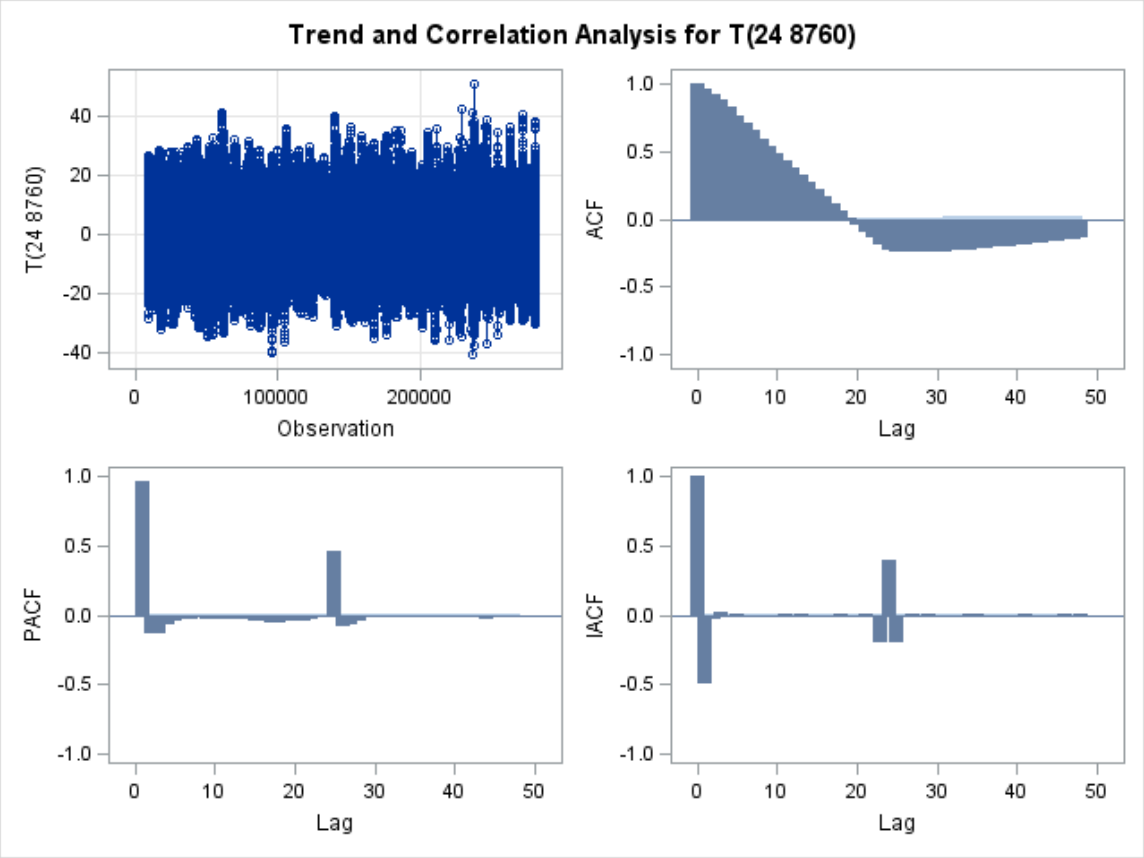

Name of Variable = T	
Period(s) of Differencing	1,24,8760
Mean of Working Series	0.000018
Standard Deviation	1.971612
Number of Observations	271535
Observation(s) eliminated by differencing	8785
Embedded missing values in working series	28

Autocorrelation Check for White Noise

To Lag	Chi-Square	DF	Pr > ChiSq	Autocorrelations					
6	8895.67	6	<.0001	0.118	0.116	0.061	0.037	0.013	0.007
12	9097.17	12	<.0001	-0.007	-0.010	-0.011	-0.014	-0.012	-0.012
18	9159.79	18	<.0001	-0.012	-0.003	-0.000	0.005	0.007	-0.002
24	9999.99	24	<.0001	-0.004	-0.015	-0.026	-0.050	-0.050	-0.489
30	9999.99	30	<.0001	-0.053	-0.059	-0.033	-0.027	-0.019	-0.015
36	9999.99	36	<.0001	-0.007	-0.006	-0.005	-0.003	-0.002	0.004
42	9999.99	42	<.0001	0.005	0.000	-0.002	-0.008	-0.012	-0.005
48	9999.99	48	<.0001	-0.004	-0.001	-0.004	-0.002	-0.005	-0.006

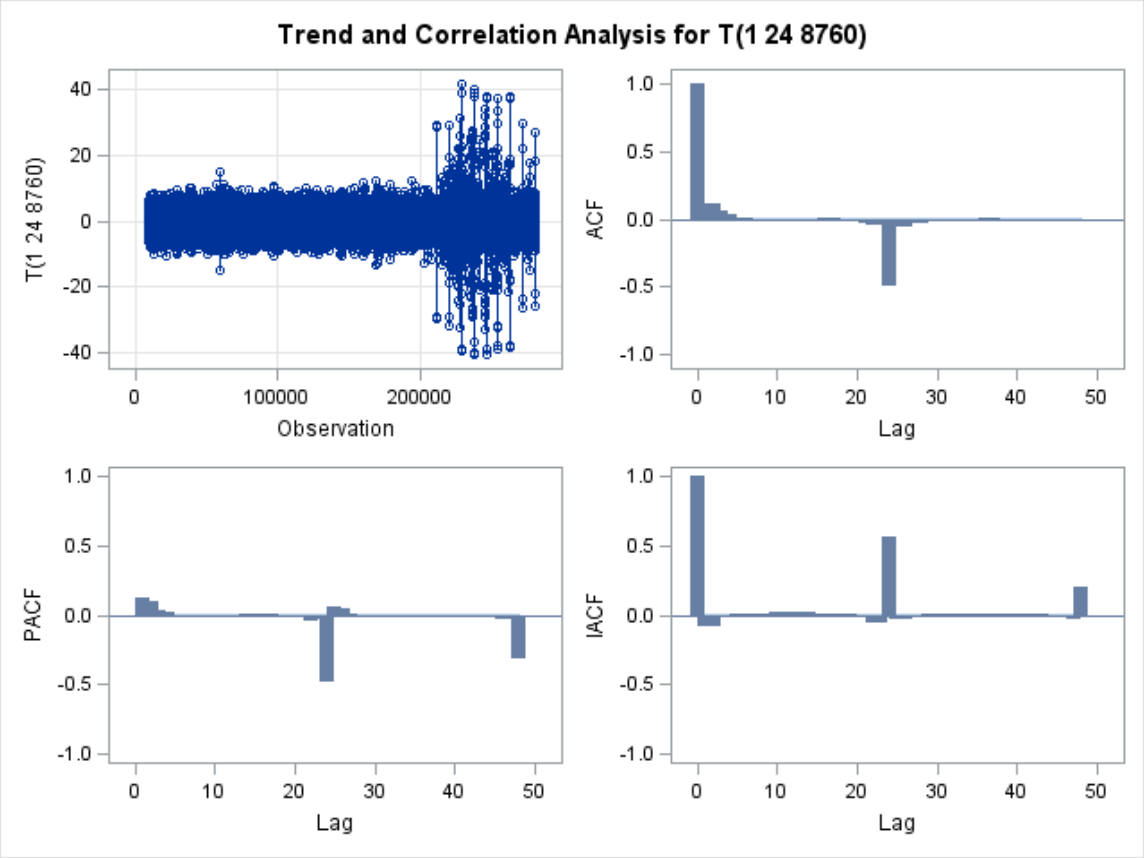

Wind

The ARIMA Procedure

Name of Variable = wind	
Mean of Working Series	4.72574
Standard Deviation	2.754792
Number of Observations	280320
Embedded missing values in working series	1

Autocorrelation Check for White Noise

To Lag	Chi-Square	DF	Pr > ChiSq	Autocorrelations					
6	9999.99	6	<.0001	0.884	0.813	0.745	0.678	0.612	0.549
12	9999.99	12	<.0001	0.490	0.434	0.383	0.336	0.296	0.260
18	9999.99	18	<.0001	0.231	0.209	0.191	0.179	0.170	0.166
24	9999.99	24	<.0001	0.164	0.165	0.167	0.168	0.167	0.162
30	9999.99	30	<.0001	0.150	0.134	0.116	0.097	0.078	0.059
36	9999.99	36	<.0001	0.042	0.027	0.016	0.006	-0.000	-0.003
42	9999.99	42	<.0001	-0.004	-0.002	0.004	0.012	0.021	0.032
48	9999.99	48	<.0001	0.045	0.057	0.070	0.082	0.090	0.094

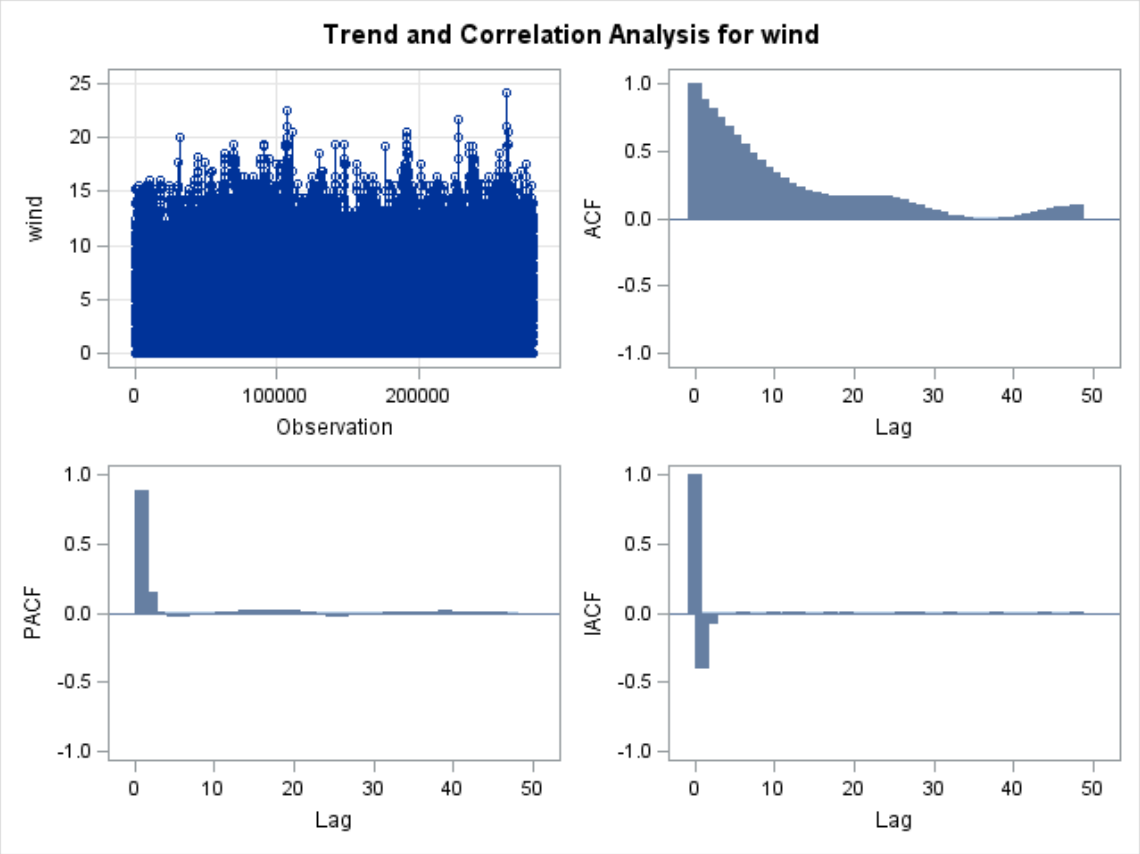

Name of Variable = wind

Name of Variable = wind	
Period(s) of Differencing	1
Mean of Working Series	6.778E-6
Standard Deviation	1.326657
Number of Observations	280319
Observation(s) eliminated by differencing	1
Embedded missing values in working series	2

Autocorrelation Check for White Noise

To Lag	Chi-Square	DF	Pr > ChiSq	Autocorrelations					
6	9999.99	6	<.0001	-0.196	-0.007	-0.008	-0.008	-0.008	-0.018
12	9999.99	12	<.0001	-0.016	-0.019	-0.021	-0.025	-0.021	-0.028
18	9999.99	18	<.0001	-0.027	-0.022	-0.021	-0.018	-0.018	-0.011
24	9999.99	24	<.0001	-0.012	-0.003	0.003	0.010	0.016	0.028
30	9999.99	30	<.0001	0.020	0.009	0.004	-0.002	-0.001	-0.006
36	9999.99	36	<.0001	-0.009	-0.015	-0.009	-0.013	-0.013	-0.012
42	9999.99	42	<.0001	-0.013	-0.013	-0.010	-0.007	-0.007	-0.005
48	9999.99	48	<.0001	-0.002	-0.000	0.007	0.012	0.021	0.032

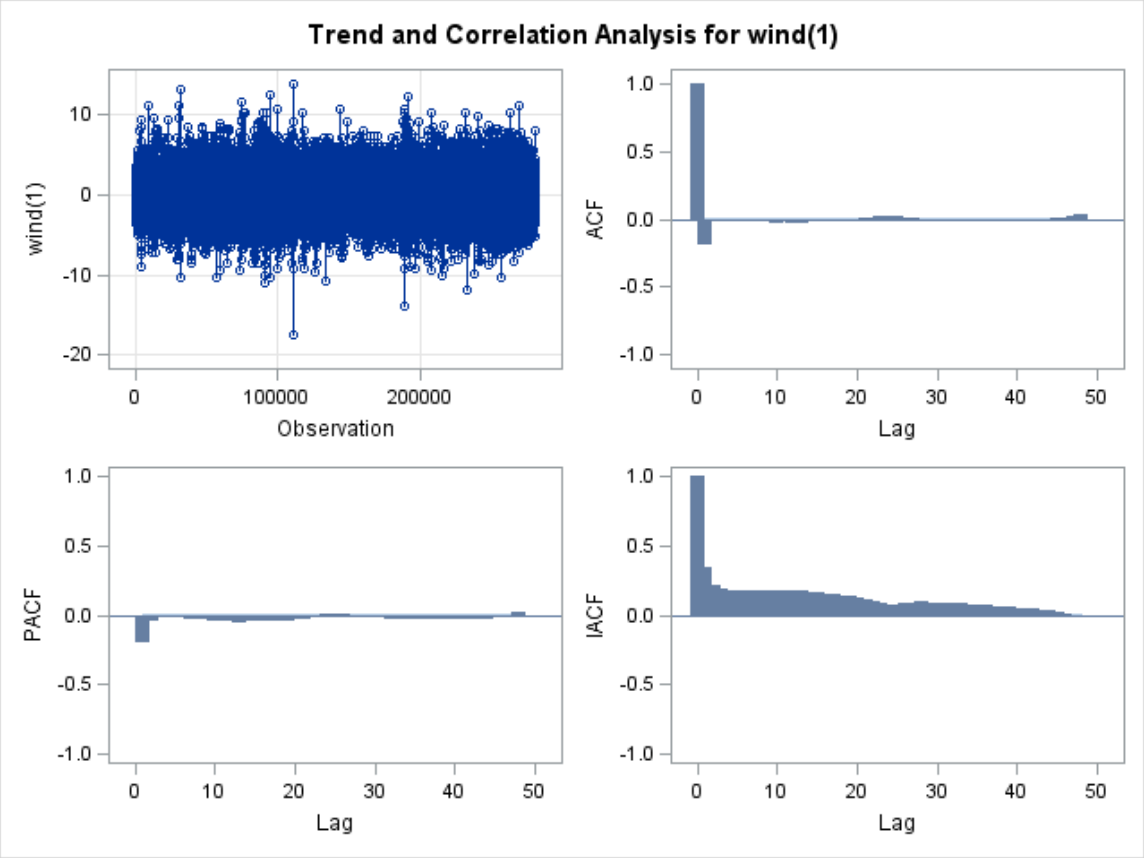

Name of Variable = wind	
Period(s) of Differencing	24
Mean of Working Series	0.000137
Standard Deviation	3.566995
Number of Observations	280296
Observation(s) eliminated by differencing	24
Embedded missing values in working series	2

Autocorrelation Check for White Noise

To Lag	Chi-Square	DF	Pr > ChiSq	Autocorrelations					
6	9999.99	6	<.0001	0.865	0.790	0.719	0.652	0.586	0.520
12	9999.99	12	<.0001	0.457	0.395	0.333	0.273	0.215	0.157
18	9999.99	18	<.0001	0.102	0.049	-0.003	-0.053	-0.102	-0.149
24	9999.99	24	<.0001	-0.196	-0.241	-0.287	-0.333	-0.382	-0.460
30	9999.99	30	<.0001	-0.402	-0.373	-0.347	-0.322	-0.297	-0.273
36	9999.99	36	<.0001	-0.250	-0.229	-0.207	-0.186	-0.167	-0.148
42	9999.99	42	<.0001	-0.132	-0.119	-0.106	-0.095	-0.085	-0.078
48	9999.99	48	<.0001	-0.071	-0.064	-0.057	-0.052	-0.046	-0.040

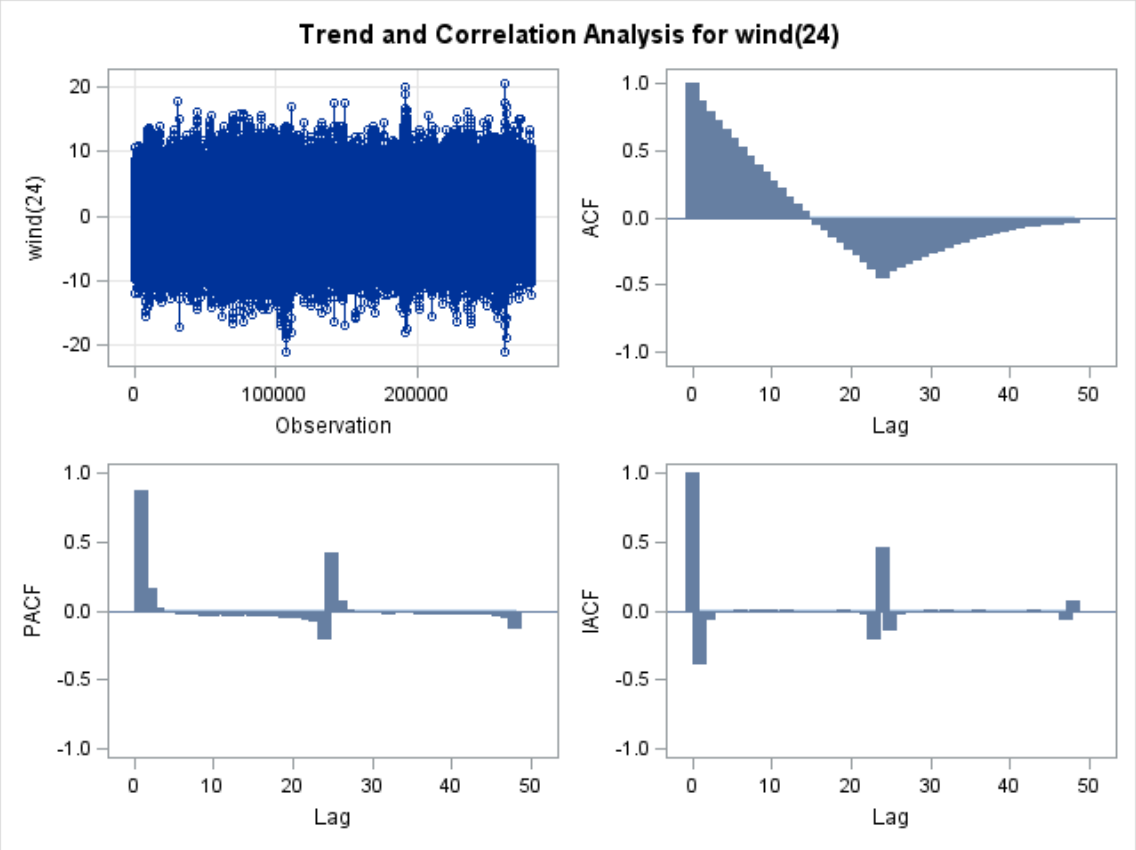

Name of Variable = wind

Name of Variable = wind	
Period(s) of Differencing	8760
Mean of Working Series	-0.00943
Standard Deviation	3.767832
Number of Observations	271560
Observation(s) eliminated by differencing	8760
Embedded missing values in working series	2

Autocorrelation Check for White Noise

To Lag	Chi-Square	DF	Pr > ChiSq	Autocorrelations					
6	9999.99	6	<.0001	0.879	0.812	0.750	0.690	0.634	0.580
12	9999.99	12	<.0001	0.529	0.480	0.434	0.391	0.351	0.315
18	9999.99	18	<.0001	0.282	0.253	0.227	0.203	0.182	0.165
24	9999.99	24	<.0001	0.148	0.134	0.121	0.110	0.100	0.091
30	9999.99	30	<.0001	0.082	0.074	0.067	0.061	0.055	0.050
36	9999.99	36	<.0001	0.045	0.040	0.037	0.033	0.031	0.028
42	9999.99	42	<.0001	0.027	0.025	0.024	0.023	0.022	0.021
48	9999.99	48	<.0001	0.020	0.019	0.019	0.019	0.020	0.020

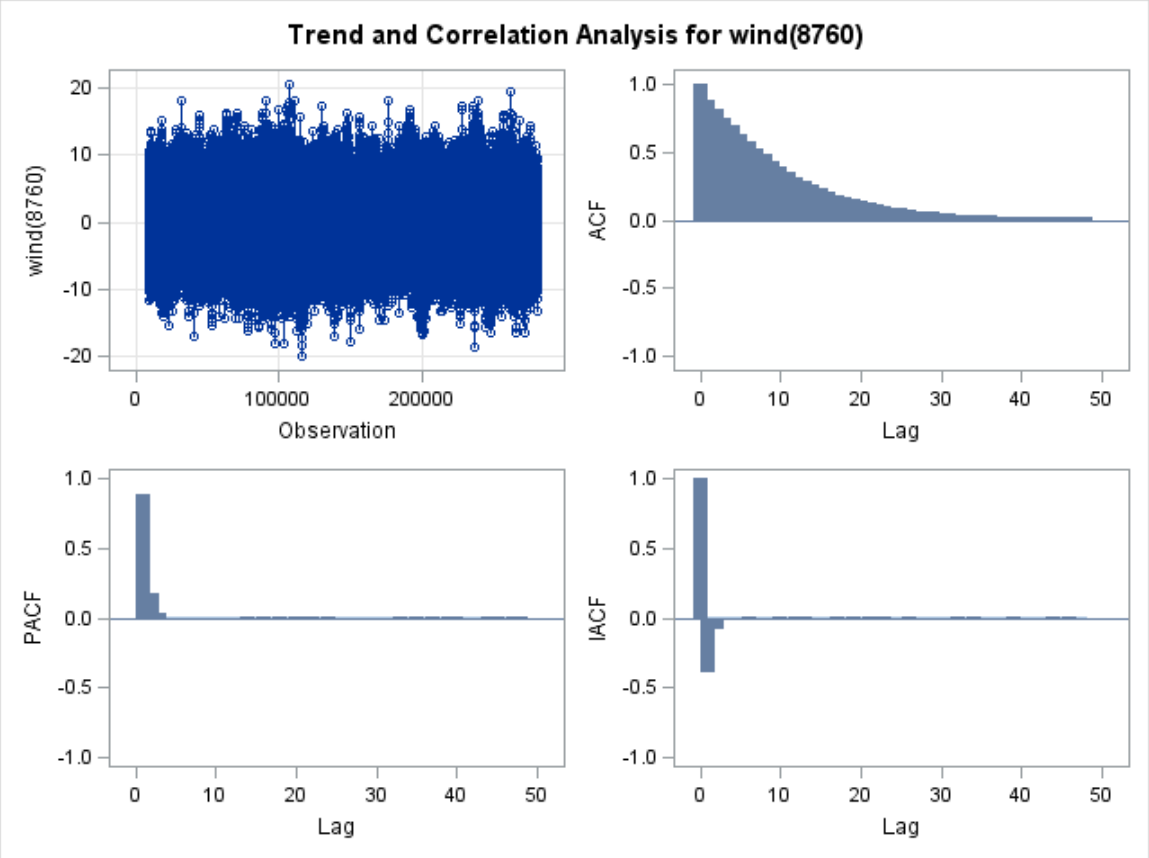

Name of Variable = wind	
Period(s) of Differencing	1,24
Mean of Working Series	-0.00002
Standard Deviation	1.850229
Number of Observations	280295
Observation(s) eliminated by differencing	25
Embedded missing values in working series	4

Autocorrelation Check for White Noise

To Lag	Chi-Square	DF	Pr > ChiSq	Autocorrelations					
6	9999.99	6	<.0001	-0.220	-0.017	-0.012	-0.005	-0.001	-0.009
12	9999.99	12	<.0001	-0.002	-0.003	-0.006	-0.008	-0.001	-0.008
18	9999.99	18	<.0001	-0.010	-0.003	-0.006	-0.005	-0.007	0.001
24	9999.99	24	<.0001	-0.007	0.001	0.004	0.008	0.107	-0.502
30	9999.99	30	<.0001	0.110	0.006	0.005	0.001	0.004	0.004
36	9999.99	36	<.0001	0.005	-0.003	0.005	0.005	0.005	0.008
42	9999.99	42	<.0001	0.008	0.003	0.007	0.005	0.007	0.002
48	9999.99	48	<.0001	0.001	0.002	0.002	-0.000	0.001	0.005

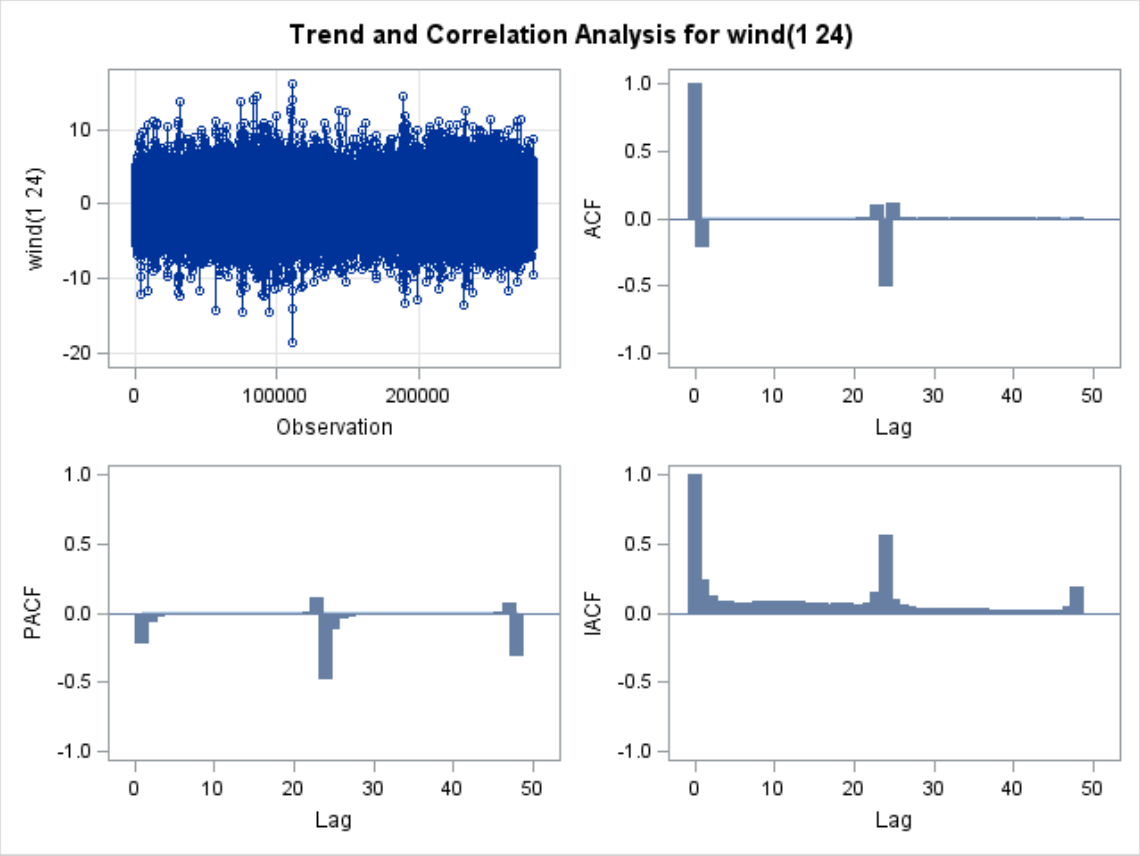

Name of Variable = wind	
Period(s) of Differencing	1,8760
Mean of Working Series	-3.31E-6
Standard Deviation	1.851927
Number of Observations	271559
Observation(s) eliminated by differencing	8761
Embedded missing values in working series	4

Autocorrelation Check for White Noise

To Lag	Chi-Square	DF	Pr > ChiSq	Autocorrelations					
6	9999.99	6	<.0001	-0.223	-0.018	-0.015	-0.011	-0.008	-0.013
12	9999.99	12	<.0001	-0.009	-0.011	-0.013	-0.016	-0.010	-0.016
18	9999.99	18	<.0001	-0.018	-0.009	-0.013	-0.010	-0.013	-0.005
24	9999.99	24	<.0001	-0.011	-0.006	-0.007	-0.003	-0.006	-0.001
30	9999.99	30	<.0001	-0.003	-0.004	-0.003	-0.003	-0.000	-0.003
36	9999.99	36	<.0001	-0.000	-0.006	0.001	-0.004	-0.001	-0.002
42	9999.99	42	<.0001	-0.001	-0.002	-0.003	0.002	0.001	0.000
48	9999.99	48	<.0001	-0.002	-0.003	0.002	-0.003	0.000	0.005

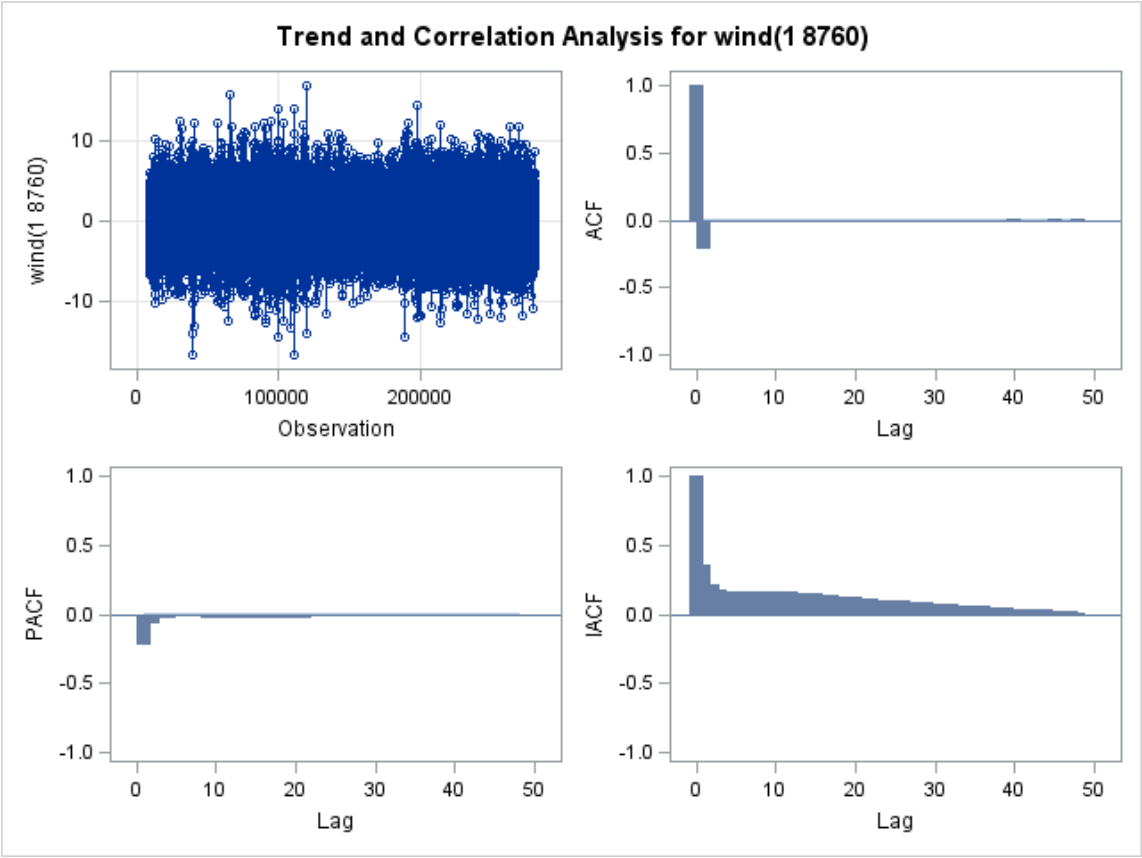

Name of Variable = wind	
Period(s) of Differencing	24,8760
Mean of Working Series	0.000105
Standard Deviation	5.080146
Number of Observations	271536
Observation(s) eliminated by differencing	8784
Embedded missing values in working series	4

Autocorrelation Check for White Noise

To Lag	Chi-Square	DF	Pr > ChiSq	Autocorrelations					
6	9999.99	6	<.0001	0.867	0.792	0.721	0.653	0.586	0.520
12	9999.99	12	<.0001	0.457	0.394	0.332	0.272	0.215	0.157
18	9999.99	18	<.0001	0.102	0.050	-0.002	-0.053	-0.103	-0.150
24	9999.99	24	<.0001	-0.197	-0.243	-0.290	-0.336	-0.385	-0.461
30	9999.99	30	<.0001	-0.404	-0.376	-0.349	-0.324	-0.299	-0.275
36	9999.99	36	<.0001	-0.252	-0.230	-0.208	-0.188	-0.169	-0.151
42	9999.99	42	<.0001	-0.134	-0.120	-0.107	-0.095	-0.085	-0.077
48	9999.99	48	<.0001	-0.070	-0.063	-0.055	-0.050	-0.044	-0.038

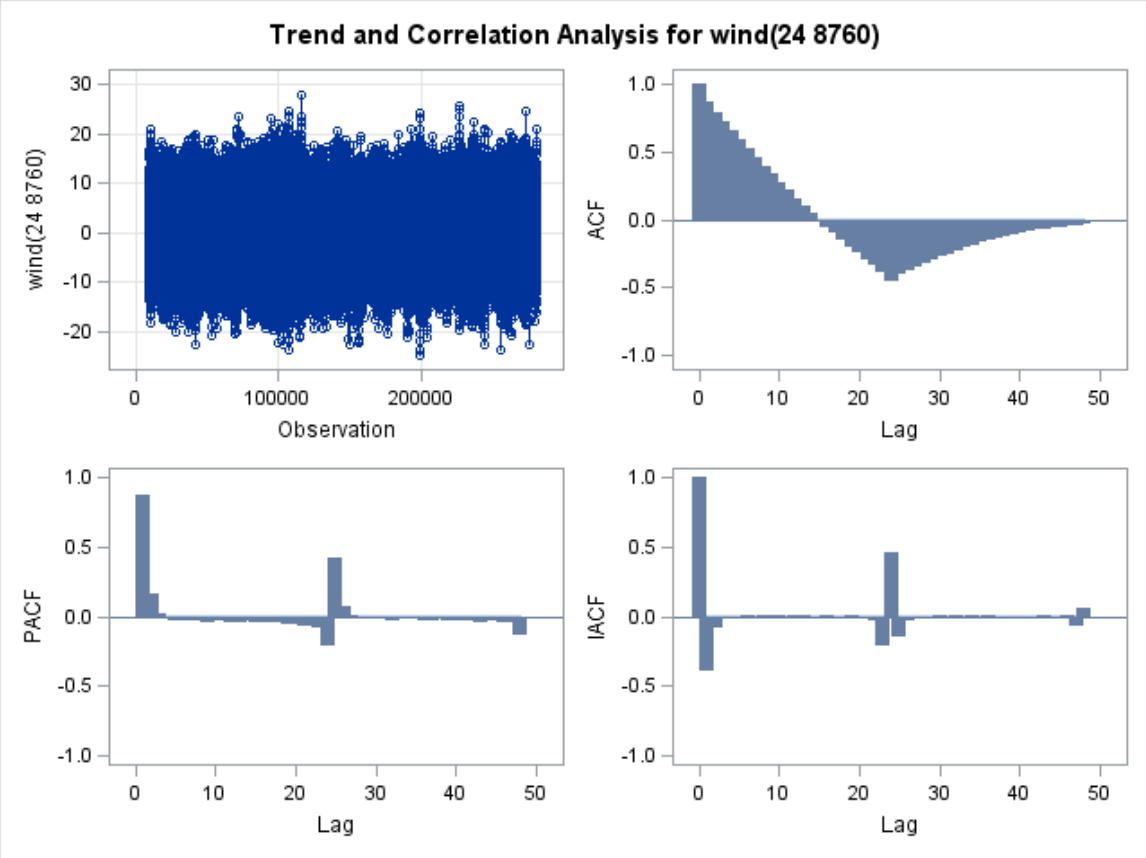

Name of Variable = wind	
Period(s) of Differencing	1,24,8760
Mean of Working Series	0.000023
Standard Deviation	2.619859
Number of Observations	271535
Observation(s) eliminated by differencing	8785
Embedded missing values in working series	8

Autocorrelation Check for White Noise

To Lag	Chi-Square	DF	Pr > ChiSq	Autocorrelations					
6	9999.99	6	<.0001	-0.218	-0.015	-0.010	-0.007	-0.003	-0.009
12	9999.99	12	<.0001	-0.003	-0.003	-0.007	-0.009	-0.001	-0.007
18	9999.99	18	<.0001	-0.012	-0.000	-0.005	-0.005	-0.009	0.002
24	9999.99	24	<.0001	-0.006	0.002	-0.001	0.008	0.105	-0.503
30	9999.99	30	<.0001	0.109	0.005	0.005	0.002	0.003	0.003
36	9999.99	36	<.0001	0.007	-0.002	0.007	0.003	0.005	0.006
42	9999.99	42	<.0001	0.009	0.001	0.008	0.005	0.009	0.002
48	9999.99	48	<.0001	-0.000	0.001	0.006	-0.003	0.003	0.005